



universität
wien

DISSERTATION

Titel der Dissertation

Specificity and transmission in two
shallow water thiotrophic symbioses

Verfasser

Mag. rer. nat. Harald Gruber-Vodicka

angestrebter akademischer Grad

Doktor der Naturwissenschaften (Dr. rer. nat.)

Wien, 2011

Studienkennzahl (lt. Studienblatt): A 091-439

Dissertationsgebiet (lt. Studienblatt): Zoologie

Betreuerin / Betreuer: Univ. Prof. i.R. Dr. Jörg Ott

für Mia, Merle, Sirii und Jana

Contents

Chapter I	1
Introduction	
Chapter II	14
First detection of thiotrophic symbiont phylotypes in the pelagic marine environment	
Chapter III	28
Sequence variability of the pattern recognition receptor Mermaid mediates specificity of marine nematode symbioses	
Chapter IV	44
A new species of symbiotic flatworms, <i>Paracatenula galateia</i> sp. nov. (Platyhelminthes: Catenulida: Retronectidae) from Belize (Central America)	
Chapter V	54
<i>Paracatenula</i>, an ancient symbiosis between thiotrophic Alphaproteobacteria and catenulid flatworms	
Chapter VI	70
Conclusions and outlook	
Appendix I	78
Summary / Zusammenfassung	
Appendix II	82
Acknowledgments	
Appendix III	84
Curriculum Vitae	

I. Introduction

In September 1683 Antony van Leeuwenhoek reported the first observation of living bacteria in plaque from his and several other persons teeth. With this description of oral cavity bacterial communities he witnessed a close relationship of very different organisms, humans and bacteria. Roughly 200 years later Heinrich Anton de Bary, a German mycologist who had worked with lichens as well as fungal crop pathogens, used the term symbiosis coined from the Ancient Greek σύν (sýn) “together” and βίος (bios) “life” (de Bary 1878) for this kind of intimate living-together of two or more unlike organisms. His definition of symbiosis encompasses mutualism (with benefits to all partners), commensalism (no partner is harmed) and parasitism (one partner is harmed) and is now widely accepted in the English speaking scientific community. It took 284 years from Leeuwenhoek’s observations to the discovery of the great role microbial symbioses played in the evolution of the eukaryote cell with its omnipresent bacterial symbionts, the mitochondria (Sagan 1967; but see also Pallen 2011; Selosse 2011). It took another 25 years to develop the sequencing and phylogenetic tools as well as the labeling and imaging tools to access the diversity and distribution of microbes in their environment using the full cycle rRNA approach (Amann et al. 1995). These and other novel molecular tools developed in the 1990s catalyzed a broadening of the focus in symbiosis research and allowed completely new approaches in microbe-animal, microbe –plant or microbe-microbe associations.

In mutualistic bacteria-animal symbioses as investigated in this thesis the microbial symbionts can have very different functions for its animal host. These functions range e.g. from providing bioluminescence such as in the bobtail squid – *Vibrio* symbiosis (Mandel et al. 2009) to defensive functions as in the leaf-cutting ants where symbiotic bacteria inhibit a fungal parasite of the gardened fungus (Currie et al. 2006) to nutritional functions as in sap feeding insects such as aphids where the bacterial symbionts supplement the insects carbohydrate rich diets by providing essential amino acids (McCutcheon and Moran 2010).

Chemoautotrophic symbiosis

In contrast to the largely oxygenated terrestrial world several large or important marine habitats are oxygen poor or free, chemically reduced and enriched in inorganic chemical energy sources such as sulfide or methane. In the steep chemical gradients from these reducing conditions to the oxygenated water column, e.g. around decomposing organic matter or sulfide rich effluents at hot vents, chemoautotrophic bacteria can successfully access both electron donors and acceptors, fix inorganic carbon and form dominating biofilms or mats. In many habitats with reduced water bodies, the optimal electron acceptor oxygen is however either temporally and/or spatially separated from the reduced compounds such as hydrogen, methane or hydrogen sulfide. In a symbiotic association with an animal hosts that bridges these gaps for its symbiont by behavioral, morphological or metabolic adaptations, the symbiont gains access to both oxygen and reduced compounds and the host is in return provisioned by its symbionts. Seen from the animal host's perspective, sulfide detoxification and nourishment through the chemoautotrophic production of its symbionts are the innovations that enable the hosts to access an otherwise inaccessible niche and apparently live on inorganic carbon and energy sources. This harnessing of chemosynthetic symbionts is a recurring evolutionary strategy (reviewed in Dubilier et al. 2008) and eukaryotes from six phyla as well as one archaeon (Muller et al. 2010) are known to harbor chemoautotrophic sulfur-oxidizing bacteria. In contrast to this broad host diversity, all bacterial partners apparently belong to two classes of bacteria – the *Gamma*- and *Epsilonproteobacteria* (Dubilier et al. 2008).

Chemosynthetic symbioses were first described from hydrothermal vents at the Galapagos Rift in the giant, mouth and gutless tubeworm *Riftia pachyptila* (Cavanaugh et al. 1981; Felbeck 1981). It only took this spectacular deep-sea discovery to have scientists realize that chemoautotrophic symbioses occur in a wide range of habitats including shallow water coastal sediments, which are much easier to access (Felbeck et al. 1981; Ott et al. 1982; Felbeck et al. 1983). For an overview of the presently known shallow-water symbioses see Figure 1.

In many of these sediments an oxygenated top layer is separated from a deeper, reduced and sulfidic layer by a layer free of both oxygen and sulfide. Meiofaunal hosts to sulfur oxidizing bacteria (SOB) such as desmodorid nematodes of the subfamily Stilbonematinae (see Fig. 2; reviewed in Ott et al. 2004a; Ott et al. 2004b) or gutless clitellate annelids of the subfamily Phallodrilinae (genera *Olavius/Inanidrilus* - commonly called 'gutless oligochaetes') (reviewed in Dubilier et al. 2006) have been shown to traverse this

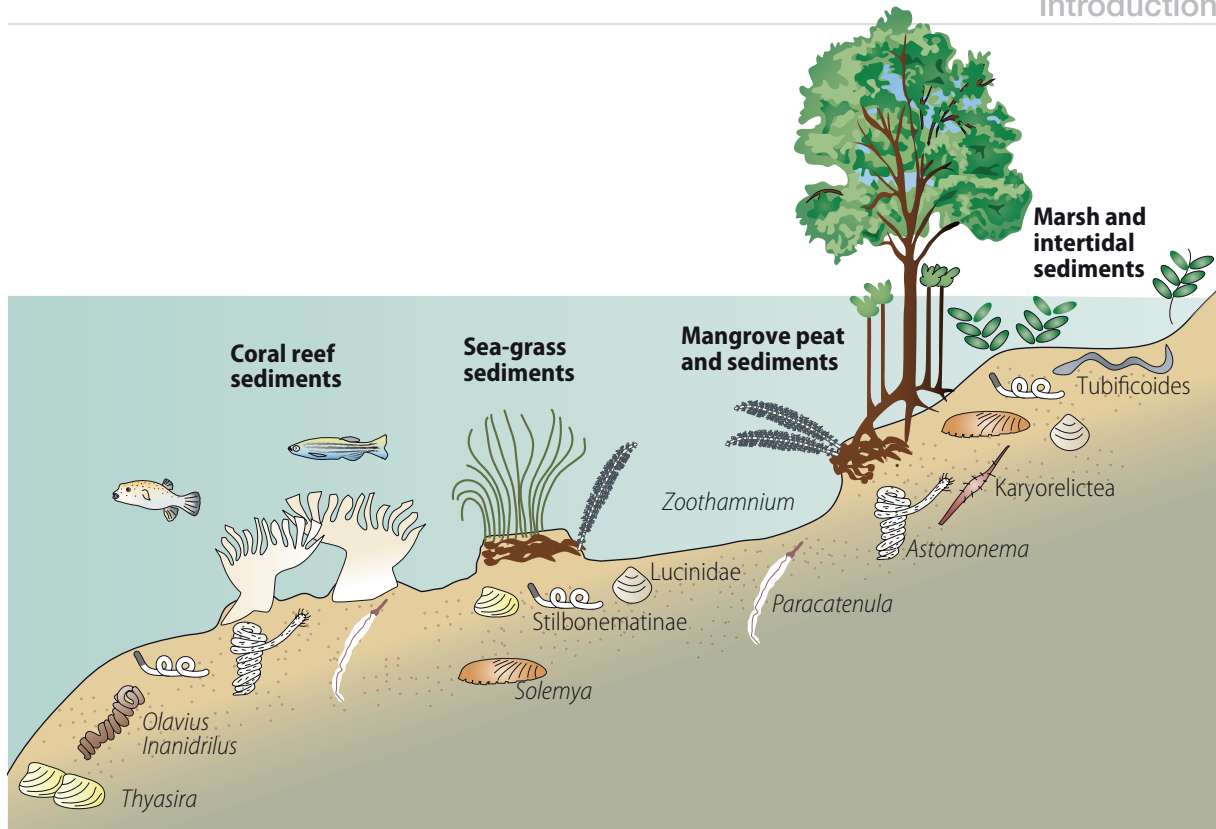


Figure 1: Overview of the presently known shallow water thiotrophic symbioses (animals not drawn to scale). Adapted after Dubilier et al 2008.

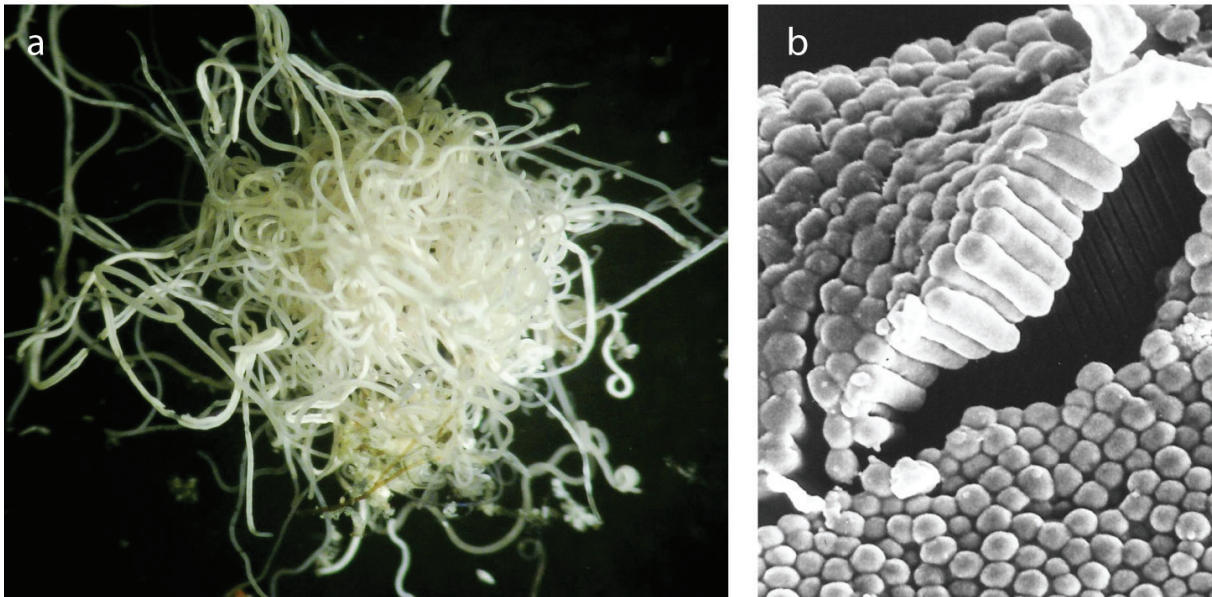


Figure 2: Stilbonematinae nematodes with thiotrophic ectosymbionts. a) A ball of freshly collected worms displaying the typical whitish color. b) Scanning electron microscopic image of the monolayer coat of ectosymbionts on the *Laxus oneistus* cuticle. Images taken by J. A. Ott and M. Polz.

chemical gradient to nourish their symbionts (Giere et al. 1991; Ott et al. 1991). Gutless oligochaetes host a consortium of symbionts with the most dominant symbiont being a gammaproteobacterial sulfur oxidizing chemoautotroph called Gamma1 (Dubilier et al. 2001; Blazejak et al. 2006). These Gamma1 symbionts form a monophyletic clade together with the ectosymbionts of stilbonematinae and the endosymbionts of the nematode *Astomonema* (Musat et al. 2007; Dubilier et al. 2008; Bayer et al. 2009).

Many hosts including stilbonematinae and gutless oligochaetes have a whitish appearance due to light refractive inclusions in their bacterial symbionts. These refractive inclusions resemble sulfur storage globules in large free-living sulfur oxidizing bacteria such as *Beggiatoa* (Pasteris et al. 2001). Due to the provisioning by the symbionts several host species with chemosynthetic symbionts have a reduced digestive system (e.g. solemyid or lucinid bivalves) or completely lack a mouth and a gut at least in adult stages (e.g. annelid taxa such as the siboglinid tubeworms and gutless oligochaetes as well as nematodes of the genus *Astomonema*). Another meiofauna member co-occurring with *Astomonema*, Stilbonematinae and gutless oligochaetes are pinkish white catenulid flatworms of the genus *Paracatenula* which also have no mouth or gut (Figure 3). Instead, they harbor intracellular microbial endosymbionts in bacteriocytes (Ott et al. 1982) that form a tissue resembling the trophosome of the mouthless Siboglinidae (Annelida). The bacteriocytes almost completely fill the posterior part of the body behind the brain (Ott et al. 1982).

Paracatenula belongs to the catenulid family of the Retronectidae, the only catenulid family with marine members (Sterrer and Rieger 1974). While the second marine genus, *Retronectes* occurs from sub-polar to tropical regions, *Paracatenula* species have only been described from the interstitial space of warm temperate to tropical subtidal sands in the Atlantic and the Caribbean Sea (Sterrer and Rieger 1974). Asexual reproduction is very common across Catenulida and led to the order's name¹. In contrast to this, no indications of asexual reproduction were found in Retronectidae and the absence of asexual reproduction was diagnosed as one of the group's synapomorphies (Sterrer and Rieger 1974). As virtually no data is available on the biology of *Paracatenula* including their reproduction, their global distribution or their diversity, all these diagnoses have to be considered preliminary. The worms' morphological adaptations, their habitat and their color however point to a chemosynthetic nature of the symbionts. In many SOB that store

1 Catenula is Latin, means 'little chain' and refers to the string of zooids which are produced in a mode of asexual reproduction called paratomy. In paratomy the agametically produced asexual offspring organ development precedes the split from the mother zooid, and daughter zooids are arranged in the anterior-posterior body axis starting with the mother zooid.

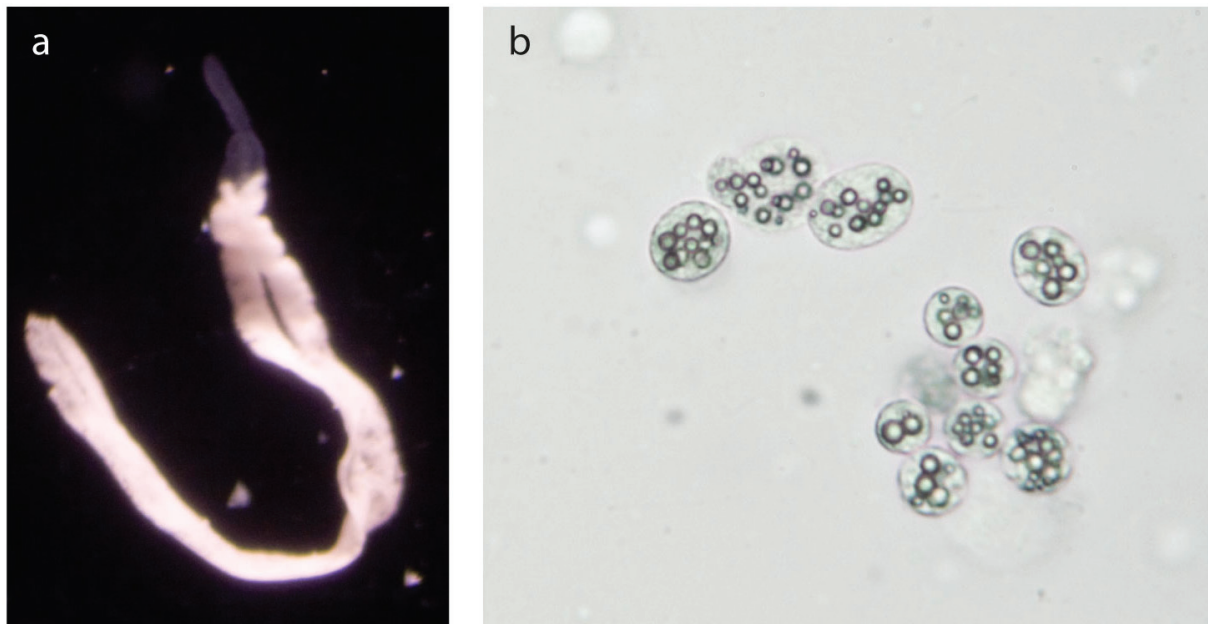


Figure 3: *Paracatenula* catenulid flatworms with endosymbiotic bacteria a) *Paracatenula* sp. worm from the Belize Barrier Reef with a pinkish-white body region housing the symbionts clearly separated from the transparent rostrum. b) Extracted symbiotic bacterial cells from a *Paracatenula* sp. host from Belize. Note the numerous light refractive inclusions in the bacterial cells.

elemental sulfur in light refractive globules, the reversely operating sirohaem dissimilatory sulfite reductase (DsrAB) enzyme system is an important part of the sulfur oxidation machinery (Loy et al. 2009). The gene for DsrAB has been found in bacteria associated with two species of *Paracatenula* and their sequences clustered together with sequences of the alphaproteobacterial sulfur oxidizing genus *Magnetospirillum*, albeit with weak node support (Loy et al. 2009). Assuming that the sequences stem from the endosymbionts and not from a contamination, a phylogenetic position of the *Paracatenula* symbionts within *Alphaproteobacteria* seems possible. A molecular identification and an assessment of the chemoautotrophic capabilities of the symbionts is however lacking.

Transmission of bacterial symbionts

The transmission of symbionts to the offspring is a crucial step in the reproduction and early development of all hosts. There are two possible sources for the symbionts of the daughter generation – a pool of free-living bacteria in the environment (environmental or horizontal transmission) or the symbionts of the parental individuals that get directly passed on to the next generation during oogenesis or development (maternal or vertical transmission) (reviewed in Bright and Bulgheresi 2010). In general, cases of strict vertical

transmission are rare and very often a mixed mode of transmission is found where vertical transmission is occasionally or regularly complemented by horizontal transmission. Complete congruence of host and symbiont phylogenies over a large number of host taxa is a good predictor for strict vertical transmission (Moran et al. 2008). The mode of transmission is inherently linked to the population size of the symbionts and therefore to the evolutionary forces acting upon them (Peek et al. 1998). Compared to a non-symbiotic free-living bacterial population, the population sizes of horizontally transmitted bacteria - which have a non-symbiotic population and an additional symbiotic population - is increased, while the population sizes of strictly vertically transmitted symbionts are largely restricted. The nearly neutral theory of molecular evolution predicts that rates of slightly deleterious nucleotide substitutions should be negatively correlated with population size due to the effects of genetic drift (Ohta 1992). Absolutely neutral mutations are only affected by the rate of mutation and deleterious mutations on the other hand are influenced more by purifying selection than by population size (Ohta 1992). Translated to symbiont evolutionary pace this should mean faster overall substitution rates in the very small populations of vertically transmitted symbionts and slower substitution rates in horizontally transmitted symbionts compared to free-living populations. Both scenarios have been demonstrated for thiotrophic symbionts with different modes of transmission (Peek et al. 1998) and accelerated evolution in vertically transmitted symbionts has been demonstrated for many insect symbiont lineages as well (Moran et al. 2008). Another typical genomic feature of vertically inherited symbionts is a tendency to have A+T enriched genomes (Moran et al. 2008). This has been documented in many insect symbiont lineages as well as in the vertically transmitted thiotrophic symbionts in vesicomid clams which have a genomic G+C content of 31.6 - 34% compared to 43.1% in the closely related free-living *Thiomicrospira crunogena* (Kuwahara et al. 2008).

Specificity in symbiotic association

A high degree of specificity has been demonstrated for a number of microbial symbioses. The degree of taxonomic specificity varies even between host species within one genus (Chaston and Goodrich-Blair 2010). In the case of Stilbonematinae nematodes the bacteria associated to *Laxus oneistus* (Polz et al. 1994), *Eubostrichus diana* (Polz et al. 1999), and three *Robbea* species (Bayer et al. 2009) have been molecularly characterized so far. Both *Laxus oneistus* and all three *Robbea* species are covered by a microbial coat composed of a single phylotype of *Gammaproteobacteria*. The molecular mechanisms mediating the selection

of cooperative microbes have been shown to be *i)* dependent on either minor variations in conserved molecules in closely related hosts or symbiont, or *ii)* on the presence / absence of host-range specificity determining genetic factors (Chaston and Goodrich-Blair 2010). Mermaid, a Ca^{2+} -dependent sugar-binding lectin secreted by stilbonematine nematodes has been detected in such minor variants (isoforms) and has been shown to be involved in symbiont attachment (Bulgheresi et al. 2006). It is feasible that the detected isoforms play a role in the acquisition and selection of the stilbonematine ectosymbionts as the symbionts are likely environmentally transmitted. Two facts point to environmental transmission (1) host and symbiont phylogenies do not match (Bayer et al. 2009) and (2) the need of developing nematodes to replace their bacterial coat through several molts, but so far no free-living closely related phylotypes have been detected.

Thesis outline

The main results of this thesis are presented in the Chapters II to VI:

This thesis studies the biology of two shallow water thiotrophic symbioses – the catenulid flatworms of the genus *Paracatenula* and stilbonematinae nematodes, both portrayed in the introduction. Host and symbiont distributions, host specificity, symbiont metabolism as well as possible modes of transmission are characterized by molecular and morphological methods in an integrative symbiosis research framework involving host and symbiont datasets.

In **chapter II - First detection of thiotrophic symbiont phylotypes in the pelagic marine environment**, we detected closely related members of the stilbonematinae / gutless oligochaete symbiont clade in offshore surface seawater of both the Caribbean and Mediterranean Sea using specific PCR-assays and FISH.

The successful selection of such environmentally transmitted partners is crucial for hosts. The stilbonematine species *Laxus oneistus* is covered by a single bacterial phylotype. The symbionts are embedded in a layer of host mucus containing the lectin Mermaid which mediates symbiont attachment. In a complementing line of work involving Stilbonematinae in **Chapter III - Sequence variability of the pattern recognition receptor Mermaid mediates specificity of marine nematode symbioses** we could show that *Stilbonema majum*—another symbiotic stilbonematine nematode co-occurring with *L. oneistus*—is covered by bacteria that are related but phylogenetically distinct to those covering *L. oneistus* using the full-cycle rRNA approach. Furthermore cDNA analysis of the host produced lectin Mermaid from both host taxa revealed

several isoforms that were differing in only one to three of the 105 aa positions in the active carbohydrate recognition domain. In agglutination experiments the isoforms showed higher affinities to the symbionts of the host they were found on. This indicates that particular isoforms of the same molecule play a role in the selection and attachment of specific symbionts, very similar to what had been documented for pathogen recognition in the innate immune system of different animals.

Paracatenula worms co-occur with Stilbonematinae and their association with endosymbiotic bacteria has been published almost 20 years earlier, but since this initial description nothing has been published on this enigmatic symbiosis.

In a first stage for the *Paracatenula* flatworm research, represented in **chapter IV - A new species of symbiotic flatworms, *Paracatenula galateia* sp. nov. (Platyhelminthes: Catenulida: Retronectidae) from Belize (Central America)**, we described our main *Paracatenula* model organism. The species *P. galateia* proved to be the most suitable in terms of reliability of sampling, ease of handling, and survival in the lab from the great diversity of *Paracatenula* species found in the vicinity of the Carrie Bow Cay field station.

In a second stage in **chapter V - *Paracatenula*, an ancient symbiosis between thiotrophic *Alphaproteobacteria* and catenulid flatworms** I characterized the *Paracatenula galateia* symbionts molecularly and gave them a name, ‘*Candidatus* Riegeria galateiae’. The intracellular endosymbionts from all studied *Paracatenula* species are closely related and form a novel family level clade of chemoautotrophic sulfur-oxidizing *Alphaproteobacteria*. I could show that the *Paracatenula* – *Candidatus* Riegeria association is ancient, likely dating back to the early evolution of flatworms more than 500 million years ago. My results indicate that up to 50% of the body volume of each worm is occupied by its mono-specific bacterial symbionts. The host and symbiont phylogenies for 16 species analyzed match perfectly and generate a first line of evidence indicating vertical transmission of the symbionts.

Literature cited

- Amann R, Ludwig W, Schleifer K (1995) Phylogenetic identification and in situ detection of individual microbial cells without cultivation. *Microbiol. Rev.* 59: 143-169
- Bayer C, Heindl NR, Rinke C, Lücker S, Ott JA, Bulgheresi S (2009) Molecular characterization of the symbionts associated with marine nematodes of the genus *Robbea*. *Environmental Microbiology Reports* 1: 136-144
- Blazejak A, Kuever J, Erseus C, Amann R, Dubilier N (2006) Phylogeny of 16S rRNA, Ribulose 1,5-Bisphosphate Carboxylase/Oxygenase, and Adenosine 5'-Phosphosulfate Reductase Genes from Gamma- and Alphaproteobacterial Symbionts in Gutless Marine Worms (Oligochaeta) from Bermuda and the Bahamas. *Applied and environmental microbiology* 72: 5527-5536
- Bright M, Bulgheresi S (2010) A complex journey: transmission of microbial symbionts. *Nature Reviews Microbiology* 8: 218-230
- Bulgheresi S, Schabussova I, Chen T, Mullin NP, Maizels RM, Ott JA (2006) A new C-type lectin similar to the human immunoreceptor DC-SIGN mediates symbiont acquisition by a marine nematode. *Appl Environ Microbiol* 72: 2950-2956
- Cavanaugh CM, Gardiner SL, Jones ML, Jannasch HW, Waterbury JB (1981) Prokaryotic Cells in the Hydrothermal Vent Tube Worm *Riftia pachyptila* Jones: Possible Chemoautotrophic Symbionts. *Science* 213: 340-342
- Chaston J, Goodrich-Blair H (2010) Common trends in mutualism revealed by model associations between invertebrates and bacteria. *FEMS Microbiology Reviews* 34: 41-58
- Currie CR, Poulsen M, Mendenhall J, Boomsma JJ, Billen J (2006) Coevolved Crypts and Exocrine Glands Support Mutualistic Bacteria in Fungus-Growing Ants. *Science* 311: 81-83
- de Bary A (1878) "Ueber Symbiose". *Tageblatt der 51. Versammlung deutscher Naturforscher und Ärzte in Cassel*: 121-126

- Dubilier N, Bergin C, Lott C (2008) Symbiotic diversity in marine animals: the art of harnessing chemosynthesis. *Nature Reviews Microbiology* 6: 725-740
- Dubilier N, Blazejak A, Rühland C (2006) Symbioses between Bacteria and Gutless Marine Oligochaetes. In: Overmann J (ed) *Molecular Basis of Symbiosis*. Springer Berlin, Heidelberg, pp 251-275
- Dubilier N, Mulders C, Ferdelman T, de Beer D, Pernthaler A, Klein M, Wagner M, Erseus C, Thiermann F, Krieger J, Giere O, Amann R (2001) Endosymbiotic sulphate-reducing and sulphide-oxidizing bacteria in an oligochaete worm. *Nature* 411: 298-302
- Felbeck H (1981) Chemoautotrophic Potential of the Hydrothermal Vent Tube Worm, *Riftia pachyptila* Jones (Vestimentifera). *Science* 213: 336-338
- Felbeck H, Childress JJ, Somero GN (1981) Calvin-Benson cycle and sulphide oxidation enzymes in animals from sulphide-rich habitats. *Nature* 293: 291-293
- Felbeck H, Liebezeit G, Dawson R, Giere O (1983) CO₂ fixation in tissues of marine oligochaetes (*Phallodrilus leukodermatus* and *P. planus*) containing symbiotic, chemoautotrophic bacteria. *Marine Biology* 75: 187-191
- Giere O, Conway N, Gastrock G, Schmidt C (1991) "Regulation" of gutless annelid ecology by endosymbiotic bacteria. *Marine Ecology Progress Series* 68: 287-299
- Kuwahara H, Takaki Y, Yoshida T, Shimamura S, Takishita K, Reimer J, Kato C, Maruyama T (2008) Reductive genome evolution in chemoautotrophic intracellular symbionts of deep-sea *Calyptogena* clams. *Extremophiles* 12: 365-374
- Loy A, Duller S, Baranyi C, Musmann M, Ott J, Sharon I, Beja O, Le Paslier D, Dahl C, Wagner M (2009) Reverse dissimilatory sulfite reductase as phylogenetic marker for a subgroup of sulfur-oxidizing prokaryotes. *Environmental Microbiology* 11: 289-299
- Mandel MJ, Wollenberg MS, Stabb EV, Visick KL, Ruby EG (2009) A single regulatory gene is sufficient to alter bacterial host range. *Nature* 458: 215-218

- McCutcheon JP, Moran NA (2010) Functional Convergence in Reduced Genomes of Bacterial Symbionts Spanning 200 My of Evolution. *Genome Biology and Evolution* 2: 708-718
- Moran NA, McCutcheon JP, Nakabachi A (2008) Genomics and evolution of heritable bacterial symbionts. *Annual Review of Genetics* 42: 165-190
- Muller F, Brissac T, Le Bris N, Felbeck H, Gros O (2010) First description of giant *Archaea* (*Thaumarchaeota*) associated with putative bacterial ectosymbionts in a sulfidic marine habitat. *Environmental Microbiology* 12: 2371-2383
- Musat N, Giere O, Gieseke A, Thiermann F, Amann R, Dubilier N (2007) Molecular and morphological characterization of the association between bacterial endosymbionts and the marine nematode *Astomonema* sp. from the Bahamas. *Environmental Microbiology* 9: 1345-1353
- Ohta T (1992) The Nearly Neutral Theory of Molecular Evolution. *Annual Review of Ecology and Systematics* 23: 263-286
- Ott JA, Bright M, Bulgheresi S (2004a) Marine microbial thiotrophic ectosymbioses. *Oceanography and marine biology - An Annual Review* 42: 95-118
- Ott JA, Bright M, Bulgheresi S (2004b) Symbioses between Marine Nematodes and Sulfur-oxidizing Chemoautotrophic Bacteria. *Symbiosis* 36: 103-126
- Ott JA, Novak R, Schiemer F, Hentschel U, Nebelsick M, Polz M (1991) Tackling the sulfide gradient: A novel strategy involving marine nematodes and chemoautotrophic ectosymbionts. *Pubblicazioni Stazione Zoologica Napoli I: Marine Ecology* 12: 261-279
- Ott JA, Rieger G, Rieger R, Enderes F (1982) New mouthless interstitial worms from the sulfide system: Symbiosis with Prokaryotes. *Pubblicazioni Stazione Zoologica Napoli I: Marine Ecology* 3: 313-333
- Pallen MJ (2011) Time to recognise that mitochondria are bacteria? *Trends in Microbiology* 19: 58-64
- Pasteris JD, Freeman JJ, Goffredi SK, Buck KR (2001) Raman spectroscopic and laser scanning confocal

microscopic analysis of sulfur in living sulfur-precipitating marine bacteria. *Chemical Geology* 180: 3-18

Peek AS, Vrijenhoek RC, Gaut BS (1998) Accelerated evolutionary rate in sulfur-oxidizing endosymbiotic bacteria associated with the mode of symbiont transmission. *Molecular Biology and Evolution* 15: 1514-1523

Polz MF, Distel DL, Zarda B, Amann R, Felbeck H, Ott JA, Cavanaugh CM (1994) Phylogenetic analysis of a highly specific association between ectosymbiotic, sulfur-oxidizing bacteria and a marine nematode. *Appl Environ Microbiol* 60: 4461-4467

Polz MF, Harbison C, Cavanaugh CM (1999) Diversity and Heterogeneity of Epibiotic Bacterial Communities on the Marine Nematode *Eubostrichus diana*. *Appl. Environ. Microbiol.* 65: 4271-4275

Sagan L (1967) On the origin of mitosing cells. *Journal of Theoretical Biology* 14: 225-274, IN221-IN226

Selosse M-A (2011) Morts d'amour: mitochondria are bacteria that sometimes become extinct through symbiosis. *Trends in Microbiology* 19: 255-256

Sterrer W, Rieger RM (1974) Retronectidae - a new cosmopolitan marine family of Catenulida (Turbellaria). In: Riser N, Morse M (eds) *Biology of the Turbellaria*. McGraw-Hill, New York, pp 63-92

II. First detection of thiotrophic symbiont phylotypes in the pelagic marine environment

Authors: Niels R. Heindl, Harald R. Gruber-Vodicka, Christoph Bayer, Sebastian Luecker, Joerg A. Ott and Silvia Bulgheresi

Publication status: published 2011 in *FEMS Microbiology Ecology* Volume 77, Issue 1, pages 223–227

Personal contributions of Harald Gruber-Vodicka

- a. performed all phylogenetic and statistical analyses
- b. edited and approved the manuscript



SHORT COMMUNICATION

First detection of thiotrophic symbiont phylotypes in the pelagic marine environment

Niels R. Heindl¹, Harald R. Gruber-Vodicka², Christoph Bayer¹, Sebastian Lücker³, Joerg A. Ott² & Silvia Bulgheresi¹

¹Department of Genetics in Ecology, University of Vienna, Vienna, Austria; ²Department of Marine Biology, University of Vienna, Vienna, Austria; and ³Department of Microbial Ecology, University of Vienna, Vienna, Austria

Correspondence: Silvia Bulgheresi, Department of Genetics in Ecology, University of Vienna, Althanstrasse 14, 1090 Vienna, Austria. Tel.: +43 (0)1 4277 57818; fax: +43 (0)1 4277 9578; e-mail: silvia.bulgheresi@univie.ac.at

Received 13 December 2010; revised 8 February 2011; accepted 5 March 2011. Final version published online 18 April 2011.

DOI:10.1111/j.1574-6941.2011.01096.x

Editor: Riks Laanbroek

Keywords

symbiosis; thiotrophic; *Gammaproteobacteria*; pelagic; sulfur-oxidizing bacteria; nematode.

Stilbonematid nematodes inhabit marine sands. Their surface is covered by sulfur-oxidizing bacteria. Frequently co-occurring with the stilbonematids are gutless oligochaetes of the genera *Inanidrilus* and *Olavius*. Both nematodes and oligochaetes do not exhibit planktonic developmental stages. Instead, they spend their entire life cycles in the sediment, where they may migrate between superficial and deep sand, thereby enabling their symbionts to access oxidants and reductants. In turn, these hosts appear to be trophically dependent on their symbionts (Ott *et al.*, 2004a, b; Dubilier *et al.*, 2008). Gutless oligochaetes harbor a consortium of symbiotic bacteria under their cuticle, the most prominent member being the Gamma 1 symbiont (Dubilier *et al.*, 2001). Metagenomic analysis allowed the identification of Gamma 1 symbiont genes encoding for enzymes involved in CO₂ fixation via the Calvin cycle, the oxidation of reduced sulfur compounds (such as adenosine 5'-phosphosulfate reductase, AprA), and sulfur-storage, supporting its chemoautotrophic, sulfur-oxidizing nature (Woyke *et al.*, 2006). In 16S rRNA gene-based phylogenetic trees, oligochaete Gamma 1 symbionts form a distinct cluster within the *Gammaproteobacteria* together with mar-

Abstract

Marine oligochaete and nematode thiotrophic symbionts (MONTs) form a phylogenetic cluster within the *Gammaproteobacteria*. For the symbionts that live on the nematode surface, environmental transmission is likely. However, until now, no free-living relatives have been found. In this study, we detected MONTs cluster members in offshore surface seawater of both the Caribbean and the Mediterranean Sea by PCR amplification of their 16S rRNA genes. This is the first evidence of members of this cluster in the pelagic environment. These may either be free-living forms of the symbionts or closely related, nonsymbiotic strains. In either case, their existence sheds light on the evolution of beneficial symbioses between shallow water invertebrates and sulfur-oxidizing bacteria.

ine nematode symbionts (Musat *et al.*, 2007; Dubilier *et al.*, 2008; Bayer *et al.*, 2009; Bulgheresi *et al.*, 2011). We will refer to this as the marine oligochaete and nematode thiotrophic symbionts (MONTs) cluster. Two 16S rRNA genes from bacteria associated with the coral *Acropora palmata* (Sunagawa *et al.*, 2010) also belong to this cluster, albeit their association with the coral needs to be confirmed by fluorescence *in situ* hybridization (FISH). So far, no free-living members of the MONTs cluster have been detected. This is surprising, given that several facts indicate that the stilbonematid symbionts are recruited – at least partially – from the environment: (1) incongruence of host and symbiont phylogenies (Bayer *et al.*, 2009); (2) lack of symbionts on the eggshell of unhatched nematode embryos (S. Bulgheresi unpublished data); and (3) the need of developing nematodes to replace their bacterial coat through several molts. As for the symbionts of gutless oligochaetes, they are transmitted vertically (Giere & Langheld, 1987), but the incongruent host and symbiont phylogenies point to additional horizontal transfer (Dubilier *et al.*, 2008).

This study was performed to determine whether members of the MONTs cluster can only be found associated to

marine metazoans or also in the pelagic environment. We therefore searched for their 16S rRNA genes in surface seawater (see Supporting Information, Table S1) offshore from where the stilbonematids *Robbea* sp. 1 (*Rmed* in the following text), sp. 2 (*Rcay*), and sp. 3 (*Rbel*) occur: Calvi on the island of Corsica (France), Little Cayman (Cayman Islands), and Carrie Bow Cay (Belize), respectively. The cuticle of these nematodes is covered by a spatially ordered monolayer of bacteria. Only one bacterial morphotype and one 16S rRNA gene phylotype were found to be associated to each given *Robbea* species. The presence and phylogeny of the *aprA* gene indicates that the bacterial symbionts may use reduced sulfur compounds as an energy source (Bayer *et al.*, 2009).

Except for the Mediterranean seawater, processed after overnight transport in a cooler, 500-mL aliquots were immediately filtered on site (0.2- μ m-pore size, 47 mm \varnothing GTTP filters, Millipore, Billerica, MA). The filters were stored deep-frozen in UltraClean™ Soil DNA Isolation Kit solution number 1 and environmental DNA was later extracted according to the manufacturer's high-yield protocol. The extracted DNA and ultrapure water, as a negative control, were randomly amplified with the GenomiPhi V2 Kit (GE Healthcare Europe). 16S rRNA gene-specific PCR primers targeting the symbionts of the three *Robbea* species mentioned above (see Table S2 for primer details) were designed using the PROBE_DESIGN tool of the ARB software package (Ludwig *et al.*, 2004) and the ARB SSU_jan04_corrected database (<http://www.arb-home.de>) updated with sequences of the MONTS cluster. The output for *Rmed* and *Rbel* symbiont-specific primers was modified by shifting mismatches to the next similar target sequences to the 3' end. Primer specificity was verified by searching GenBank, SILVA, and Greengenes databases with probeCheck (Loy *et al.*, 2008). From each randomly amplified environmental DNA, a pool of 16S rRNA gene fragments was generated with the eubacterial primers 616V (Juretschko *et al.*, 1998) and 1492R (Kane *et al.*, 1993). Each 16S rRNA gene pool was then used as a template for amplification with nested, symbiont-specific primers. One microliter of template per 50 μ L reaction volume was used for PCR amplification (Invitrogen Life Technologies, Darmstadt, Germany) [4 min at 94 °C; 35 \times (45 s at 94 °C, 30 s at T_A , 1 min 30 s at 72 °C); 10 min at 72 °C]. All PCR products were cloned into the pCR2.1-TOPO cloning vector (Invitrogen Life Technologies), Sanger-sequenced, and assembled using CodonCode Aligner 3.5 (CodonCode Corporation, Dedham, MA). Most of the sequences obtained from the seawater samples were closely related to those of nematode symbionts (EU711427, EU711426, and EU71142, 98.1–100% sequence identity; see Table S1).

We compiled a 16S rRNA gene dataset with those sequences obtained from our environmental samples that

had MONTS cluster members among their 20 BLASTN top hits (BLASTN was used with standard parameters; Altschul *et al.*, 1990). GenBank sequences retrieved using BLASTN and displaying $\geq 95\%$ similarity to the 16S rRNA genes of three stilbonematid symbionts (EU711426, EU711427, and EU711428) were also included. We also BLASTN searched the CAMERA, IMG/G, and SAR databases for sequences $\geq 95\%$ identical to EU711426, EU711427, and EU711428, but retrieved no hits. This absence of pelagic MONTS 16S rRNA gene fragments from public databases could indicate that they might represent low-abundance phylotypes (Sogin *et al.*, 2006; Reeder & Knight, 2009). After the removal of chimeric sequences identified using MALLARD (Ashelford *et al.*, 2006) the dataset was aligned using RDPII (<http://rdp.cme.msu.edu>; Cole *et al.*, 2009) and manually corrected in the GENEIOUS 5 software (Drummond *et al.*, 2010). Several of the environmentally derived clones displayed a maximum of nine nucleotide differences over a fragment length of 403 nt compared with all published symbiont sequences – for example clone BeLOW-5 (HQ141157), 98.6% identical to the *Rmed*-, 98.6% to the *Rcay*-, and 97.8% to the *Rbel*-symbiont, but only 97.3% identical to uncultured bacteria outside the MONTS cluster (DQ256693 from the Great Barrier Reef) and 95% identical to cultured *Halochromatium* sp. bacteria (AJ401219). Alignment analysis shows that – within the obtained environmental sequences – at least six of all nucleotide changes can be identified as single nucleotide polymorphisms (10 sequences minimum alignment coverage, 0.25 minimum variant frequency). These results clearly indicate a hitherto hidden diversity among members of the MONTS cluster, for which PCR and sequencing errors cannot solely account for. To analyze the phylogenetic position of the environmental sequences, we used maximum likelihood- (PHYML at the phylogeny.fr web service; Guindon & Gascuel, 2003; Dereeper *et al.*, 2008) and Bayesian inference-based (MRBAYES; Ronquist & Huelsenbeck, 2003) algorithms. The GTR+I+G model was used in both analyses and *Ectothiorhodospira variabilis* (AM943121) and *Alkalilimnicola ehrlichii* (AF406554) served as outgroup sequences. Node stability was evaluated using posterior probabilities (pp – Bayesian inference) and aLRT (maximum likelihood; Anisimova & Gascuel, 2006; Guindon *et al.*, 2010) for two datasets – one consisting only of sequences longer than 1000 nt and one including 400–1000 nt-long sequences. The addition of these short sequences did not alter the topologies of the trees, and therefore we only considered phylogenetic analyses including the short sequences. Our tree reconstruction (Fig. 1, Fig. S1 and Table S1) shows that: (1) 16S rRNA gene sequences retrieved from the public databases displaying $\geq 95\%$ identity to those of MONTS members are from metazoan-associated bacteria, sediment samples (of marine or freshwater origin) or bacterial mats; none of the sequences

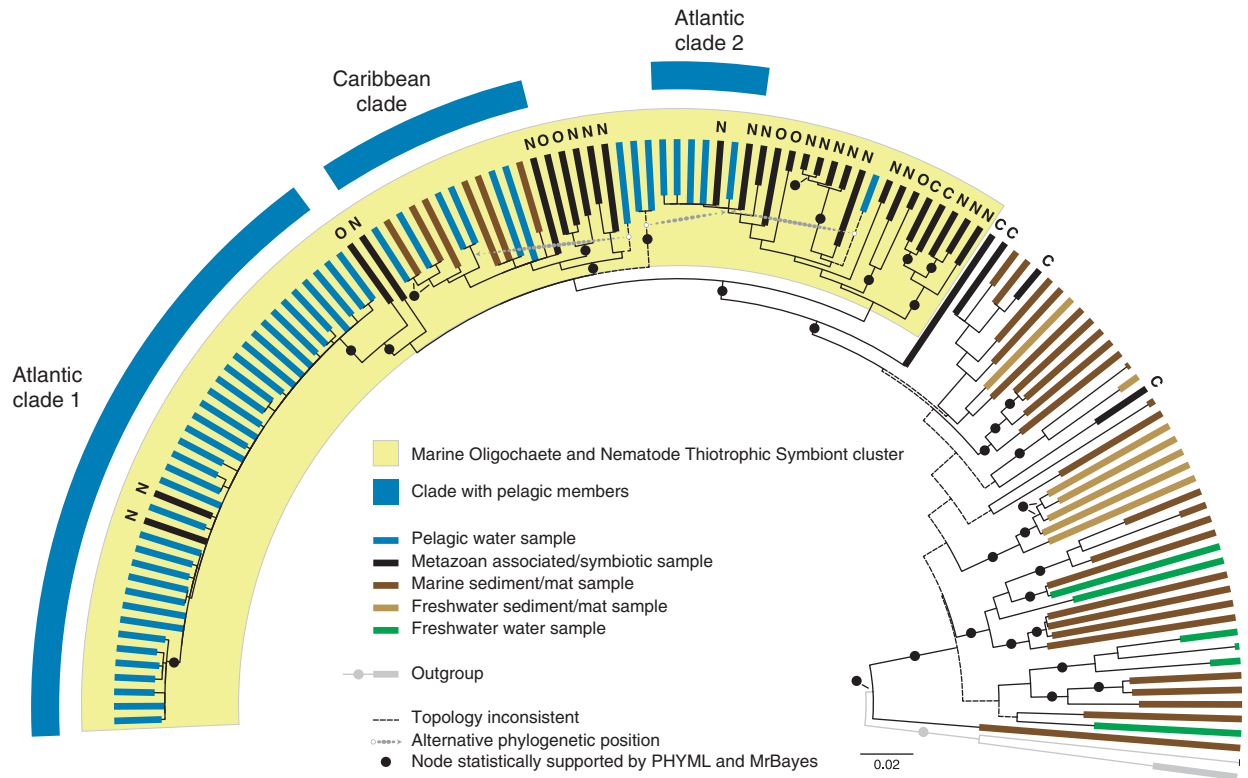


Fig. 1. 16S rRNA gene-based phylogenetic reconstruction of the MONTs cluster showing the position of the clones obtained from offshore water samples. The tree shown here is based on the most likely *PHYML* tree (GTR+I+G model of substitution). Two clades with pelagic members present in the *PHYML* analysis are absent in the *MRBAYES* trees. Their alternative positions according to *MRBAYES* analysis are indicated by dotted arrows. Clades with pelagic members supported by both algorithms are highlighted with dark blue bars. Filled circles indicate the nodes statistically supported in both *PHYML* and *MRBAYES* analysis (aLRT \geq 0.87, pp \geq 0.9). For symbiotic bacteria, taxonomic affiliations of the metazoan hosts are indicated above the respective branches (N, nematode; O, oligochaete; and C, coral). Scale bar represents 2% estimated sequence divergence. See Fig. S1 for GenBank accession numbers.

retrieved from the databases are from marine pelagic samples. (2) All selected 16S rRNA gene fragments PCR amplified with symbiont-specific primers from offshore seawater belong to the MONTs cluster (pp 0.95, aLRT 0.9). (3) Three stable clades contain pelagic clones and symbionts, and each clade is included in one of the three MONTs major groups. The existence of three different clades of pelagic phylotypes indicates that a free-living lifestyle may be common among the MONTs members. (4) Phylotypes most closely related to *Rbel* and *Rmed* symbionts are found in both Caribbean and Mediterranean Sea, whereas phylotypes related to the *Rcay* symbionts were only found locally, in Cayman Islands seawater. We also performed FISH on offshore seawater filtrates using *Gamma-proteobacteria*-specific probes together with probes targeting members of the three pelagic clades to ensure that the amplified 16S rRNA genes originated from environmental bacteria (Fig. S2 and Table S3).

The high sequence identity between symbiotic and pelagic 16S rRNA gene fragments suggests that the latter originated either from free-living forms of the symbionts or nonsymbiotic members of the MONTs cluster. Environ-

mental transmission of thiotrophic symbionts from a pool of free-living bacteria has already been proven for the gill symbionts of the lucinid clam *Codakia orbicularis* (Gros *et al.*, 2003) and is suggested for the beard worm *Oligobrachia mashikoi* (Aida *et al.*, 2008) and the giant tubeworm *Riftia pachyptila* (Nussbaumer *et al.*, 2006). Nevertheless, putative free-living forms of these three thiotrophic symbionts have only been found in the vicinity of their hosts (Gros *et al.*, 2003; Aida *et al.*, 2008; Harmer *et al.*, 2008). The lack of evidence for coevolution between the stilbonematid nematodes and their symbionts (Bayer *et al.*, 2009) and the intermingled phylogeny of oligochaete and nematode symbionts within the MONTs cluster indicate that in the course of evolution, multiple recruitment events between hosts and associated bacteria occurred. The pelagic members of the MONTs cluster might represent the pool of environmental bacteria from which symbionts may be – or may have been – recruited by the hosts. Although their close phylogenetic relationship with the symbiotic members of the MONTs cluster does not imply their ability to engage in symbiotic interactions, it suggests a predisposition to a life in association with invertebrate hosts.

Acknowledgements

This work was supported by the Austrian Science Fund (FWF) projects P17710-B12 (S.B., N.R.H., C.B.), P20394-B03 (J.A.O., H.R.G.-V.), and S10002-B17 (S.L.). Part of this work was carried out using the resources of the Computational Biology Service Unit from Cornell University, which is partially funded by Microsoft Corporation. We are very grateful to Monika Bright and Ulrich Dirks for valuable discussions, to Michael Stachowitsch for editing, and to Markus Möseneder and Marc Mußmann for technical suggestions.

Statement

Contribution 901 from the Carrie Bow Cay Laboratory, Caribbean Coral Reef Ecosystem Program, NMNH, Washington, DC.

References

- Aida M, Kanemori M, Kubota N, Matada M, Sasayama Y & Fukomari Y (2008) Distribution and population of free-living cells related to endosymbiont A harbored in *Oligobrachia mashikoi* (a siboglinid polychaete) inhabiting Tsukumo bay. *Microbes Environ* **23**: 81–88.
- Altschul SF, Gish W, Miller W, Myers EW & Lipman DJ (1990) Basic local alignment search tool. *J Mol Biol* **215**: 403–410.
- Anisimova M & Gascuel O (2006) Approximate likelihood-ratio test for branches: a fast, accurate, and powerful alternative. *Syst Biol* **55**: 539–552.
- Ashelford KE, Chuzhanova NA, Fry JC, Jones AJ & Weightman AJ (2006) New screening software shows that most recent large 16S rRNA gene clone libraries contain chimeras. *Appl Environ Microb* **72**: 5734–5741.
- Bayer C, Heindl NR, Rinke C, Lückner S, Ott JA & Bulgheresi S (2009) Molecular characterization of the symbionts associated with marine nematodes of the genus *Robbea*. *Environ Microbiol Rep* **1**: 136–144.
- Bulgheresi S, Gruber-Vodicka HR, Heindl NR, Dirks U, Kostadinova M, Breiteneder H & Ott JA (2011) Sequence variability of the pattern recognition receptor Mermaid mediates specificity of marine nematode symbioses. *ISME J*. <http://dx.doi.org/10.1038/ismej.2010.198>.
- Cole JR, Wang Q, Cardenas E *et al.* (2009) The Ribosomal Database Project: improved alignments and new tools for rRNA analysis. *Nucleic Acids Res* **37**: D141–D145.
- Dereeper A, Guignon V, Blanc G *et al.* (2008) Phylogeny.fr: robust phylogenetic analysis for the non-specialist. *Nucleic Acids Res* **36**: W465–W469.
- Drummond A, Ashton B, Buxton S *et al.* (2010) Geneious v5.1. <http://www.geneious.com/>.
- Dubilier N, Mulders C, Ferdelman T *et al.* (2001) Endosymbiotic sulphate-reducing and sulphide-oxidizing bacteria in an oligochaete worm. *Nature* **411**: 298–302.
- Dubilier N, Bergin C & Lott C (2008) Symbiotic diversity in marine animals: the art of harnessing chemosynthesis. *Nat Rev Microbiol* **6**: 725–740.
- Giere O & Langheld C (1987) Structural organisation, transfer and biological fate of endosymbiotic bacteria in gutless oligochaetes. *Mar Biol* **93**: 641–650.
- Gros O, Liberge M, Heddi A, Khatchadourian C & Felbeck H (2003) Detection of the free-living forms of sulfide-oxidizing gill endosymbionts in the lucinid habitat (*Thalassia testudinum* environment). *Appl Environ Microb* **69**: 6264–6267.
- Guindon S & Gascuel O (2003) A simple, fast, and accurate algorithm to estimate large phylogenies by maximum likelihood. *Syst Biol* **52**: 696–704.
- Guindon S, Dufayard J-F, Lefort V, Anisimova M, Hordijk W & Gascuel O (2010) New algorithms and methods to estimate maximum-likelihood phylogenies: assessing the performance of PhyML 3.0. *Syst Biol* **59**: 307–321.
- Harmer TL, Rotjan RD, Nussbaumer AD, Bright M, Ng AW, DeChaine EG & Cavanaugh CM (2008) Free-living tube worm endosymbionts found at deep-sea vents. *Appl Environ Microb* **74**: 3895–3898.
- Juretschko S, Timmermann G, Schmid M, Schleifer KH, Pommerening-Roser A, Koops HP & Wagner M (1998) Combined molecular and conventional analyses of nitrifying bacterium diversity in activated sludge: *Nitrosococcus mobilis* and *Nitrospira*-like bacteria as dominant populations. *Appl Environ Microb* **64**: 3042–3051.
- Kane MD, Poulsen LK & Stahl DA (1993) Monitoring the enrichment and isolation of sulfate-reducing bacteria by using oligonucleotide hybridization probes designed from environmentally derived 16S rRNA sequences. *Appl Environ Microb* **59**: 682–686.
- Loy A, Arnold R, Tischler P, Rattei T, Wagner M & Horn M (2008) probeCheck – a central resource for evaluating oligonucleotide probe coverage and specificity. *Environ Microbiol* **10**: 2894–2898.
- Ludwig W, Strunk O, Westram R *et al.* (2004) ARB: a software environment for sequence data. *Nucleic Acids Res* **32**: 1363–1371.
- Musat N, Giere O, Gieseke A, Thiermann F, Amann R & Dubilier N (2007) Molecular and morphological characterization of the association between bacterial endosymbionts and the marine nematode *Astomonema* sp. from the Bahamas. *Environ Microbiol* **9**: 1345–1353.
- Nussbaumer AD, Fisher CR & Bright M (2006) Horizontal endosymbiont transmission in hydrothermal vent tubeworms. *Nature* **441**: 345–348.
- Ott JA, Bright M & Bulgheresi S (2004a) Symbioses between marine nematodes and sulfur-oxidizing chemoautotrophic bacteria. *Symbiosis* **36**: 103–126.
- Ott JA, Bright M & Bulgheresi S (2004b) Marine microbial thiotrophic ectosymbioses. *Oceanogr Mar Biol* **42**: 95–118.
- Reeder J & Knight R (2009) The ‘rare biosphere’: a reality check. *Nat Methods* **6**: 636–637.

- Ronquist F & Huelsenbeck JP (2003) MrBayes 3: Bayesian phylogenetic inference under mixed models. *Bioinformatics* **19**: 1572–1574.
- Sogin ML, Morrison HG, Huber JA *et al.* (2006) Microbial diversity in the deep sea and the underexplored 'rare biosphere'. *P Natl Acad Sci USA* **103**: 12115–12120.
- Sunagawa S, Woodley CM & Medina M (2010) Threatened corals provide underexplored microbial habitats. *PLoS One* **5**: e9554.
- Woyke T, Teeling H, Ivanova NN *et al.* (2006) Symbiosis insights through metagenomic analysis of a microbial consortium. *Nature* **443**: 950–955.

Supporting Information

Additional Supporting Information may be found in the online version of this article:

Appendix S1. Methods.

Fig. S1. Detailed 16S rRNA gene-based phylogenetic reconstruction showing the position of the clones from offshore

seawater samples in the MONTS cluster and highlighting the specificity ranges of the employed FISH probes.

Fig. S2. FISH photographs of pelagic bacteria triple stained with DAPI (A, E, and I), a *Gammaproteobacteria*-specific probe (B, F, and J, green), and a *Rmed* symbiont-specific (C, red) or a *Rcay/Inanidrilus leukodermatus* symbiont-specific (G, red) or a *Rbel* symbiont-specific probe (K, red).

Table S1. Presence/absence (+/–) of pelagic members of the three MONTS clades in the environmental samples.

Table S2. Sequences, annealing temperatures and expected product sizes of MONTS member-specific primer sets.

Table S3. FISH probes description.

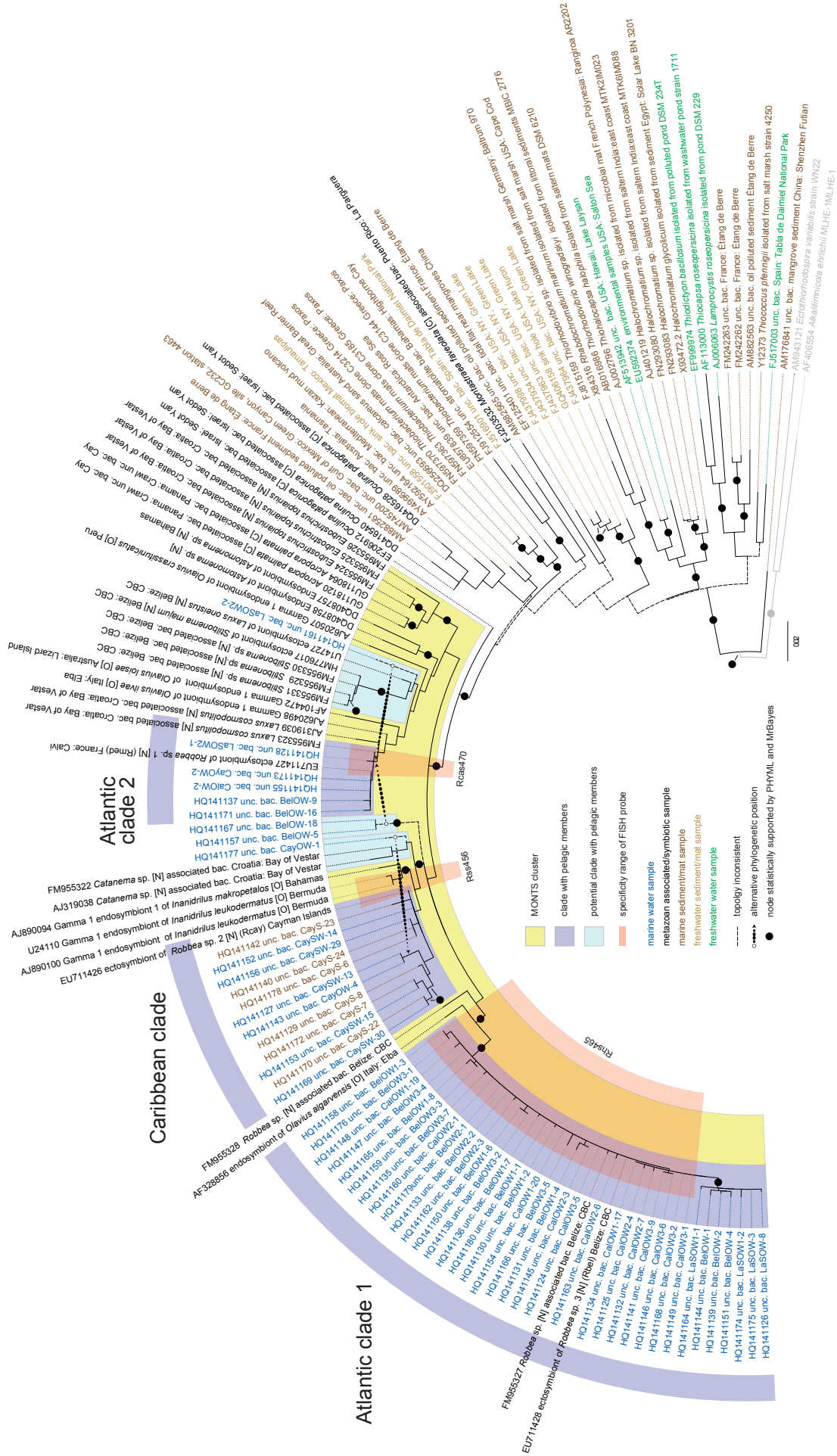
Please note: Wiley-Blackwell is not responsible for the content or functionality of any supporting materials supplied by the authors. Any queries (other than missing material) should be directed to the corresponding author for the article.

Supplementary Materials

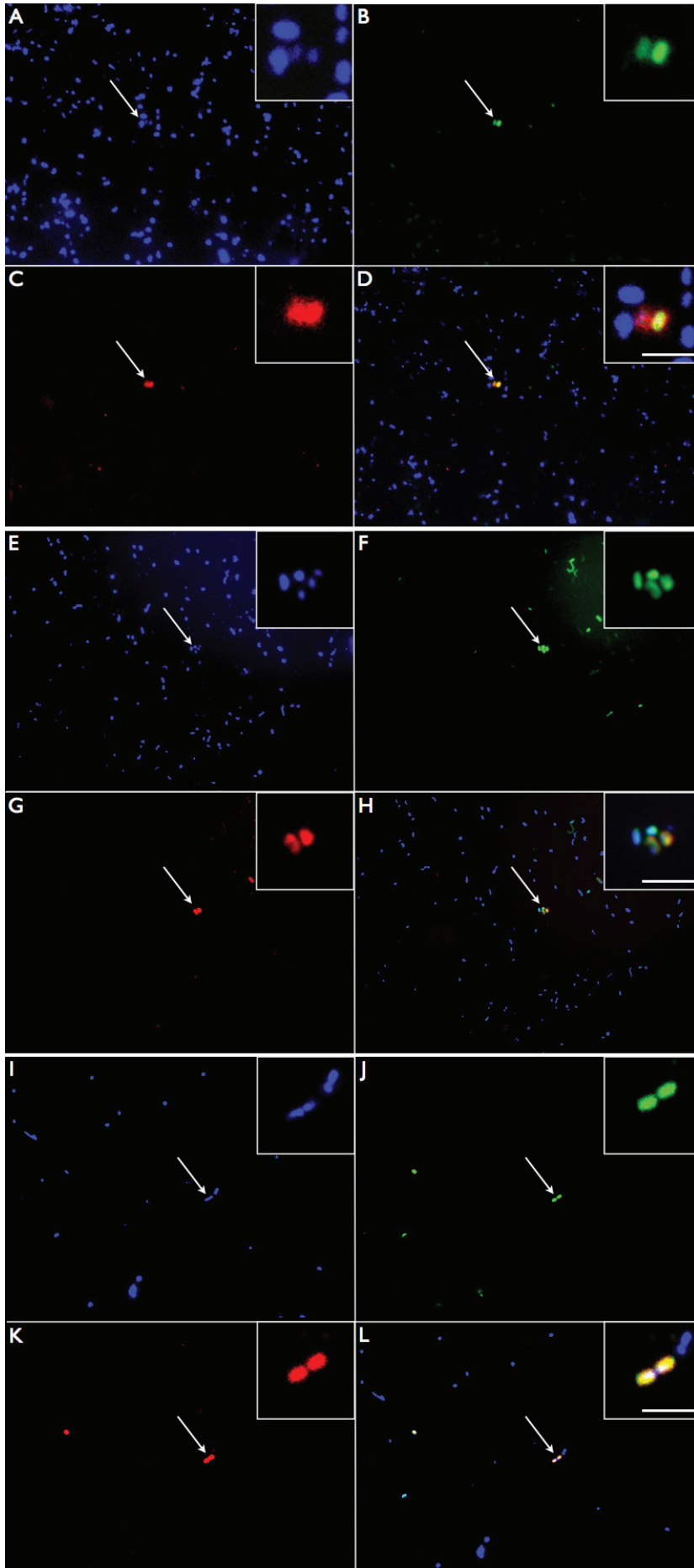
Supplementary Methods

FISH

We performed FISH on surface seawater collected offshore from La Spezia, Mediterranean Sea (LaSOW), a seawater sample which yielded 16S rRNA-gene fragments belonging to both Atlantic clades (see Supplementary Table 1 for details). After overnight transport in a cooler, samples were fixed overnight in 1.6% formaldehyde at 4°C. 94 ml-aliquots were then vacuum filtered ($p < 130$ mbar) through 0.22 μm pore size 47 mm GTTP filters (Millipore, USA). Filters were subsequently washed with PBS, air dried on a cellulose sheet and stored airtight at 4°C in 6 cm sterile Petri dishes. Fixed bacteria were transferred from the filters onto the wells of epoxy resin masked slides (Marienfeld, Germany) after these were moistened with 0.1% agarose. 1 cm^2 pieces were cut from the filters and placed face down onto the wells. Slides were then vacuum-dried for approximately 10 min in a desiccator before peeling off the pieces (Hicks, *et al.*, 1992). Transferred bacteria were hybridized with the fluorescein-labeled probe Gam42a (Manz, *et al.*, 1992) and with the Cy3-labelled probes Rca470, Rss456 and Rhs465, specifically targeting the 16S rRNA-genes of the symbionts of *Rmed*, *Rcay* and *Rbel*, respectively. Hybridization and washing were performed according to Manz et al. (Manz, *et al.*, 1992) and under hybridization conditions described in (Bayer, *et al.*, 2009). See Supplementary Table 3 for FISH probe details. Specimens were mounted in DAPI Vectashield (Vector Labs, USA) and examined under a Zeiss AX10 epifluorescence microscope.



Supplementary Figure 1: Detailed 16S rRNA-gene based phylogenetic reconstruction showing the position of the clones from offshore seawater samples in the MONTS cluster and highlighting the specificity ranges of the employed FISH probes. The tree shown here is based on the most likely PHYML tree (GTR+I+G model of substitution). Two clades with pelagic members present in the PHYML analysis are absent in the MrBayes trees. Their alternative positions are indicated by dotted arrows. Clades with pelagic members supported by both algorithms are highlighted with purple arcs. Filled circles indicate nodes statistically supported in PHYML and MrBayes analysis (aRLT \geq 0.87, pp \geq 0.9). The outgroup is indicated in gray. Scale bar represents 2% estimated sequence divergence. GenBank accession numbers precede names of bacteria.



Supplementary Figure 2: FISH photographs of pelagic bacteria triple stained with DAPI (A, E and I), a *Gammaproteobacteria*-specific probe (B, F, and J, green), and a *Rmed* symbiont-specific (C, red) or a *Rgay/Inanidrilus leukodermatus* symbiont-specific (G, red) or a *Rbel* symbiont-specific probe (K, red). D, H and L are overlays of A-C, E-G, and I-K, respectively. Inserts display high magnification photographs of the triple stained bacteria indicated by arrows. Scale bars correspond to 2 μm .

Supplementary Table 1: Presence/absence (+/–) of pelagic members of the three MONTS clades in the environmental samples. Sequence identities between environmental 16S rRNA-gene fragments and those of the respective *Robbea* symbionts are given in parentheses. Atlantic clade 1 members are compared to the *Rbel* ectosymbiont (EU711428), Atlantic clade 2 members to the *Rmed* ectosymbiont (EU711427) and Caribbean clade members to the *Rcay* ectosymbiont (EU711426). n.d.: not determined.

		Mediterranean Sea		Caribbean Sea	
		Calvi (France) Offshore Water (CalOW)	La Spezia (Italy) Offshore Water (LaSOW)	Carrie Bow Cay (Belize) Offshore Water (BelOW)	Little Cayman (Cayman Islands) Offshore Water (CayOW)
	water sample				
	geographical coordinates	42°35'55N 08°43'30W	44°02'32N 09°49'14W	16°48'15N 88°04'73W	19°22'18N 80°04'11W
	approx. water depth at collection site	80 m	30 m	25 m	300 m
	collection date	Aug. 2008	Aug. 2008	Nov. 2007	Oct. 2006
Atlantic clade 1	presence/absence (sequence identity)	+ (99.1-100%)	+ (99.2-99.5%)	+ (99.2-100%)	–
	# of clones analyzed	12	4	19	–
Atlantic clade 2	presence/absence (sequence identity)	+ (100%)	+ (99.1-99.7%)	+ (98.5-99.8%)	+ (100%)
	# of clones analyzed	1	7	4	1
Caribbean clade	presence/absence (sequence identity)	n.d.	–	–	+ (98.1-99.2%)
	# of clones analyzed	n.d.	–	–	2

24 **Supplementary Table 2:** Sequences, annealing temperatures and expected product sizes of MONTS member-specific primer sets.

Specificity	Primer set	T _A (°C)	<i>E. coli</i> position ^c	Expected product size (nt)
<i>Rmed</i> symbiont 16S rRNA-gene	Rcas627F: 5' -GGAATGGCATTGATACTGTTC-3'	53	627-648	403
	+ Rcas1008R: 5' -GGCACCTGCCTAICTCTAGAC-3'		1008 - 1028	
<i>Rcaj</i> symbiont 16S rRNA-gene	Rss457F: 5' - CTTGGGTTAATAGCTCAGGGT -3'	60	457-477	1004
	+ Rss1439R: 5' - GCTCCCCGAAAGGCACCTATCT-3'		1018-1037	
<i>Rbel</i> symbiont 16S rRNA-gene	Rhs439F: 5' -TCAGTCGGGAAGAAAAGGTCTC-3'	50	439-459	581
	+ Rhs999R: 5' -CCATCTCTGGAAAAGTTCACAG-3'		999-1019	
	Rhs439F: 5' -TCAGTCGGGAAGAAAAGGTCTC-3'		439-459	
	+ 1492R: ^a 5' -GGYTACCTTGTTACGACTT-3'		1492-1510	
<i>Rbel</i> symbiont 16S rRNA-gene	616V: ^b 5' -AGAGTTTGATYMTGGGCTC -3'	53	8-26	1012
	+ Rhs999R: 5' -CCATCTCTGGAAAAGTTCACAG-3'		999-1019	

^a Kane et al., 1993

^b Juretschko et al., 1998

^c Brosius et al., 1978

Supplementary Table 3: FISH probes description.

Probe	Standard probe name ^a	Specificity	Sequence/ 5' -modification	target rRNA	Position ^{b,c}	Formamide percentage/ incubation time (h)/ probe concentration ng/ μ l ⁻¹	Reference
GAM42a	L-C-gProt-1027-a-A-17	gamma-proteobacteria	5' -GCC TTC CCA CAT CGT TT-3' / Cy5	23S	1027-1043	35%/1.5-0.n./3-9	Manz et al., 1992
Rcas471	S*-Robs1-0471-a-A-21	<i>Rmedsymbiont</i>	5' -TCG GTA ACG TCA AGA CCC TGG -3' / Cy3	16S	471-491	35%/1.5/2-3	Bayer et al., 2009
Rss457	S*-Robs2-0457-a-A-21	<i>Rcay</i> symbiont, <i>Inanidrilus</i> <i>leukodermatius</i> endosymbiont 1 (AJ890100)	5' -ACC CTG AGC TAT TAA CCC AAG -3' / Cy3	16S	457-477	35%/0.n./2-3	Bayer et al., 2009
Rhs466	S*-Robs3-0466-a-A-21	<i>Rbel</i> symbiont	5' -AAC GTC AGG ATC CCG AGC TAT -3' / Cy3	16S	466-486	35%/3/2-3	Bayer et al., 2009

^aaccording to Alm et al., 1996

^b16SrRNA position, *E. coli* numbering according to Brosius et al., 1978

^c23SrRNA position, *E. coli* numbering according to Brosius et al., 1981

o.n.: overnight

Supplementary References

- Alm EW, Oerther DB, Larsen N, Stahl DA & Raskin L (1996) The oligonucleotide probe database. *Appl. Environ. Microbiol.* 62: 3557-3559.
- Bayer C, Heindl NR, Rinke C, Lückner S, Ott JA & Bulgheresi S (2009) Molecular characterization of the symbionts associated with marine nematodes of the genus *Robbea*. *Environ. Microbiol. Reports* 1: 136-144.
- Brosius J, Palmer ML, Kennedy PJ & Noller HF (1978) Complete nucleotide sequence of a 16S ribosomal RNA gene from *Escherichia coli*. *Proc. Natl. Acad. Sci. U. S. A.* 75: 4801-4805.
- Brosius J, Dull TJ, Sleeter DD & Noller HF (1981) Gene organization and primary structure of a ribosomal RNA operon from *Escherichia coli*. *J. Mol. Biol.* 148: 107-127.
- Hicks RE, Amann RI & Stahl DA (1992) Dual staining of natural bacterioplankton with 4',6-diamidino-2-phenylindole and fluorescent oligonucleotide probes targeting kingdom-level 16S rRNA sequences. *Appl. Environ. Microbiol.* 58: 2158-2163.
- Juretschko S, Timmermann G, Schmid M, Schleifer KH, Pommerening-Roser A, Koops HP & Wagner M (1998) Combined molecular and conventional analyses of nitrifying bacterium diversity in activated sludge: *Nitrosococcus mobilis* and *Nitrospira*-like bacteria as dominant populations. *Appl. Environ. Microbiol.* 64: 3042-3051.
- Kane MD, Poulsen LK & Stahl DA (1993) Monitoring the enrichment and isolation of sulfate-reducing bacteria by using oligonucleotide hybridization probes designed from environmentally derived 16S rRNA sequences. *Appl. Environ. Microbiol.* 59: 682-686.
- Manz W, Amann R, Ludwig W, Wagner M & Schleifer K-H (1992) Phylogenetic oligodeoxynucleotide probes for the major subclasses of proteobacteria: Problems and solutions. *Syst. Appl. Microbiol.* 15: 593-600.

III. Sequence variability of the pattern recognition receptor Mermaid mediates specificity of marine nematode symbioses

Authors: Silvia Bulgheresi*, Harald R. Gruber-Vodicka*, Niels R. Heindl, Ulrich Dirks, Maria Kostadinova, Heimo Breiteneder and Joerg A. Ott

* These authors contributed equally to this work

Publication status: published 2011 in *The ISME Journal* Volume 5, pages 986–998

Personal contributions of Harald Gruber-Vodicka

- a. designed parts of the study
- b. collected material on a field trip to Carrie Bow Caye
- c. sequenced symbiont 16S and host 18S rRNA genes
- d. performed alignments, structural analyses and 3-D models of lectins
- e. performed all phylogenetic analyses and statistical analyses
- f. wrote parts of the manuscript and edited and approved the manuscript



ORIGINAL ARTICLE

Sequence variability of the pattern recognition receptor Mermaid mediates specificity of marine nematode symbioses

Silvia Bulgheresi^{1,4}, Harald R Gruber-Vodicka^{2,4}, Niels R Heindl¹, Ulrich Dirks², Maria Kostadinova³, Heimo Breiteneder³ and Joerg A Ott²

¹Department of Genetics in Ecology, University of Vienna, Althanstrasse 14, 1090 Vienna, Austria;

²Department of Marine Biology, University of Vienna, Althanstrasse 14, 1090 Vienna, Austria and ³Center for Physiology, Pathophysiology and Immunology, Medical University of Vienna, Währinger Gürtel 18-20, 1090 Vienna, Austria

Selection of a specific microbial partner by the host is an all-important process. It guarantees the persistence of highly specific symbioses throughout host generations. The cuticle of the marine nematode *Laxus oneistus* is covered by a single phylotype of sulfur-oxidizing bacteria. They are embedded in a layer of host-secreted mucus containing the mannose-binding protein Mermaid. This Ca²⁺-dependent lectin mediates symbiont aggregation and attachment to the nematode. Here, we show that *Stilbonema majum*—a symbiotic nematode co-occurring with *L. oneistus* in shallow water sediment—is covered by bacteria phylogenetically distinct to those covering *L. oneistus*. Mermaid cDNA analysis revealed extensive protein sequence variability in both the nematode species. We expressed three recombinant Mermaid isoforms, which based on the structural predictions display the most different carbohydrate recognition domains (CRDs). We show that the three CRDs (DNT, DDA and GDA types) possess different affinities for *L. oneistus* and *S. majum* symbionts. In particular, the GDA type, exclusively expressed by *S. majum*, displays highest agglutination activity towards its symbionts and lowest towards its *L. oneistus* symbionts. Moreover, incubation of *L. oneistus* in the GDA type does not result in complete symbiont detachment, whereas incubation in the other types does. This indicates that the presence of particular Mermaid isoforms on the nematode surface has a role in the attachment of specific symbionts. This is the first report of the functional role of sequence variability in a microbe-associated molecular patterns receptor in a beneficial association.

The ISME Journal (2011) 5, 986–998; doi:10.1038/ismej.2010.198; published online 13 January 2011

Subject Category: microbe–microbe and microbe–host interactions

Keywords: symbiosis; C-type lectin; sulfur-oxidizing bacteria; nematode; microbe-associated molecular pattern receptor; marine sediment

Introduction

A high degree of specificity has been experimentally demonstrated for a number of microbial symbioses. The degree of taxonomic specificity (that is, genus, species and strain) varies among the associations, and certain host species within one genus may display stricter symbiont selectivity than others (Chaston and Goodrich-Blair, 2010). In the case of thiotrophic marine nematodes—Stilbonematinae, Chromadoria (Ott *et al.*, 2004a,b)—the bacteria

associated with *Laxus oneistus* (Polz *et al.*, 1994), *Eubostrichus diana* (Polz *et al.*, 1999) and three *Robbea* species (Bayer *et al.*, 2009) have been molecularly characterized so far. Except for *E. diana*, all these stilbonematids are covered by a microbial coat composed of a single phylotype of Gammaproteobacteria. Symbionts not only appear to be a major component of the diet of the stilbonematids, but may also protect their hosts against sulfide poisoning (Ott *et al.*, 1991; Hentschel *et al.*, 1999). Although in this small sub-family of nematodes, a high degree of specificity seems to be the rule, we still know little about the molecular mechanisms underlying the selection of cooperative microbes and the exclusion of potential cheating or non-performing ones. As pointed out by Chaston and Goodrich-Blair (2010), specificity may be mediated either by (1) minor variations in molecules conserved among phylogenetically related symbiotic

Correspondence: S Bulgheresi, Department of Marine Biology, University of Vienna, Althanstrasse 14, Vienna 1090, Austria.
E-mail: silvia.bulgheresi@univie.ac.at

Contribution 894 from the Carrie Bow Cay Laboratory, Caribbean Coral Reef Ecosystem Program, NMNH, Washington, DC.

⁴These authors contributed equally to this work.

Received 26 July 2010; revised 18 November 2010; accepted 21 November 2010; published online 13 January 2011

partners, or (2) by the presence or absence of genetic determinants of host-range specificity in a given symbiotic partner. A good molecular candidate for mediating stilbonematid symbiosis specificity is Mermaid (Bulgheresi *et al.*, 2006), a secreted Ca^{2+} -dependent sugar-binding protein (C-type lectin). Lectins are proteins that have at least one non-catalytic domain that reversibly and non-enzymatically binds specific mono- or oligosaccharides (carbohydrate recognition domain (CRD)); (Peumans and Van Damme, 1995; De Hoff *et al.*, 2009). They are found in cells, membranes and secretomes of plants, animals and bacteria. The degree of sequence variation the lectins tolerate in their ligand-binding pocket is remarkable and comparable to that of immunoglobulins (McMahon *et al.*, 2005). This sequence variation mirrors carbohydrate variability, which itself arises by differences in (1) carbon backbone length of the monomer, (2) anomericity, (3) side-group orientation, (4) substitution and (5) branching. As a result, cells exposing a characteristic carbohydrate repertoire can be recognized by specific lectins. Like most lectins, Mermaid appears to be multivalent and may therefore clump cells together. The mature protein is composed of one CRD, structurally and functionally similar to the human dendritic cell-specific immunoreceptor dendritic cell-specific ICAM-3 grabbing non-integrin; (DC-SIGN) (Bulgheresi *et al.*, 2006; Zhang *et al.*, 2006, 2008; Nabatov *et al.*, 2008; Mittal *et al.*, 2009). Mermaid is expressed and secreted from subcuticular glandular sense organs (Nebelsick *et al.*, 1992) onto the cuticle of *L. oneistus*. Only the posterior glandular sense organs underlying the bacterial coat secrete this lectin, whereas it is absent from the anterior part of cuticle to which no symbionts are attached. Moreover, a recombinant form of Mermaid aggregated the symbionts and competed with native Mermaid for symbiont attachment (Bulgheresi *et al.*, 2006). All these data point to a pivotal role of Mermaid in *L. oneistus*-symbiont attachment. As for the bacterial symbiont, it is predicted to utilize surface-exposed mannose residues to bind to the host lectin (Nussbaumer *et al.*, 2004), consistently with the ability of recombinant Mermaid to bind mannotriose in glycan specificity assays (Nabatov *et al.*, 2008). Moreover, recombinant Mermaid may bind to the core lipopolysaccharide (LPS) of a rough *Escherichia coli* strain (Zhang *et al.*, 2006), and inhibits the interaction of *Yersinia pestis* core LPS with dendritic cell-specific immunoreceptor (Zhang *et al.*, 2008).

Mermaid genes are also expressed by *Stilbonema majum*, another stilbonematid nematode, thriving in the same microhabitat as *L. oneistus*. Whereas the latter carries a monolayer of $2.1 \times 0.6 \mu\text{m}$ rods, the former bears up to 10 layers of $1.3 \times 0.6 \mu\text{m}$ oval bacteria. Because of the different symbiont morphology and coat architecture, the two co-occurring nematodes were long hypothesized to carry distinct symbiont phylotypes. Moreover, they were found to

express two and three Mermaid isoforms, respectively. These differed at three amino acid positions (105, 108 and 109). On the basis of a three-dimensional model of Mermaid CRD, these substitutions were speculated not to dramatically affect the protein conformation (Bulgheresi *et al.*, 2006).

The hypothesis behind the present work is that minor variations in the protein sequence of their CRD might mediate attachment of specific symbionts to the nematode cuticle. We first assessed the phylogenetic position of the *S. majum* symbiont to confirm that it differs from that of the *L. oneistus* symbiont. Subsequently, we assessed the degree of both *L. oneistus* and *S. majum* Mermaid sequence variability by screening Mermaid cDNA libraries obtained from each species to saturation. We then selected three Mermaid isoforms which, based on structural predictions, were expected to bear the most different CRDs. Finally, we expressed recombinant forms thereof and tested whether their binding activity towards different symbionts would significantly differ.

Materials and methods

Nematode collection

L. oneistus and *S. majum* were collected in March 2009 in ~ 1 m depth from a shallow water back-reef sandbar, off Carrie Bow Cay, Belize ($16^{\circ}48'11 \text{ N}$, $88^{\circ}04'55 \text{ W}$). The worms were extracted from the sand by shaking it in seawater and pouring the supernatant through a $63\text{-}\mu\text{m}$ -pore-size mesh screen. Single individuals were then picked by hand under a dissecting microscope. For DNA extraction and fluorescence *in situ* hybridization (FISH), worms were fixed in methanol. For mRNA extraction, batches of freshly collected nematodes were flash frozen in liquid nitrogen. All samples were deep frozen for transportation and storage, except for the live *L. oneistus* nematodes used in the *in vivo* dissociation experiments. In the case of *S. majum*, their identity was confirmed by direct sequencing of an 18S rRNA gene fragment (data not shown).

Symbionts collection

Batches of 500 and 150 freshly collected *L. oneistus* and *S. majum*, respectively, were incubated for 3 min in an MgSO_4 solution, isotonic to seawater, to induce symbiont dissociation. Dissociated symbionts were collected by 2 min centrifugation at 6K r.p.m. Symbiont pellets were washed three times in filtered seawater and deep frozen for transport and storage.

DNA extraction, PCR amplification and cloning of the *S. majum* 18S rRNA gene and of the *S. majum* symbiont 16S rRNA gene

DNA was extracted from three separate *S. majum* individuals as described (Schizas *et al.*, 1997), and

2 µl of each extraction were used as PCR template. A 1720 nt-long fragment of the 18S rRNA gene was amplified for each *S. majum* worm by PCR with the general eukaryotic primers 1f (5'-CTGGTTGAT YCTGCCAGT-3') and 2023r (5'-GGTTCACCTACGG AAACC-3') (Pradillon *et al.*, 2007). Cycling conditions were as follows: 94 °C for 4 min followed by 35 cycles of 94 °C for 45 s, 49 °C for 30 s, 72 °C for 1 min and a final elongation step of 72 °C for 10 min. The PCR products obtained from the three *S. majum* individuals were purified using the MinElute PCR purification kit (Qiagen, Hilden, Germany) and directly sequenced with the PCR primers.

A 1499-nt long fragment of the 16S rRNA gene was amplified for each *S. majum* worm by PCR with bacterial primers 616 V (5'-AGAGTTTGATYMTGGC TC-3'; Juretschko *et al.*, 1998) and 1492R (5'-GGYTA CCTTGTTACGACTT-3'; Kane *et al.*, 1993). Cycling conditions were as follows: 94 °C for 5 min, followed by 35 cycles of 94 °C for 45 s, 47 °C for 45 s, 72 °C for 1 min 30 s and a final elongation step of 72 °C for 10 min. PCR products were gel purified and cloned into pCR2.1-TOPO using the TOPO TA Cloning Kit (Invitrogen Life Technologies, Darmstadt, Germany). We randomly picked and fully sequenced eight, seven and six clones from each of the three 16S rRNA gene libraries obtained from the three *S. majum* individuals. Sequences were aligned and compared with CodonCode Aligner 1.6.3 software (CodonCode Corporation, Dedham, MA, USA).

16S rRNA gene-based phylogenetic analysis

A bacterial 16S rRNA gene data set was compiled adding closely related sequences from the GenBank using BLASTN (Altschul *et al.*, 1990). The data set was aligned using MAFFT G-INS-I (Katoh *et al.*, 2005). We used Bayesian inference- (MrBayes; Ronquist and Huelsenbeck, 2003), maximum likelihood- (RAxML; Stamatakis, 2006), parsimony- and distance-based algorithms to reconstruct the phylogenetic position of the symbiont. Node stability was evaluated using posterior probabilities (Bayesian inference) and bootstrapping (all other algorithms). Sequences of *Alkalimnicola halodurans* (AJ404972) and *Nitro-coccus mobilis* (L35510) served as out-groups.

Fluorescence in situ hybridization

We designed a FISH probe (Sms444) specific to the *S. majum* ectosymbiont 16SrRNA gene (GenBank accession number HM776017) by using the ARB PROBE_DESIGN tool (arb software package Ludwig *et al.*, 2004; Table 1), and confirmed its specificity by comparing it with all available sequences in GenBank, SILVA and Greengenes using probeCheck (Loy *et al.*, 2008). The sequence most similar to Sms444, found in these databases, has a weighted mismatch of 2.6 and corresponds to a fragment of the 16S rRNA gene of the *Robbea* sp. 3 ectosymbiont (EU711428). Accordingly, an unlabeled competitor

Table 1 Probes used for FISH

Probe	Standard probe name ^a	Specificity	Sequence/5' modification	Target RNA	Position ^{b,c}	Formamide percentage/incubation time (h)/probe concentration (ng µl ⁻¹)	Reference
EUB338	S-* -BactV-0338-a-A-18	Most bacteria	5'-GCTGCCTCCCGTAGGAGT-3', fluorescein	16S	338-355	40%/3/3.6	Amann <i>et al.</i> (1990)
NON338	Not named	None	5'-ACTCTACGGGAGGAGCGAGG-3', Cy3	16S	338-355	40%/3/2.1	Wallner <i>et al.</i> (1993)
Sms444	S-* -Sms-444-a-A-20	<i>S. majum</i> ectosymbiont (HM776017)	5'-AACCCAGACCTTCTCCCG-3', Cy3	16S	444-464	40%/3/2.1	This paper
Rhs 444	S-* -Rhs-444-a-A-20	<i>Robbea</i> sp.3 ectosymbiont (EU711428)	5'-AACCCGAGACCTTCTCCCG-3', none	16S	444-464	40%/3/2.1	This paper
GAM42a	L-C-gProt-1027-a-A-17	Gammaproteobacteria	5'-GCCTTCCCACATCGTTT-3', Cy5	23S	1027-1043	40%/3/2.1	Manz <i>et al.</i> (1992)
BET42a	L-C-bProt-1027-a-A-17	Betaproteobacteria	5'-GCCTTCCCACATCGTTT-3', fluorescein	23S	1027-1043	40%/3/3.6	Manz <i>et al.</i> (1992)

Abbreviation: FISH, fluorescence in situ hybridization.

^aAccording to Alm *et al.* (1996).

^b16S rRNA position, *E. coli* numbering Brosius *et al.* (1978).

^c23S rRNA position, *E. coli* numbering Brosius *et al.* (1981).

probe (Rhs444) was designed (Eurofins MWG Operon, Ebersberg, Germany). All other probes used were fluorescently labeled on their 5' end (Thermo Fisher Scientific, Ulm, Germany). FISH was performed according to Manz *et al.*, 1992. To determine stringent hybridization conditions, a formamide series was conducted for all the probes (0%, 10%, 15%, 20%, 25%, 30%, 35%, 40%, 45%, 55% and 70%). Fixed *S. majum* nematodes were incubated at 46 °C in hybridization buffer containing the optimal formamide concentration and respective probes (0.46 M NaCl, 20 mM TrisHCl (pH 8.0) and 0.001% sodium dodecyl sulfate; refer to Table 1 for optimal incubation time, formamide percentage and probe concentrations). Hybridization was stopped by incubation in washing buffer (70 mM NaCl, 20 mM Tris:HCl (pH 8.0) and 0.125 M EDTA) for 15 min at 48 °C and subsequently in ice-cold ddH₂O for 3 sec. Nematodes were dried quickly under compressed air, mounted in DAPI Vectashield (Vector Labs, Burlingame, CA, USA) and examined using a Leica TCS-SP2 confocal laser-scanning microscope combined to an inverted DM-IRE2 microscope (Leica Microsystems, Heidelberg, Germany).

Mermaid cDNA libraries

L. oneistus and *S. majum* mRNA were extracted with the QuickPrep Micro mRNA Purification Kit (Amersham Biosciences, Freiburg, Germany) from deep-frozen batches of 500 individuals each, and cDNA was synthesized with the Ready-To-Go T-primed first-strand kit (Amersham Biosciences). Full-length Mermaid cDNA libraries of *L. oneistus* and *S. majum* were obtained using primer SB34 binding the 5'-untranslated region (5'-TTTTTTATTTCACAGCCATCGGTTTCC-3') and primer SB27 binding the 3'-untranslated region (5'-CTAACAGTCACTGACTCTCAACGAATCC-3'). Cycling conditions were as described (Bulgheresi *et al.*, 2006). Full-length Mermaid cDNA from both *L. oneistus* and *S. majum* was gel purified and cloned into pCR2.1-TOPO using the TOPO TA Cloning Kit (Invitrogen Life Technologies). We randomly picked and fully sequenced 89 *L. oneistus* and 113 *S. majum* cDNA clones.

Immunofluorescence

A custom-made rabbit polyclonal antibody was raised against a synthetic peptide corresponding to Mermaid amino acids 65–81 (Genosphere Biotechnologies, Paris, France). Antibody specificity was tested and immunostaining performed as described (Bulgheresi *et al.*, 2006). In brief, methanol-fixed *S. majum* individuals were rehydrated and washed in phosphate-buffered saline containing 0.1% Tween-20 (washing solution). Blocking was carried out for 1 h in washing solution containing 2% (wt/vol) bovine serum albumin (blocking solution). Worms were incubated overnight under gentle agitation at 4 °C in blocking solution containing

peptide antibody anti-Mermaid or rabbit preimmune serum as the negative control (1:500 dilution each). Unbound primary antibody was removed by three washing steps in washing solution and Alexa488-conjugated secondary anti-rabbit antibody (Molecular Probes, Eugene, OR, USA) was then applied at a 1:500 dilution in blocking solution for 1 h at room temperature. After three washing steps, worms were mounted in the Slow-Fade Antifade kit (Molecular Probes). Images were recorded on a laser-scanning confocal microscope (described above).

Mermaid isoforms sequence alignment and analysis

The sequences of each worm were translated, aligned and compared using the software package Geneious (Biomatters, Auckland, New Zealand; Drummond *et al.*, 2009). Only isoforms encoded by at least two clones were aligned to eliminate random sequencing errors as a source of variation. Secondary structure predictions were carried out by using the NetSurfP tool available online at <http://www.cbs.dtu.dk/services> (Petersen *et al.*, 2009). The tertiary structure was homology modeled by SWISS-MODEL (<http://swissmodel.expasy.org>; Guex and Peitsch, 1997) on the basis of the available crystal structure of the C-type lectin DC-SIGNR (deposited in the protein data bank (PDB) code 1sl6c) and then visualized with PyMOL 1.2r1 (Schrödinger, LLC, New York, NY, USA).

Mermaid isoforms expression and purification

Recombinant His-Mermaid-3 corresponds to the previously published His-Mermaid, and was expressed and purified exactly as described (Bulgheresi *et al.*, 2006). PCR fragments corresponding to amino acids 20–161 of (Sm-) Mermaid-1 and -2 were *NdeI/BamHI* cloned into pET15b (Novagen, Merck, Darmstadt, Germany). The resulting His-Mermaid-1 and -2 fusion proteins contained an N-terminal hexahistidine tag (His-tag) and were expressed in the *E. coli* strain BL21-AI (Invitrogen) according to the manufacturer's instructions. Bacterial lysates containing His-Mermaid-1, -2 and -3 were individually applied to nickel-chelated resins (1 ml HisTrap chelating HP, Amersham Biosciences, charged with 50 mM NiSO₄) in binding buffer (8 M urea, 20 mM Na₂HPO₄/NaH₂PO₄, 0.5 M NaCl, 10 mM imidazole) and were eluted with the same buffer (except for the imidazole concentration, which was increased to 0.5 M). Eluted proteins were dialysed against phosphate-buffered saline-containing decreasing urea concentrations to allow renaturation.

Agglutination assays

Bacterial pellets obtained as described above were re-suspended in filter-sterilized seawater to a final density corresponding to OD₆₀₀ = 1. His-Mermaid-1, -2 and -3 were each added to

separate 50 µl aliquots of *L. oneistus* and *S. majum* symbionts (starting with a concentration of 10 µg ml⁻¹, and using a dilution series to determine the minimum concentration sufficient to induce visible aggregation). Agglutination was carried out in 1.5 ml tubes for 3 h at room temperature. For each symbiont and each Mermaid isoform, agglutination was performed in triplicate. Agglutinated and control symbionts were mounted onto glass slides for photographic documentation. For each treatment and the control, the size of the particles appearing in three randomly photographed microscopic fields were measured using ImageJ (National Institutes of Health, Bethesda, MD, USA), and compared the particle size distribution by rank-based Kruskal–Wallis analysis of variance followed by Dunn’s test for differences among groups. $P < 0.01$ was considered to be statistically significant.

Dissociation assays

Dissociation assays were conducted as described (Bulgheresi *et al.*, 2006). In brief, nine batches of 50 *L. oneistus* individuals were collected and each batch was immediately added to a tube containing 300 µl filter-sterilized seawater. Each His-Mermaid isoform was added to three worm batches (of 50 individuals each, for a total of 150 worms per Mermaid isoform) to a make a final concentration of

10 µg ml⁻¹. Dissociation assays were carried out for 24 h at room temperature under gentle agitation. Worms were transferred to petridishes for photographic documentation after <1 h, 2 h, 5 h, 9 h, 20 h and 24 h.

Results

S. majum symbionts are phylogenetically distinct from *L. oneistus* symbionts

Direct sequencing of a 16S rRNA gene fragment of the *L. oneistus* symbiont provided a single unambiguous sequence (Polz *et al.*, 1994). Therefore, in this study we only constructed 16S rRNA gene libraries from *S. majum* individuals. Comparison of the 1,499 nt-long 16S rRNA gene sequences of randomly picked clones obtained from three individuals showed that they consistently differed at a single-nucleotide position (sequence identity among them >99.9%). Therefore, we used only one *S. majum*-derived 16S rRNA gene sequence (clone #3–5) for phylogenetic analysis (HM776017). The tree displayed in Figure 1 shows that: (1) the obtained 16S rRNA gene sequence is most closely related to three sequences (FM955329–FM955331) that originated from bacteria associated to an unknown *Stilbonema* species; (2) *S. majum* and *L. oneistus* symbionts are phylogenetically distinct (97% sequence identity) and (3) they form a highly

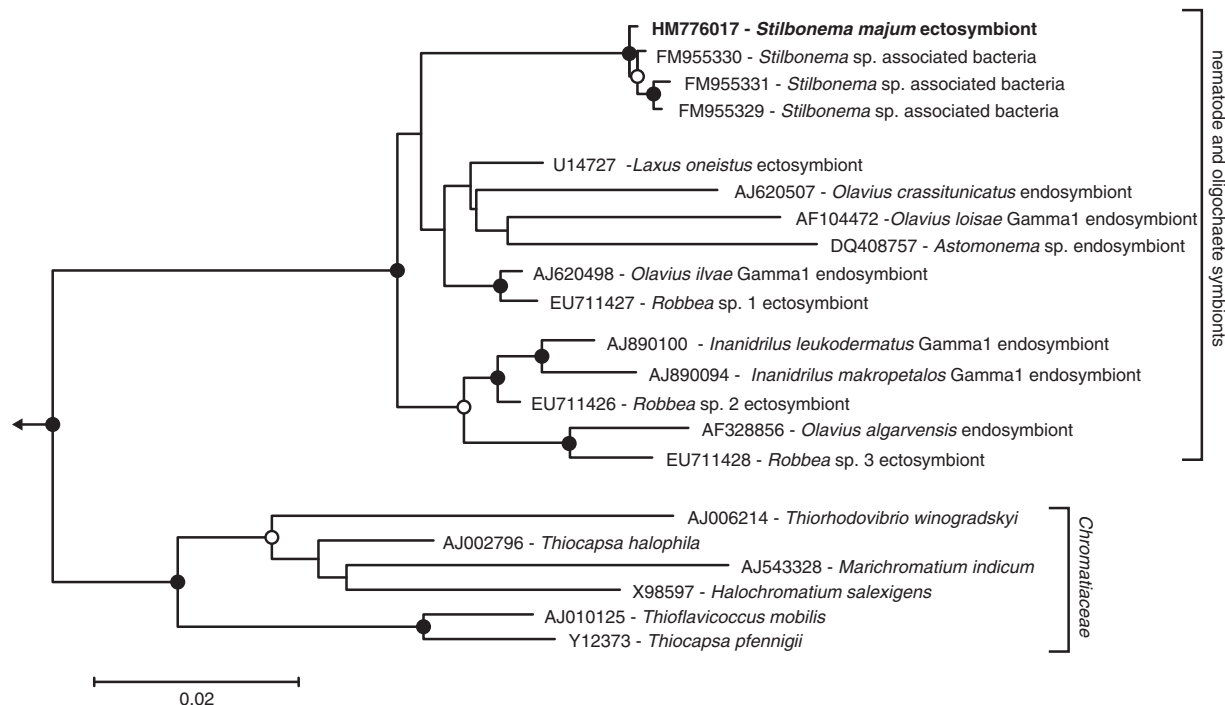


Figure 1 16S rRNA gene tree based on the most likely RAxML tree (GTR + I + G model of substitution). Filled and open circles indicate nodes supported by all four or at least two reconstruction methods, respectively (bootstrapping support ≥ 0.75 , posterior probabilities ≥ 0.9). The arrow points to the out-group. Scale bar represents 2% estimated sequence divergence. GenBank accession numbers precede the names of the bacteria.

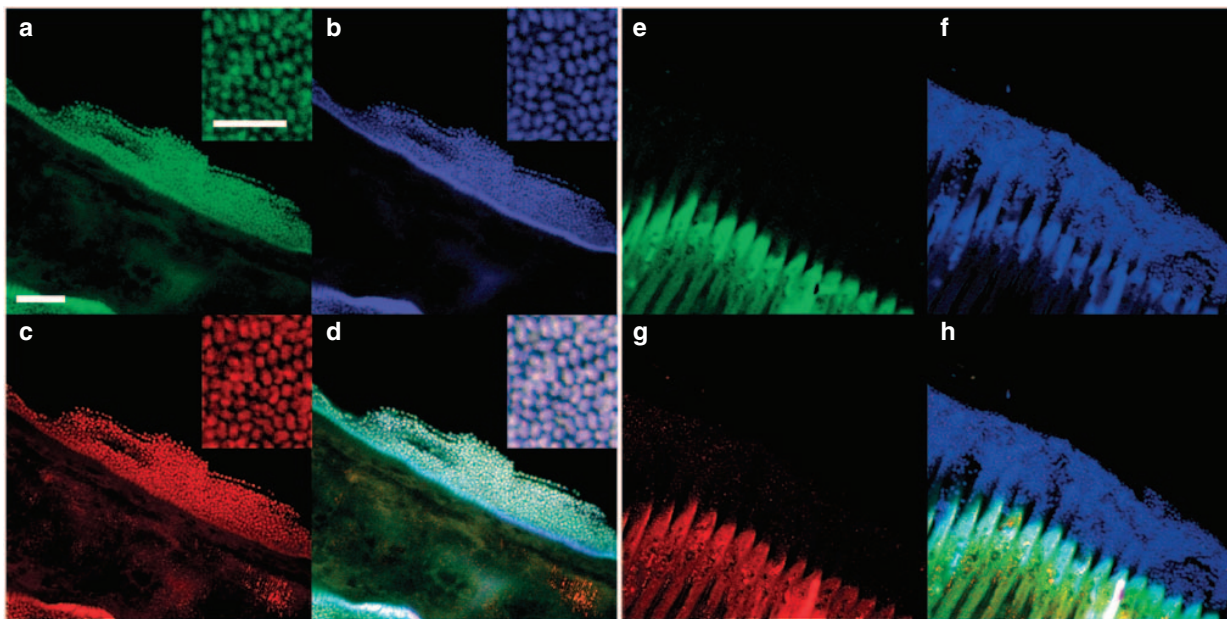


Figure 2 FISH LSCM of symbionts attached to the surface of a *S. majum* worm. Each symbiont is triple stained with specific probes targeting eubacteria (a), Gammaproteobacteria (b) and the *S. majum* symbiont (c). All symbionts are stained with a Gammaproteobacteria-specific probe (f) but not with a nonsense control probe (e) or a Betaproteobacteria-specific probe (g). Panels (d) and (h) are overlay pictures of a–c and e–g, respectively. Scale bar is 6 μm in a–h and 3 μm in the inserts.

supported phylogenetic group (all algorithms bootstrap support and posterior probability ≥ 0.99) together with the sulfur-oxidizing symbionts of other thiotrophic nematodes (*Robbea* sp. and *Astomonema* sp.) and of marine gutless oligochaetes (*Inanidrilus* and *Olavius* spp.); and (4) this nematode–oligochaete symbiont cluster is most closely related to free-living sulfur-oxidizing Gammaproteobacteria from the family *Chromatiaceae* (Dubilier *et al.*, 2008).

To confirm that the Gammaproteobacterial 16S rRNA gene sequences derived from the *S. majum* symbionts, we carried out FISH with the symbiont-specific probe Sms444 (refer to Table 1 for detailed description of all the FISH probes used in this study). The bacteria attached to the worms were triple stained by this specific probe, as well as by the bacterial probe EUB338, and by the Gammaproteobacteria-specific probe GAM42a (Figure 2). In contrast, no FISH signal was detectable with the control probe NON338 or with a Betaproteobacteria-specific probe, which differs from GAM42a at a single-nucleotide position (Figure 2). Moreover, use of the non-fluorescent competitor Rhs444 did not decrease the hybridization signal of the *S. majum* symbiont-specific probe (Supplementary Figure 1). FISH indicates that the bacteria covering *S. majum* belong to a single phylotype. This is consistent with our highly homogeneous 16S rRNA gene library, and with the scanning electron microscopy analysis showing only one bacterial morphotype covering this nematode species (Ott *et al.*, 2004a, b).

L. oneistus and *S. majum* express different repertoires of Mermaid isoforms

To assess the degree of variation in the primary structure of the lectin CRD, we screened *Mermaid* cDNA libraries obtained from *L. oneistus* and *S. majum* to saturation. In the case of *L. oneistus*, besides Lo-Mermaid-1 and -2, we discovered nine isoforms bearing novel CRDs. As for *S. majum*, we identified 10 isoforms bearing novel CRDs, besides the three already known (Sm-Mermaid-1, -2 and -3). Figure 3 displays an alignment of all unique CRDs. For each species, new isoforms were numbered according to the order in which they were discovered. At least two cDNA clones encoded for each of them, which allows us to exclude sequencing mistakes as a source of variability. The amino acid substitution sites were conserved and occurred non-randomly in the 119 amino acid long CRD (12 and 15 variable positions in *L. oneistus* and *S. majum*, respectively). None of them directly affected the conserved amino acids, including those involved in calcium- or sugar-binding (black circles and arrowheads in Figure 3). Substitutions of hydrophilic with hydrophobic amino acids and *vice versa* (defined as non-conservative and underlined in Figure 3) never occurred in the helical structures or β -sheets. This also holds true for substitutions at positions 105, 108 and 109. These, however, occurred in the long-loop region, close to a core of amino acids always involved in sugar binding (black arrowheads in Figure 3). The additional amino acids participating in ligand-binding can

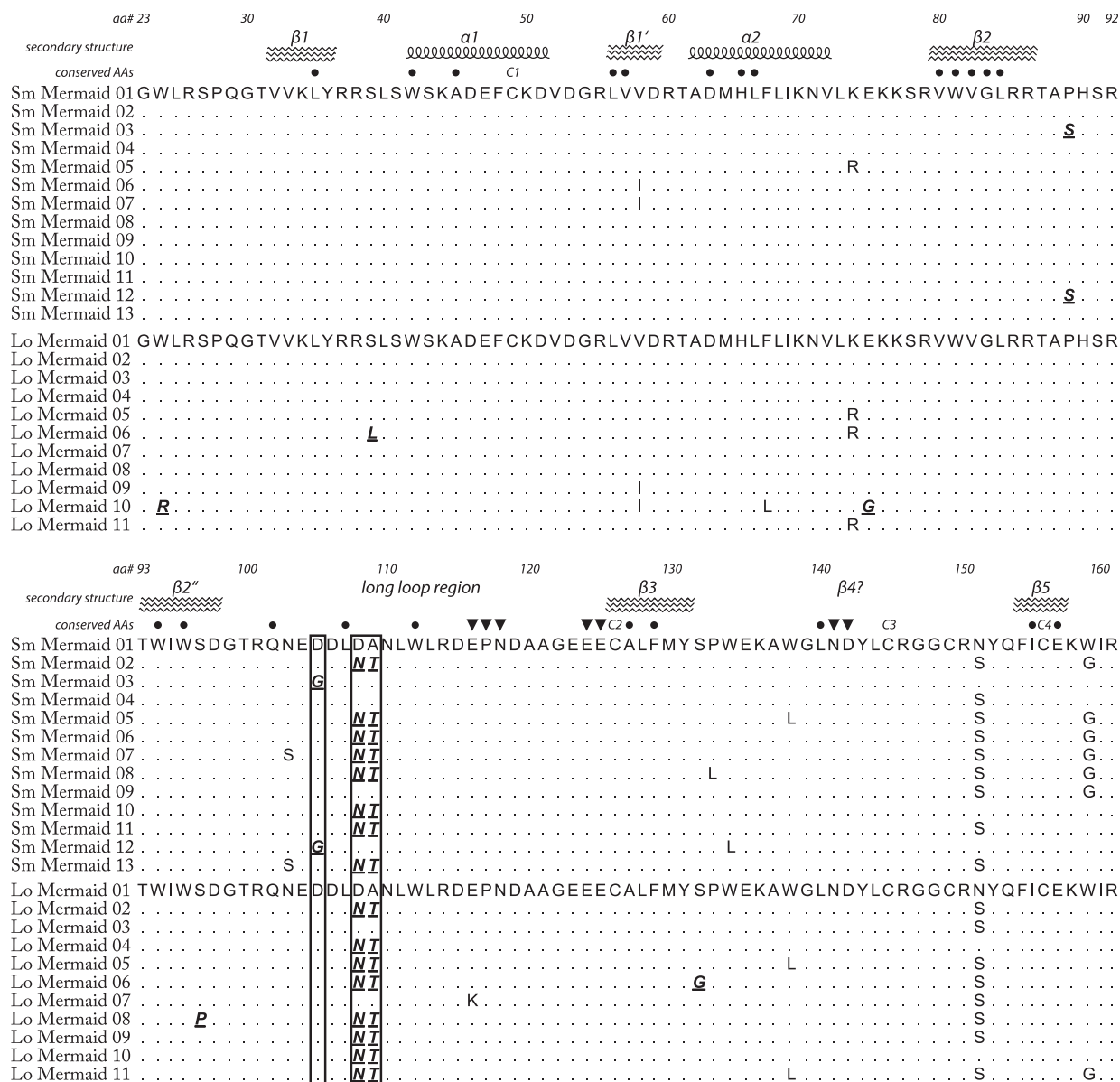


Figure 3 Protein sequence alignment of the CRDs of *L. oneistus* (Lo) and *S. majum* (Sm) Mermaid isoforms. Amino acid (aa) numbering, NetSurfP-predicted secondary structures (helices and β -sheets), and conserved aas symbols overlaid the alignments and were selected and named according to Zelensky & Gready (2003): C1–C4 are the four Cysteines implicated in the formation of two disulfide bridges; black arrowheads mark conserved aas for sugar- and calcium-binding; black circles mark other structurally important conserved aas. Dots represent aas identical to isoform 1. Non-conservative aa substitutions (see text for a definition) are in italics and underlined. Non-conserved aa substitutions occurring in the vicinity of the ligand-binding region (105, 108 and 109) are boxed. GenBank accession numbers of Sm-Mermaid-4 to -13 are HM804996–HM805005; GenBank accession numbers of Lo-Mermaid-3 to -11 are HM805006–HM805014.

only be determined for a given sugar and only with a yet unavailable crystal structure. Nevertheless, in the DC-SIGNR-based tertiary structure predictions (Figure 4), positions 105, 108 and 109 are in a protein fold that is easily accessible and close to the conserved sugar-binding amino acids, and may therefore participate in sugar-binding (Feinberg et al., 2001).

By considering only these three amino acid positions, we classified all *L. oneistus* and *S. majum* CRDs

into three types. The isoforms bearing the DDA-type CRD display amino acids Asp, Asp and Ala at these positions, those belonging to the DNT-type display Asp, Asn and Thr, and those belonging to the GDA-type display Gly, Asp and Ala. In the case of *L. oneistus*, 63% of the cDNA clones encoded for DNT-type CRDs and 37% for DDA-type CRDs. In the case of *S. majum*, 52% encoded for DNT-type CRDs, 34% for DDA type and 14% for GDA type. Notably, no *L. oneistus* cDNA encoded for a GDA-type CRD.

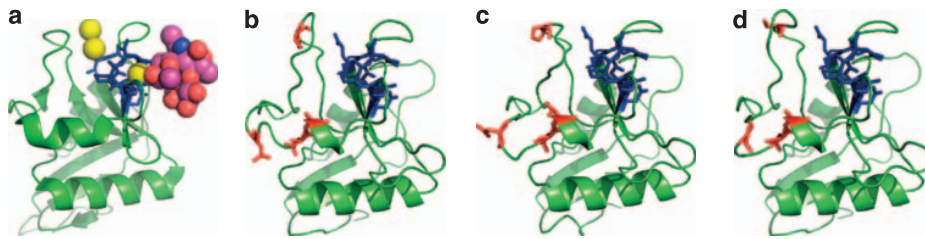


Figure 4 Three-dimensional model of the CRDs of DC-SIGNR (a) and Mermaid isoforms 1, 2 and 3 (b, c and d, respectively). All PyMOL renderings are based on the resolved structure of DC-SIGNR 1SL6. (a–d) conserved ligand-binding sites (as in Figure 3) are shown in blue, variable positions are shown in red. (a) Calcium atoms are indicated as yellow spheres and carbohydrate ligand (Lewis X) by a ball molecular model.

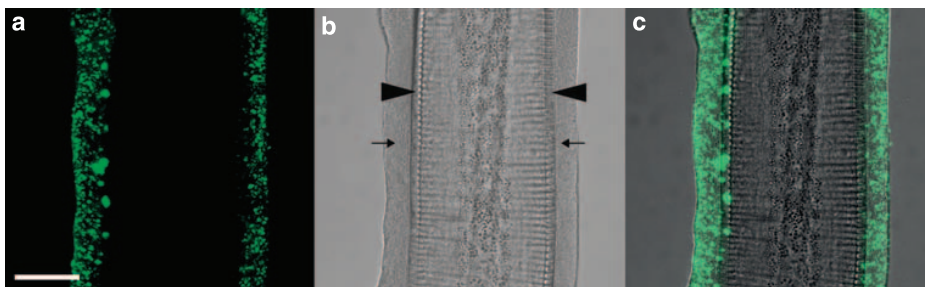


Figure 5 *S. majum* Mermaid localization pattern. LSCM picture of the bacterial coat of a *S. majum* nematode, immunostained with a specific anti-Mermaid antibody and Alexa488-conjugated secondary anti-rabbit antibody (a), corresponding differential contrast image (b) and overlay (c). Arrows point to the bacterial coat and arrowheads to the nematode cuticle. Scale bar is 20 μm .

To prove that *S. majum* expresses not only the mRNA but also the Mermaid protein, we immunostained it with a specific anti-Mermaid antibody. The pronounced staining of the bacterial coat indicates that the lectin is secreted by *S. majum* onto its cuticle (Figure 5). Immunostaining with rabbit pre-immune serum did not result in any significant staining (Supplementary Figure 2).

L. oneistus symbionts are most efficiently aggregated by Mermaid-2 and *S. majum* symbionts by Mermaid-3

To assess whether the three CRD types described above agglutinate *L. oneistus* and *S. majum* symbionts with different efficiency, we expressed recombinant forms of three isoforms, His-Mermaid-1, -2 and -3, bearing CRD types DDA, DNT and GDA, respectively; His-Mermaid-3 corresponds to the recombinant form His-Mermaid produced and analyzed in Bulgheresi *et al.* (2006). As shown in Figure 6, His-Mermaid-2 induced the largest aggregates of *L. oneistus* symbionts, whereas His-Mermaid-3 incubation resulted in the largest *S. majum* symbiont aggregates. His-Mermaid-1-induced aggregates were comparable to those obtained with His-Mermaid-2 in both *L. oneistus* and *S. majum* symbionts. Moreover, dilution series showed that the minimum concentration sufficient to induce visible aggregation varied significantly among different Mermaid isoforms. Only $1 \mu\text{g ml}^{-1}$ of His-Mermaid-2 or -1, but $10 \mu\text{g ml}^{-1}$ of His-Mermaid-3 that is, a 10-fold higher concentration, is necessary to induce *L. oneistus*

symbiont aggregation. As for *S. majum* symbionts, a $5 \mu\text{g ml}^{-1}$ concentration of His-Mermaid-3 was sufficient to aggregate them (data not shown).

Taken together, our data show that the three tested isoforms, bearing three distinct CRDs, agglutinate *L. oneistus* and *S. majum* symbionts with different efficiency. In particular, we expect the DNT type (Mermaid-2) to have a central role in *L. oneistus* symbiont aggregation, and the GDA type (Mermaid-3) to predominantly mediate *S. majum* symbiont aggregation. Therefore, expression of different isoform repertoires, or of the same isoforms at different concentrations, can underlie the attachment of different symbionts to the two co-occurring nematodes.

Incubation of *L. oneistus* in His-Mermaid-2 leads to complete symbiont detachment

In a previous report, we showed that incubation of live *L. oneistus* in recombinant His-Mermaid-3 resulted in significant symbiont detachment from all treated nematodes (Bulgheresi *et al.*, 2006). This effect was attributed to competition of the recombinant lectin with the native one. Nonetheless, symbiont patches persisted on the surface of lectin-incubated nematodes, leading to the speculation that other lectins, or other lectin isoforms, might be needed to achieve complete symbiont detachment.

We tested whether His-Mermaid-1 or -2, both displaying higher affinity for *L. oneistus* symbionts than His-Mermaid-3 in agglutination experiments, can cause complete host–symbiont dissociation.

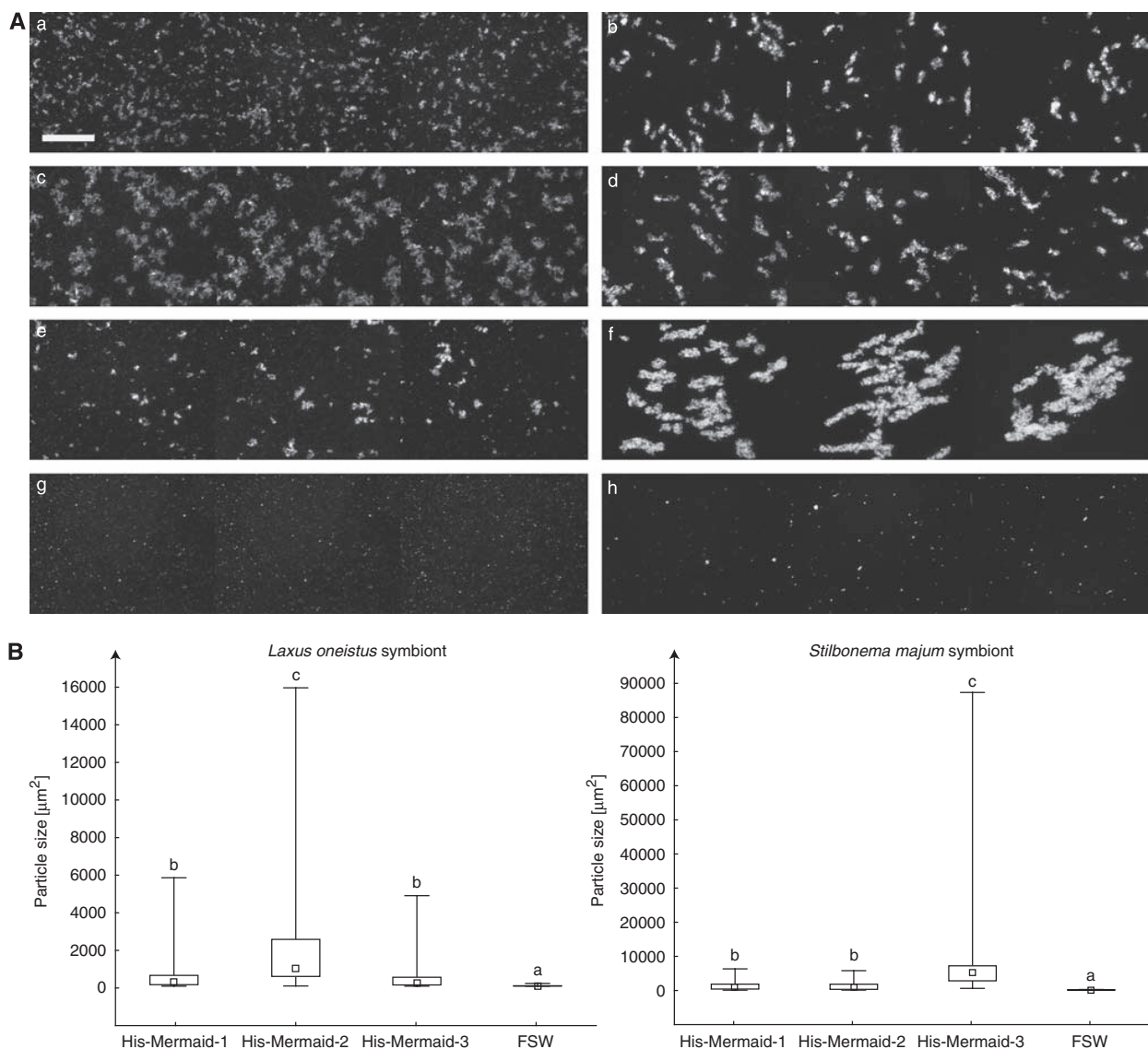


Figure 6 Agglutination assays. (A). Light microscope images of *L. oneistus* and *S. majum* symbionts incubated in $10\ \mu\text{g ml}^{-1}$ His-Mermaid-1 (a and b), His-Mermaid-2 (c and d), His-Mermaid-3 (e and f) and no lectin (g and h). Each panel was obtained by merging the photographs of three randomly chosen microscopic fields. Scale bar is $200\ \mu\text{m}$. (B) Box plot of particles size of *L. oneistus* (left plot) and *S. majum* symbionts (right plot) incubated in $10\ \mu\text{g ml}^{-1}$ His-Mermaid-1, His-Mermaid-2, His-Mermaid-3 and lectin-free filtered seawater as control. The bars indicate maximum and minimum, the boxes indicate the 25–75% quartiles and the squares indicate the median of the particle size distribution. Different letters above the graphs indicate statistically different (Dunn's *post-hoc* $P < 0.01$) particle size distributions of the treatments for each of the symbionts. For details on the P -values see Supplementary Table 1.

Figure 7 shows that *L. oneistus* individuals incubated in His-Mermaid-2 (b) started to lose the bacteria earlier than those incubated in His-Mermaid-1 or -3 (a and c, respectively). Moreover, after 20 h incubation in His-Mermaid-1 or -2, the nematodes completely lost their bacterial coat (e, f, i and j), whereas, as previously reported (Bulgheresi *et al.*, 2006), symbiont patches are still visible on His-Mermaid-3-incubated nematodes (g and k).

The ability of the three isoforms to cause different degrees of host–symbiont dissociation confirms what we observed in the agglutination experiments:

the three isoforms are functionally different, for example, they aggregate *L. oneistus* symbionts with different efficiency. Moreover, we expect the DNT-type CRD (Mermaid-2) to have a predominant role in *L. oneistus* symbiont attachment.

Discussion

Several stilbonematid species have been reported to establish monospecific ectosymbioses. The cuticles of *L. oneistus* (Polz *et al.*, 1994) and of three *Robbea* species (Bayer *et al.*, 2009) are each covered by one

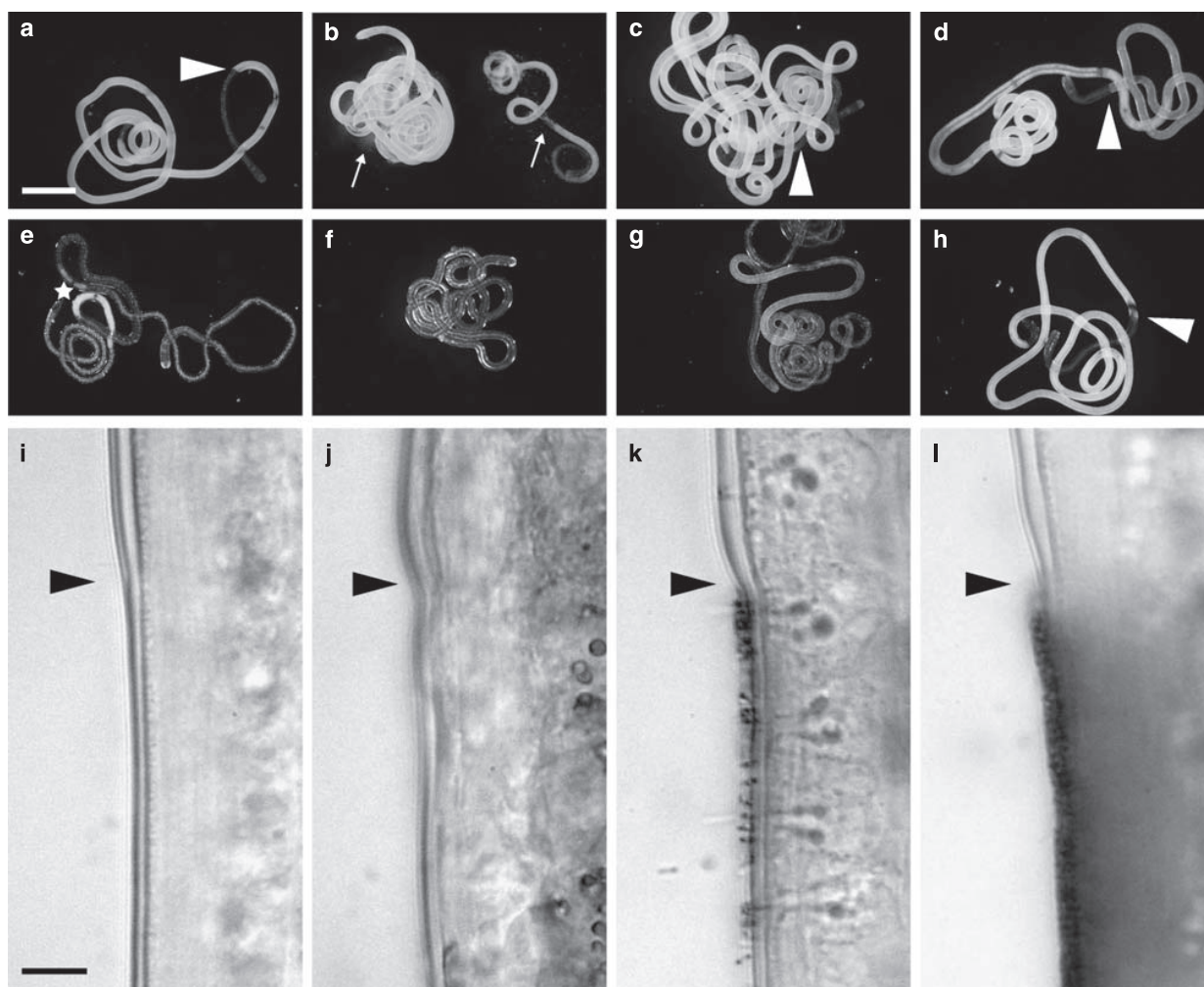


Figure 7 Dissociation assays. Light microscope images of *L. oneistus* individuals incubated in $10 \mu\text{g ml}^{-1}$ His-Mermaid-1 (a, e and i), His-Mermaid-2 (b, f and j), His-Mermaid-3 (c, g and k) and no lectin (d, h and l). Nematodes were photographed after < 1 h (a–d) and 20 h (e–l) incubation. White and black arrowheads point to the beginning of the bacterial coat. White arrows in (b) point to a nematode region where symbionts are detaching (left) and already detached (right). Two eggs inside the nematode (star) are visible after symbiont detachment. Scale bar is $200 \mu\text{m}$ in a–h and $20 \mu\text{m}$ in i–l.

phylogroup of Gammaproteobacteria, each displaying a certain morphotype and spatial arrangement on the host. The present work adds *S. majum* to those hosts able to engage in a binary association. This high degree of specificity has so far been reported for only two other bacterial ectosymbioses: the cave amphipod *Niphargus ictus* (Dattagupta *et al.*, 2009) and the leaf-cutting ant *Acromyrmex* (Poulsen *et al.*, 2005). The identification of the *S. majum* symbiont 16S rRNA gene and its phylogenetic placement within the Gammaproteobacteria reiterates earlier findings: (1) stilbonematid symbionts tightly cluster with the sulfide-oxidizing endosymbionts of a marine nematode and of gutless marine oligochaetes (Musat *et al.*, 2007) (Dubilier *et al.*, 2008); (2) all the phylotypes contained in this cluster cannot be grouped according to the geographical origin of their hosts; and (3) their closest relatives are free

living and not symbiotic. Given that stilbonematid and symbiont phylogenies do not match (Bayer *et al.*, 2009), the partners probably did not co-speciate.

Protein–sugar interactions have a central role in host–symbiont attachment in virtually all microbial symbioses, including plant–rhizobia, ectomycorrhiza, cnidarian–zooxanthellae, lucinid mussels and the ones established by thiotrophic marine nematodes (Wood-Charlson *et al.*, 2006; Gourdine and Smith-Ravin, 2007; Kvennefors *et al.*, 2008; De Hoff *et al.*, 2009; Bright and Bulgheresi, 2010; Chaston and Goodrich-Blair, 2010). Here, we showed that one to three amino acid replacements in a host-secreted sugar-binding protein are sufficient to radically affect its ability to agglutinate two different symbiont phylotypes. More specifically, incubation of *L. oneistus* symbionts in a DNT-type CRD results in

the largest bacterial aggregates, whereas a GDA type induces the largest *S. majum* symbiont aggregates. Therefore, acquisition of specific symbionts by two co-occurring stilbonematids might be mediated by minor differences in lectin protein sequence. This is the first report of lectin isoforms differing in their symbiont-binding capacity. cDNA analysis of a family of *Acropora millepora* mannose-binding proteins (Millelectins; Kvennefors *et al.*, 2008) revealed extensive sequence variation. As observed for the Mermaids, some substitutions occur in the vicinity of the ligand-binding region. Kvennefors *et al.* (2008) speculated that amino acid variability would enable the coral-secreted Millelectins to recognize a variety of symbionts and pathogens.

Agglutination and dissociation assays indicate that the three CRD types differ in their symbiont-binding activity. This might be because of their different polymerization capacities or sugar specificities. Detailed analysis of the latter, as well as of the lipopolysaccharide composition of the two symbiont phylotypes, promise to disclose the effects of the three analyzed amino acid substitutions on Mermaid activity. It is possible that the specificity of the DNT-type CRD (displayed by Mermaid-2) matches the sugar composition of *L. oneistus* symbiont lipopolysaccharide and the specificity of the GDA-type CRD (displayed by Mermaid-3) that of the *S. majum* symbiont. Although we did not attempt to dissociate the latter from its host by incubation in different recombinant Mermaid isoforms, as *S. majum* does not tolerate long incubations outside the marine environment, agglutination tests suggest that GDA-type Mermaids are predominantly mediating symbiont attachment to this stilbonematid species.

The Mermaids are not the first molecules to vary between phylogenetically related hosts, thereby affecting symbiosis specificity. Other very well-known examples are the plant flavonoids and, on the symbiont side, the rhizobial *Nod* factors (Cooper, 2007). This study does not exclude that other host (C-type) lectins might participate in symbiont discrimination. Additionally, the presence of another given gene (symbiosis specificity mechanism (b), see introduction) could be involved. Examples of genes that can specify the host range are the nematode intestine localization (*nil*) *B* and *C* genes of insect-killing nematode symbionts (Cowles and Goodrich-Blair, 2008) and the regulator of symbiotic colonization sensor (*rscS*) gene of squid symbionts (Mandel *et al.*, 2009).

A high rate of amino acid substitutions is a hallmark of positive selection. This is defined as an excess in the non-synonymous nucleotide substitution rate (dN) relative to the synonymous rate (dS) when compared with neutral expectations (Hughes and Nei, 1988). Positive selection acts on a multigenes family and favours diversity at the amino acid level. Evidence of positive selection has been reported for many immunity genes

(Hughes, 1994; Tiffin and Moeller, 2006; Hayes *et al.*, 2010). Molecular population genetics studies are needed to find out whether the Mermaids are evolving adaptively under diversifying, selective pressure exerted by the symbionts. Moreover, quantitative PCR and/or isoform-specific antibodies are required to define the relative abundance of each isoform transcript/protein in each stilbonematid species.

The finding that different Mermaid isoforms can discriminate different symbionts is a true step forward in understanding the mechanisms of symbiosis specificity. So far, only pathogen-associated molecular pattern receptors were known to be tailored in such a custom-made manner. New research avenues will be to investigate whether the different Mermaid CRDs display different affinity for pathogens such as the human immunodeficiency virus-1 (HIV-1) and their role in stilbonematid innate immunity defense.

Acknowledgements

We are very grateful to Anja Spang for her insightful comments on the manuscript. This work was supported by the Austrian Research Promotion Agency (FFG) project 814324 (SB and NRH) and by the Austrian Science Fund (FWF) project 20394 (JAO, HG and UD).

References

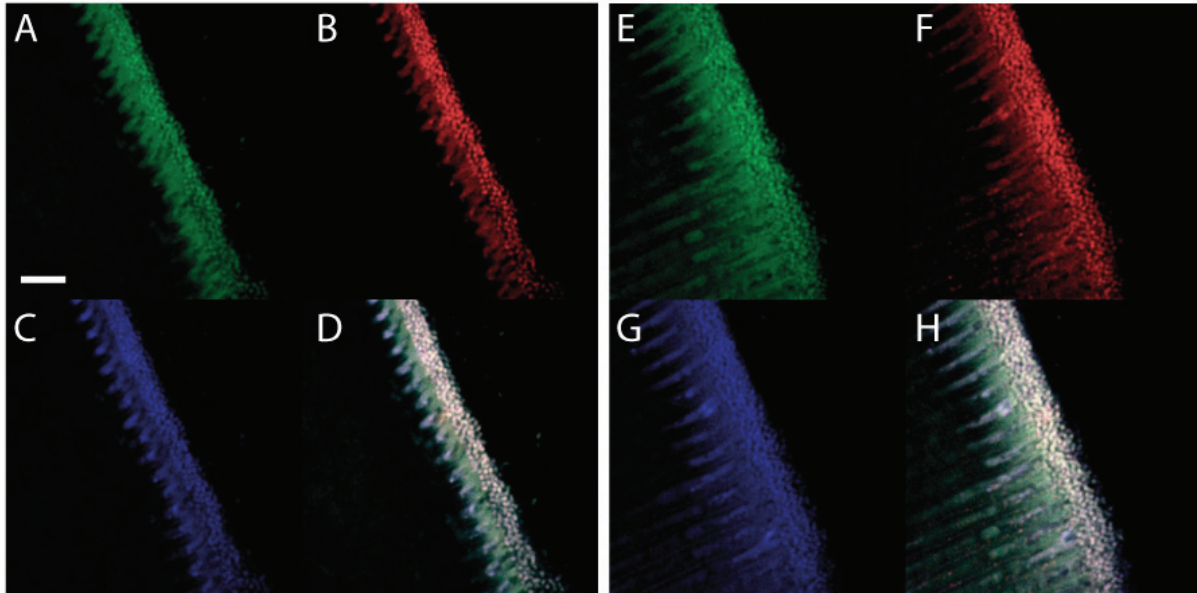
- Alm EW, Oerther DB, Larsen N, Stahl DA, Raskin L. (1996). The oligonucleotide probe database. *Appl Environ Microbiol* **62**: 3557–3559.
- Altschul SF, Gish W, Miller W, Myers EW, Lipman DJ. (1990). Basic local alignment search tool. *J Mol Biol* **215**: 403–410.
- Amann RI, Krumholz L, Stahl DA. (1990). Fluorescent-oligonucleotide probing of whole cells for determinative, phylogenetic, and environmental studies in microbiology. *J Bacteriol* **172**: 762–770.
- Bayer C, Heindl NR, Rinke C, Lückner S, Ott JA, Bulgheresi S. (2009). Molecular characterization of the symbionts associated with marine nematodes of the genus *Robbea*. *Environ Microbiol Rep* **1**: 136–144.
- Bright M, Bulgheresi S. (2010). A complex journey: transmission of microbial symbionts. *Nat Rev Microbiol* **8**: 218–230.
- Brosius J, Dull TJ, Sleeter DD, Noller HF. (1981). Gene organization and primary structure of a ribosomal RNA operon from *Escherichia coli*. *J Mol Biol* **148**: 107–127.
- Brosius J, Palmer ML, Kennedy PJ, Noller HF. (1978). Complete nucleotide sequence of a 16S ribosomal RNA gene from *Escherichia coli*. *Proc Natl Acad Sci USA* **75**: 4801–4805.
- Bulgheresi S, Schabussova I, Chen T, Mullin NP, Maizels RM, Ott JA. (2006). A new C-type lectin similar to the human immunoreceptor DC-SIGN mediates symbiont acquisition by a marine nematode. *Appl Environ Microbiol* **72**: 2950–2956.

- Chaston J, Goodrich-Blair H. (2010). Common trends in mutualism revealed by model associations between invertebrates and bacteria. *FEMS Microbiol Rev* **34**: 41–58.
- Cooper JE. (2007). Early interactions between legumes and rhizobia: disclosing complexity in a molecular dialogue. *J Appl Microbiol* **103**: 1355–1365.
- Cowles CE, Goodrich-Blair H. (2008). The *Xenorhabdus nematophila* *niABC* genes confer the ability of *Xenorhabdus* spp. to colonize *Steinernema carpocapsae* nematodes. *J Bacteriol* **190**: 4121–4128.
- Dattagupta S, Schaperdorth I, Montanari A, Mariani S, Kita N, Valley JW *et al*. (2009). A novel symbiosis between chemoautotrophic bacteria and a freshwater cave amphipod. *ISME J* **3**: 935–943.
- De Hoff P, Brill L, Hirsch A. (2009). Plant lectins: the ties that bind in root symbiosis and plant defense. *Mol Genet Genomics* **282**: 1–15.
- Drummond A, Ashton B, Cheung M, Heled J, Kearse M, Moir R *et al*. (2009). Geneious v4.7 available from <http://www.geneious.com/>.
- Dubilier N, Bergin C, Lott C. (2008). Symbiotic diversity in marine animals: the art of harnessing chemosynthesis. *Nat Rev Microbiol* **6**: 725–740.
- Feinberg H, Mitchell DA, Drickamer K, Weis WI. (2001). Structural basis for selective recognition of oligosaccharides by DC-SIGN and DC-SIGNR. *Science* **294**: 2163–2166.
- Gourdine JP, Smith-Ravin EJ. (2007). Analysis of a cDNA-derived sequence of a novel mannose-binding lectin, codakine, from the tropical clam *Codakia orbicularis*. *Fish Shellfish Immunol* **22**: 498–509.
- Guex N, Peitsch M. (1997). SWISS-MODEL and the Swiss-Pdbviewer: an environment for comparative protein modeling. *Electrophoresis* **18**: 2714–2723.
- Hayes M, Eytan R, Hellberg M. (2010). High amino acid diversity and positive selection at a putative coral immunity gene (tachylectin-2). *BMC Evol Biol* **10**: 150.
- Hentschel U, Berger EC, Bright M, Felbeck H, Ott JA. (1999). Metabolism of nitrogen and sulfur in ectosymbiotic bacteria of marine nematodes (Nematoda, Stilbonematinae). *Mar Ecol Prog Ser* **183**: 149–158.
- Hughes AL. (1994). The evolution of functionally novel proteins after gene duplication. *Proc Biol Sci* **256**: 119–124.
- Hughes AL, Nei M. (1988). Pattern of nucleotide substitution at major histocompatibility complex class I loci reveals overdominant selection. *Nature* **335**: 167–170.
- Juretschko S, Timmermann G, Schmid M, Schleifer KH, Pommerening-Roser A, Koops HP *et al*. (1998). Combined molecular and conventional analyses of nitrifying bacterium diversity in activated sludge: *Nitrosococcus mobilis* and *Nitrospira*-like bacteria as dominant populations. *Appl Environ Microbiol* **64**: 3042–3051.
- Kane MD, Poulsen LK, Stahl DA. (1993). Monitoring the enrichment and isolation of sulfate-reducing bacteria by using oligonucleotide hybridization probes designed from environmentally derived 16S rRNA sequences. *Appl Environ Microbiol* **59**: 682–686.
- Katoh K, Kuma K-I, Toh H, Miyata T. (2005). MAFFT version 5: improvement in accuracy of multiple sequence alignment. *Nucleic Acids Res* **33**: 511–518.
- Kvennefors ECE, Leggat W, Hoegh-Guldberg O, Degnan BM, Barnes AC. (2008). An ancient and variable mannose-binding lectin from the coral *Acropora millepora* binds both pathogens and symbionts. *Dev Comp Immunol* **32**: 1582–1592.
- Loy A, Arnold R, Tischler P, Rattei T, Wagner M, Horn M. (2008). Probecheck—a central resource for evaluating oligonucleotide probe coverage and specificity. *Environ Microbiol* **10**: 2894–2898.
- Ludwig W, Strunk O, Westram R, Richter L, Meier H, Yadhukumar *et al*. (2004). ARB: a software environment for sequence data. *Nucleic Acids Res* **32**: 1363–1371.
- Mandel MJ, Wollenberg MS, Stabb EV, Visick KL, Ruby EG. (2009). A single regulatory gene is sufficient to alter bacterial host range. *Nature* **458**: 215–218.
- Manz W, Amann R, Ludwig W, Wagner M, Schleifer K-H. (1992). Phylogenetic oligodeoxynucleotide probes for the major subclasses of proteobacteria: problems and solutions. *Syst Appl Microbiol* **15**: 593–600.
- McMahon SA, Miller JL, Lawton JA, Kerkow DE, Hodes A, Marti-Renom MA *et al*. (2005). The C-type lectin fold as an evolutionary solution for massive sequence variation. *Nat Struct Mol Biol* **12**: 886–892.
- Mittal R, Bulgheresi S, Emami C, Prasadarao NV. (2009). *Enterobacter sakazakii* targets DC-SIGN to induce immunosuppressive responses in dendritic cells by modulating MAPKs. *J Immunol* **183**: 6588–6599.
- Musat N, Giere O, Gieseke A, Thiermann F, Amann R, Dubilier N. (2007). Molecular and morphological characterization of the association between bacterial endosymbionts and the marine nematode *Astomonema* sp. from the Bahamas. *Environ Microbiol* **9**: 1345–1353.
- Nabatov AA, de Jong MA, de Witte L, Bulgheresi S, Geijtenbeek TB. (2008). C-type lectin Mermaid inhibits dendritic cell mediated HIV-1 transmission to CD4+ T cells. *Virology* **378**: 323–328.
- Nebelsick M, Blumer M, Novak R, Ott JA. (1992). A new glandular sensory organ in *Catanema* sp. (Nematoda, Stilbonematinae). *Zoomorphology* **112**: 17–26.
- Nussbaumer AD, Bright M, Baranyi C, Beisser CJ, Ott JA. (2004). Attachment mechanism in a highly specific association between ectosymbiotic bacteria and marine nematodes. *Aquat Microb Ecol* **34**: 239–246.
- Ott JA, Bright M, Bulgheresi S. (2004a). Marine microbial thiotrophic ectosymbioses. *Oceanogr Mar Biol Annu Rev* **42**: 95–118.
- Ott JA, Bright M, Bulgheresi S. (2004b). Symbioses between marine nematodes and sulfur-oxidizing chemoautotrophic bacteria. *Symbiosis* **36**: 103–126.
- Ott JA, Novak R, Schiemer F, Hentschel U, Nebelsick M, Polz M. (1991). Tackling the sulfide gradient: a novel strategy involving marine nematodes and chemoautotrophic ectosymbionts. *PSZN I: Mar Ecol* **12**: 261–279.
- Petersen B, Petersen TN, Andersen P, Nielsen M, Lundegaard C. (2009). A generic method for assignment of reliability scores applied to solvent accessibility predictions. *BMC Struct Biol* **9**: 51.
- Peumans WJ, Van Damme E. (1995). Lectins as plant defense proteins. *Plant Physiol* **109**: 347–352.
- Polz MF, Distel DL, Zarda B, Amann R, Felbeck H, Ott JA *et al*. (1994). Phylogenetic analysis of a highly specific association between ectosymbiotic, sulfur-oxidizing bacteria and a marine nematode. *Appl Environ Microbiol* **60**: 4461–4467.
- Polz MF, Harbison C, Cavanaugh CM. (1999). Diversity and heterogeneity of epibiotic bacterial communities on the marine nematode *Eubostriechus diana*. *Appl Environ Microbiol* **65**: 4271–4275.
- Poulsen M, Cafaro M, Boomsma JJ, Currie CR. (2005). Specificity of the mutualistic association between

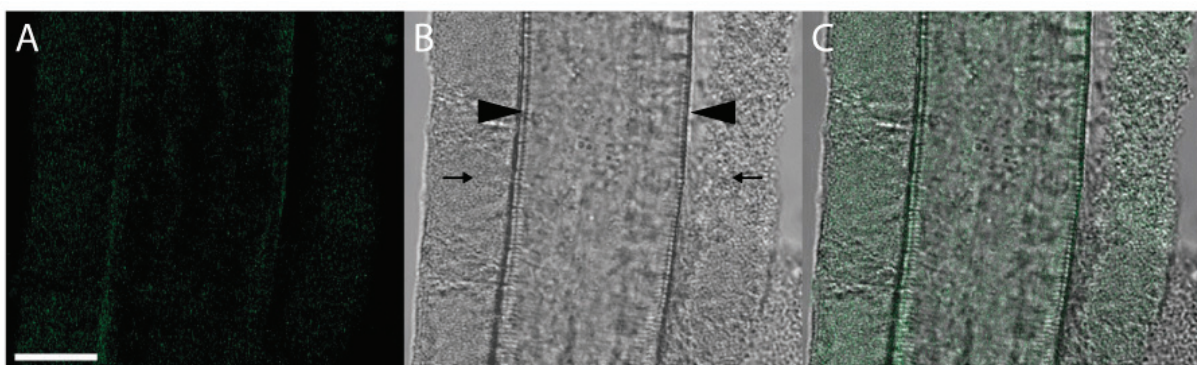
- actinomycete bacteria and two sympatric species of *Acromyrmex* leaf-cutting ants. *Mol Ecol* **14**: 3597–3604.
- Pradillon F, Schmidt A, Peplies J, Dubilier N. (2007). Species identification of marine invertebrate early stages by whole-larvae *in situ* hybridisation of 18S ribosomal RNA. *Mar Ecol Prog Ser* **333**: 103–116.
- Ronquist F, Huelsenbeck JP. (2003). MrBayes 3: bayesian phylogenetic inference under mixed models. *Bioinformatics* **19**: 1572–1574.
- Schizas NV, Street GT, Coull BC, Chandler GT, Quattro JM. (1997). An efficient DNA extraction method for small metazoans. *Mol Mar Biol Biotechnol* **6**: 381–383.
- Stamatakis A. (2006). RAxML-VI-HPC: maximum likelihood-based phylogenetic analyses with thousands of taxa and mixed models. *Bioinformatics* **22**: 2688–2690.
- Tiffin P, Moeller DA. (2006). Molecular evolution of plant immune system genes. *Trends Genet* **22**: 662–670.
- Wallner G, Amann R, Beisker W. (1993). Optimizing fluorescent *in situ* hybridization with rRNA-targeted oligonucleotide probes for flow cytometric identification of microorganisms. *Cytometry* **14**: 136–143.
- Wood-Charlson EM, Hollingsworth LL, Krupp DA, Weis VM. (2006). Lectin/glycan interactions play a role in recognition in a coral/dinoflagellate symbiosis. *Cell Microbiol* **8**: 1985–1993.
- Zelensky AN, Gready JE. (2003). Comparative analysis of structural properties of the C-type-lectin-like domain (CTLD). *Proteins* **52**: 466–477.
- Zhang P, Skurnik M, Zhang SS, Schwartz O, Kalyanasundaram R, Bulgheresi S *et al*. (2008). Human dendritic cell-specific intercellular adhesion molecule-grabbing nonintegrin (CD209) is a receptor for *Yersinia pestis* that promotes phagocytosis by dendritic cells. *Infect Immun* **76**: 2070–2079.
- Zhang P, Snyder S, Feng P, Azadi P, Zhang S, Bulgheresi S *et al*. (2006). Role of N-acetylglucosamine within core lipopolysaccharide of several species of gram-negative bacteria in targeting the DC-SIGN (CD209). *J Immunol* **177**: 4002–4011.

Supplementary Information accompanies the paper on The ISME Journal website (<http://www.nature.com/ismej>)

Supplementary Materials



Supplementary Fig. 1 FISH LSCM of *S. majum* symbionts attached to the worm surface. Symbionts are stained with specific probes targeting eubacteria (A, E), Gammaproteobacteria (B, F), and the *S. majum* symbiont in the presence (C) or absence (G) of an unlabeled competitor. D and H are overlay pictures of A-C and E-G, respectively. Scale bar is 6 μm in A-H.



Supplementary Fig. 2 LSCM picture of the bacterial coat of a *S. majum* nematode immunostained with rabbit preimmune serum and Alexa488-conjugated secondary anti-rabbit antibody (A), corresponding differential contrast image (B) and overlay (C). The degree of signal is negligible in comparison to that obtained in Fig.5. Arrows point to the bacterial coat and arrowheads to the nematode cuticle. Scale bar is 20 μm .

Supplementary Table 1. Symbiont agglutination assay. Dunn's post-hoc multiple comparisons p-values after Kruskal-Wallis nonparametric ANOVA.

	<i>L. oneistus</i> symbiont agglutination				<i>S. majum</i> symbiont agglutination			
	FSW	His-Mermaid-1	His-Mermaid-2	His-Mermaid-3	FSW	His-Mermaid-1	His-Mermaid-2	His-Mermaid-3
FSW	-	0,000	0,000	0,001	-	0,000	0,000	0,000
His-Mermaid-1	0,000	-	0,000	1,000	0,000	-	1,000	0,000
His-Mermaid-1	0,000	0,000	-	0,000	0,000	1,000	-	0,000
His-Mermaid-1	0,001	1,000	0,000	-	0,000	0,000	0,000	-

IV. A new species of symbiotic flatworms, *Paracatenula galateia* sp. nov. (Platyhelminthes: Catenulida: Retronectidae) from Belize (Central America)

Authors: Ulrich Dirks*, Harald R. Gruber-Vodicka*, Nikolaus Leisch, Wolfgang Sterrer and Jörg A. Ott

* These authors contributed equally to this work

Publication status: published 2011 in *Marine Biology Research* Volume 7, pages 769 - 777

Personal contributions of Harald Gruber-Vodicka

- a. designed the study together with JAO
- b. collected material on two field trips to Carrie Bow Cay (Belize)
- c. sequenced all 18S and 28S rRNA genes
- d. contributed light microscopic images and measurements
- e. performed all phylogenetic and statistical analyses
- f. wrote the manuscript together with UD and JAO.



ORIGINAL ARTICLE

A new species of symbiotic flatworms, *Paracatenula galateia* sp. nov. (Platyhelminthes: Catenulida: Retronectidae) from Belize (Central America)

ULRICH DIRKS^{1†}, HARALD R. GRUBER-VODICKA^{1†}, NIKOLAUS LEISCH¹, WOLFGANG STERRER² & JÖRG A. OTT^{1*}

¹Department of Marine Biology, University of Vienna, Vienna, Austria, and ²Bermuda Aquarium, Natural History Museum and Zoo (BAMZ), Bermuda

Abstract

Paracatenula galateia sp. nov. is a mouthless marine catenulid platyhelminth with bacterial intracellular endosymbionts. The worms live in shallow back-reef sands in the Belize Barrier Reef system and are distinguished from the four previously described members of the genus by their large size combined with a ribbon-shaped body and characteristic bipartite inclusions in cells, which are interpreted as sperm. The bacteria are presumed to be sulphur-oxidizing chemoautotrophs. They are found in bacteriocytes which fill the body region ('trophosome region') posterior to the brain, whereas the anterior part of the worm (rostrum) is bacteria-free. Phalloidin staining reveals a delicate system of subepithelial circular and longitudinal muscles and dorsoventral fibres. The serotonergic nervous system consists of a brain at the base of the rostrum and longitudinal fibres extending both anteriorly and posteriorly, the latter being concentrated in a structure called the 'dorsal cord'.

Key words: *Interstitial meiofauna, intracellular symbiosis, subtidal sand*

Introduction

Catenulida are an order of small, free-living Platyhelminthes ('Turbellaria', Tyler et al. 2006–2010). Originally thought to occur exclusively in freshwater except for the questionable *Tyrrheniella sigillata* (Riedl, 1959), they were first reported from marine sandy bottoms by Sterrer (1966). Sterrer & Rieger (1974) described nine marine species from NE and W Atlantic coasts, belonging to two new genera (*Retronectes* and *Paracatenula*) for which they erected the family Retronectidae, named for their ability to swim backward by reversing the ciliary beat. Usually found only as isolated, fragile specimens, and difficult to identify for their paucity of consistent morphometric features, retronectids are characterized by an often polyolithoporous statocyst (which may be lacking in some species or specimens), and a simple, anterior-dorsally opening mixed gonad. Reproductive biology is

as yet unresolved: oocytes were observed in only one, and a mature egg in another species of *Retronectes* of at least 50 specimens studied (Sterrer & Rieger 1974). A small proportion of specimens contained cells with distinctly shaped inclusions that have been interpreted as spermatozoa and their nuclei; spermatids contain ciliary rudiments (Rieger 1978). In *Paracatenula*, distinct gonads are apparently lacking; in fact, no oocytes or eggs have ever been found. Instead, cells containing characteristic rod-, ribbon-, banana- or even spicule-shaped inclusions were found along a strand of tissue named 'dorsal cord' (Sterrer & Rieger 1974), which extends throughout the body in median position. These inclusions often clustered behind the brain (in a *vesicula seminalis*?), where a dorsal pore to the outside may be located.

The peculiar retronectid gonad with its large, oocyte-like sperm prompted Sterrer & Rieger

*Correspondence: Jörg A. Ott, Department of Marine Biology, University of Vienna, Althanstraße 14, 1090 Vienna Austria. E-mail: joerg.ott@univie.ac.at

†These authors contributed equally

Published in collaboration with the University of Bergen and the Institute of Marine Research, Norway, and the Marine Biological Laboratory, University of Copenhagen, Denmark

(1974) to suggest 'a completely new mode of reproduction – such as parthenogenesis from sperm' along the transformation of male cells into oocytes described by Borkott (1970) for the freshwater catenulid *Stenostomum*; see also Schuchert & Rieger (1990) – and further 'underlines the isolated position of the Catenulida within the Turbellaria and the Platyhelminthes' (Rieger 1978). Recent multilocus phylogenetic studies corroborate the placement of the genus *Paracatenula* within the Catenulida and also the status of the Catenulida as the basal taxon of Platyhelminthes (Larsson & Jondelius 2008).

While members of *Retronectes* have a mouth, ciliated pharynx and gut lumen, those of *Paracatenula* were described to lack mouth, pharynx and gut lumen; rather, the tissue filling most of the body volume consists of large turgescient cells containing 'granular bodies'. These have been identified as intracellular bacteria in *P. erato* Sterrer and Rieger, 1974 (Ott et al. 1982). Subsequent investigations have shown that this is the case for all members of the genus *Paracatenula* (own unpublished observations). The bacteria are presumably symbiotic sulphur-oxidizers, since the bacteria from two *Paracatenula* species have been shown to possess a reverse dissimilatory sulphite reductase (DsrAB) gene, an important gene in bacterial sulphur metabolism, which clustered with the sequences of other sulphur-oxidizing bacteria (Loy et al. 2009). In addition, the bacteria contain highly refractive granules, appearing white in incident light, which resemble the elemental sulphur storage granules known from many sulphur-oxidizing bacteria (Pasteris et al. 2001). Members of *Paracatenula* have a symbiont-free anterior body region (rostrum) and a posterior body region filled by symbiont-containing cells (bacteriocytes), which together form a distinct organ, which we call 'trophosome' in analogy to the symbiont-containing organ in the vestimentiferan annelids.

Only three more species of Retronectidae have been described since Sterrer & Rieger's (1974) original nine: one new genus, *Myoretronectes paransensis* Noreña-Jansson & Faubel, 1996 from Argentina, and two species of *Retronectes*: *R. sterreri* Faubel, 1976 from the North Sea and *R. atypica* Doe & Rieger, 1977 from North Carolina. During investigations of the meiofauna in back-reef sediments of the Mesoamerican barrier reef system at Belize, a large, conspicuous new species was found to be common in subtidal sands close to the field station of the US National Museum of Natural History (Washington, DC) on the island of Carrie Bow Cay (Rützler & Macintyre 1982). This species is currently subject to intensive studies of its biology and ecology. Here we present the description of this species new to science.

Materials and methods

Specimens were collected between 2007 and 2010 at several locations in the vicinity of the field station of the US National Museum of Natural History (Washington, DC) on the island of Carrie Bow Cay (Figure 1). The worms were extracted by shaking sand samples in seawater and pouring the supernatant through a 32- μ m pore-size mesh. Individual specimens were picked by hand and inspected using a dissecting microscope. Squeeze preparations of live animals were analysed using bright field and phase contrast microscopy at 16–1000 \times magnification. Digital photomicrographs were collected and used for measurements with the analysis tool of Adobe Photoshop CS5.

Fluorescent staining of whole mounts

Musculature in whole mounts of individual worms was made visible by staining F-actin with fluorescently labelled phalloidin (Alexa Fluor 568; Invitrogen, Austria); the nervous system by staining of serotonergic nerves with an anti-serotonin antiserum

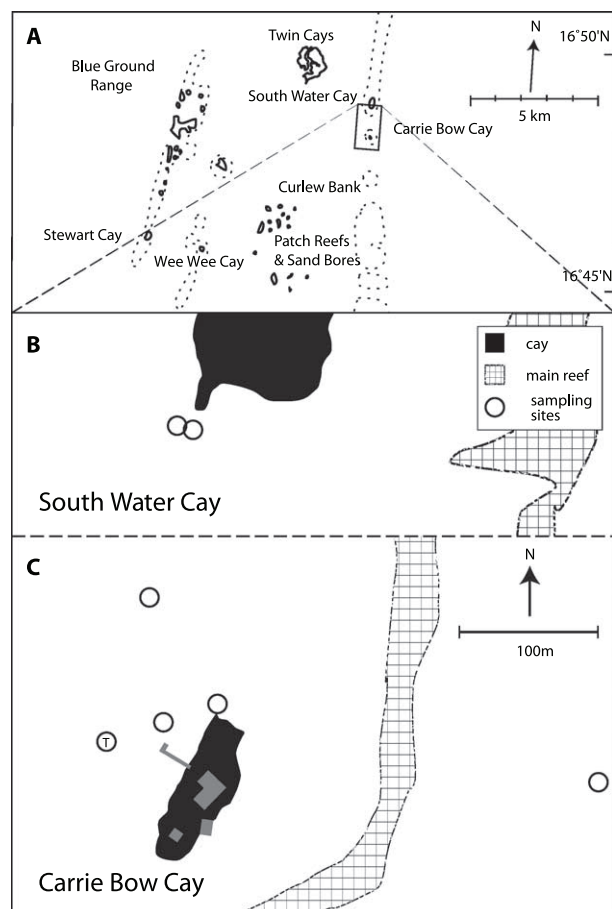


Figure 1. A. Map of the southern part of the Belize Barrier Reef. B and C. Sample locations in the vicinity of Carrie Bow Cay where *Paracatenula galateia* sp. nov. was found. T, type location.

produced in rabbit (Sigma Aldrich, Austria) followed by a staining with an Alexa Fluor 568-conjugated secondary antibody. Freshly collected specimens were first relaxed in a magnesium chloride solution isotonic to seawater, fixed for 12 h in 4% (w/v) formaldehyde at 4°C, rinsed in phosphate-buffered saline (PBS) and stored in PBS at 4°C (for phalloidin staining) or in methanol at -20°C (for serotonin staining). For phalloidin staining the specimens were washed and permeabilized in PBS with 0.2% (v/v) Triton X-100 (PBS-T) and then stained for 30 min with phalloidin-Alexa 568 diluted 1:200 in PBS-T. After three washes in PBS and a DAPI staining for 5 min, the specimens were mounted on slides in Vecta shield (Vector Laboratories). For antibody staining the fixed animals were transferred into PBS-T and digested for 6 min at room temperature in 0.1 mg/ml proteinase K in PBS-T. Digestion was stopped by adding 2 N hydrochloric acid. Animals were then washed in PBS-T and blocked in BSA-T (bovine serum albumin (BSA) plus 0.2% Triton X-100) for 30 min. Serotonin was stained with the anti-serotonin antiserum 1:2000 diluted in BSA-T overnight at 4°C. After three washing steps in PBS-T, an Alexa 547 conjugated secondary antibody was applied for 1 h at room temperature at 1:300 dilution in BSA-T. DAPI staining and mounting was done as described above. Slides were either scanned with a confocal laser-scanning microscope (Zeiss LSM 510) or examined and photographed with an epifluorescence microscope (Zeiss Axio Imager).

DNA extraction, PCR amplification and sequencing

DNA was extracted from ten worms using the Blood and Tissue DNA extraction kit (Qiagen, Germany) and 2 µl of each extraction was used as PCR template. Fragments of the 18S and 28S rRNA gene (1750 and 1350 nt long, respectively) were amplified for each worm by PCR with the general eukaryotic primers 1f (5'-CTGGTTGATYCTGC CAGT-3') and 2023r (5'-GGTTCACCTACG GAAACC-3') for 18S (Pradillon et al. 2007) and the Primers D1a (5'-CCC(C/G)CGTAA(T/C)TTAAG CATAT-3') and D5b2 (5'-CGCCAGTTCTGCT TACC-3') initially developed for Arthropoda for 28S (von Reumont et al. 2009). Cycling conditions for both genes were: 94°C for 3 min followed by 40 cycles of 94°C for 45 s, 49°C for 30 s, 72°C for 1 min, and a final elongation step of 72°C for 10 min. The PCR products obtained were purified using the MinElute PCR purification kit (Qiagen) and directly sequenced with the PCR primers. All sequences

were deposited in Genbank, accession numbers HQ231330–HQ231344.

rRNA genes-based phylogenetic analysis

18S and 28S rRNA gene data sets were constructed with our sequences and selected Catenulida sequences available in Genbank. The 18S and 28S rRNA gene data sets were separately aligned using MAFFT Q-INS-I, which considers the secondary structure of RNA (Katoh et al. 2005). The 5' and 3' ends of both alignments were trimmed, final length of alignments were 1816 nt (18S) and 1676 nt (28S). The nucleotide sequence identity between individuals was calculated based on these alignments using Geneious 5 (Drummond et al. 2010). The alignments were concatenated and we reconstructed the phylogenies using maximum likelihood- (PHYML at the phylogeny.fr web service; Guindon & Gascuel 2003; Dereeper et al. 2008) and Bayesian inference-based (MrBayes; Ronquist & Huelsenbeck 2003) algorithms. Substitution models for both genes were evaluated using MrModeltest 2.3 (Nylander 2008). The GTR + I + G model was chosen using the Akaike information criterion. MrBayes was run for five Mio generations using four chains. Convergence was evaluated by plotting the generations versus logL and the burn-in was set to two Mio generations. Node stability was evaluated using posterior probabilities (pp, Bayesian inference) and aLRT (maximum likelihood; Anisimova & Gascuel 2006; Guindon et al. 2010). Sequences of Macrostromida served as out-group.

Taxonomy

***Paracatenula galateia* sp. nov.**

Material

Of more than 100 individuals from back-reef sediments at a variety of sampling sites in the vicinity of Carrie Bow Cay (Belize) (see Figure 1), 19 adults were studied live in squeeze preparation, six by serial semithin sections, and about 10 each as whole mounts stained with phalloidin and serotonin antibody, respectively.

Type specimens

Holotype: 1 specimen fixed in formaldehyde 4% and mounted on a microscope slide embedded in glycerol; USNM 1154145.

Paratype: 2 specimens fixed in Bouin's fluid in separate vials; USNM 1154146 and 1154147.

772 U. Dirks et al.

Type locality

Carrie Bow Cay, Belize Barrier Reef (16°48'10.50"N, 88°04'56.30"W). Subtidal sand in approximately 1 m water depth, 50 m west of the island in front of the pier (Figure 1).

Etymology

Galateia refers to the silky, milky white appearance of the worm under incident light. In Greek mythology this is an attribute of the skin of the nymph Galateia (Greek Γαλατεία, 'the milky white').

Diagnosis

Ribbon-shaped *Paracatenula* up to 6 mm long, with or without a statocyst. Inclusions bipartite, with conical to ladyfinger-shaped parts, 12–19 µm long and 3 µm wide.

External appearance

Paracatenula galateia is a ribbon-shaped worm up to 6 mm long (Figures 2A, 3). The length of the

animals is extremely variable because the fragile worms tend to break, probably due to the extraction process. Only rarely are individuals found that are apparently complete and show an undamaged posterior end. Many worms show constrictions or an irregular outline (Figure 3C). The width of the trophosome region, which makes up the largest part of the animal, is 225–315 µm (271 ± 30.6 µm, $n = 19$); its dorsoventral height, however, is much smaller, and difficult to measure or even estimate in living worms. Fixed specimens have a width/height ratio of approximately 4.6–5.5. The trophosome is pinkish-white in incident light and has a characteristic silky appearance (Figure 3A). The transparent dorsal cord appears to divide the trophosome into two parts along the midline (Figures 3 and 9A).

The rostrum is 330–460 µm (398 ± 37.5 µm, $n = 19$) long and has a characteristic shape. The anterior part is cylindrical or club-shaped, with a rounded tip (Figures 2A,C and 3). Its diameter is 100–176 µm (129 ± 17.7 µm, $n = 19$). The posterior part is conical and widens to match the width of the trophosome region. This widening begins at about 60% of the length of the rostrum, where it has its

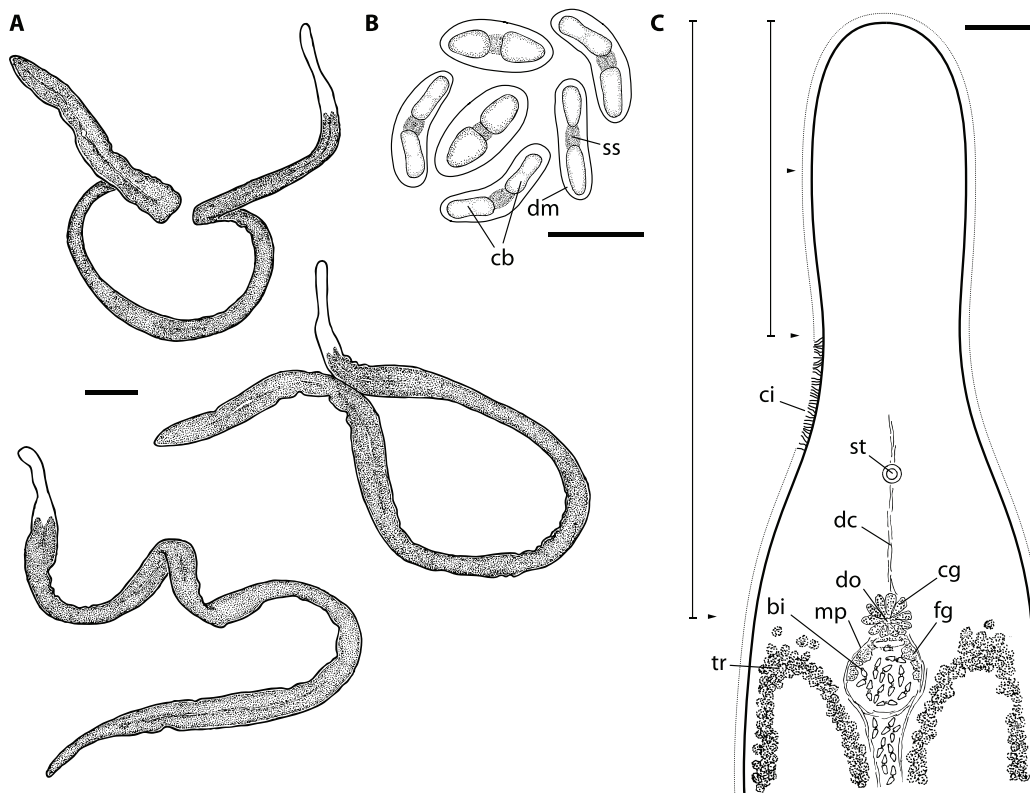


Figure 2. *Paracatenula galateia* sp. nov. A. Habitus of live specimens. B. Drawings of bipartite inclusions showing the conical to ladyfinger-shaped bodies (cb) connected by a short strand (ss) and surrounded by a dense matrix (dm). C. Morphology and organization of the rostrum showing the ciliated epidermis (ci), the monolithophorous statocyst (st), the dorsal cord (dc), the trophosome (tr), the dorsal opening (do) with surrounding gland cells with coarse granules (cg) adjacent to the muscular pouch (mp) which is filled with bipartite inclusions (bi) and has gland cells with fine granules (fg). The positions where measurements of width (arrowheads) and length (bars) were taken are indicated. Scale bars indicate 250 µm (A), 10 µm (B) and 50 µm (C).

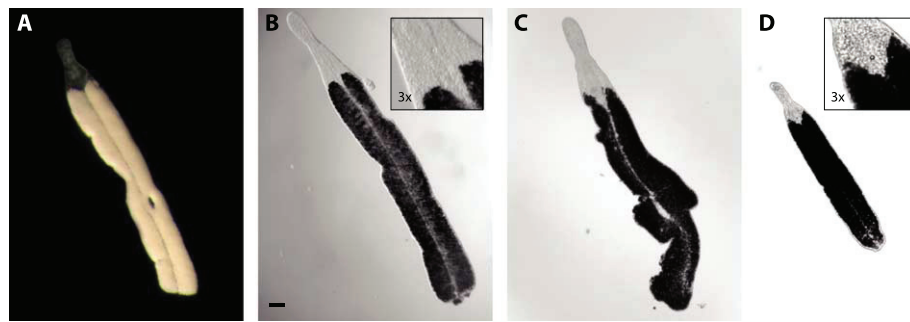


Figure 3. *Paracatenula galateia* sp. nov. Micrographs of live specimens. A. Incident light showing smooth silky appearance of trophosome. B. Transmitted light showing characteristic shape of extended rostrum and dorsal chord. C. Specimen with irregular outline and constriction. D. Small (juvenile?) specimen. Note position of the statocysts in inserts to B and D. A–D at same scale, bar indicates 100 μ m.

minimum diameter of 94–145 μ m (119 ± 14.9 μ m, $n = 19$). In 5 of 19 specimens studied in detail, the rostrum contained a monolithophorous statocyst (Figure 4) of 12.8 ± 0.63 μ m in diameter; the diameter of the statolith was 6.5 ± 0.43 μ m. In small (juvenile?) worms the statocyst lies close to the brain (Figure 3D), which nestles between the anterior tips of the two trophosome parts, whereas in large (adult?) animals it is in a more forward position (Figure 3B).

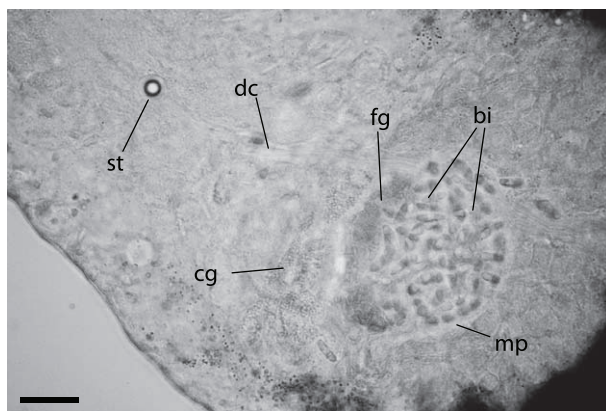


Figure 4. *Paracatenula galateia* sp. nov. Statocyst (st) anterior of brain connected to the dorsal cord (dc), gland cells with coarse granules (cg) adjacent to the muscular pouch (mp) filled with bipartite inclusions (bi) and gland cells with fine granules (fg). Scale bar 25 μ m.

Anatomy

A cross-section in the trophosome region (Figure 5) shows a thin (3.7–4.7 μ m thick), ciliated epidermis. The nuclei of the epidermis cells are sunk into the underlying muscle layer that consists of fine longitudinal and even finer circular muscle fibres (Figure 6A,B). Numerous dorsoventral muscle fibres run through the body. The ‘dorsal cord’ is a muscular strand that also contains the major longitudinal nerves. The remainder of the body is filled with the bacteriocytes. Approximately 50 bacteriocytes can be distinguished in a cross-section; each bacteriocyte contains numerous bacteria. The symbionts show different shapes in the section (Figure 7). When squeezed out of the worm, they attain a coccoid shape with a diameter of 8.26 ± 0.63 μ m ($n = 10$). The refractive granules are contained in vacuoles and are approximately 0.5 μ m in diameter.

The serotonergic nervous system (Figure 8) is centralized in a brain, which is located at the boundary of trophosome and rostrum. Originating in the brain, there are four nerve cords innervating the rostrum in an anterior direction, two on the dorsal and two on the ventral side. In the median of the DV-axis we find two prominent nerves originating in the brain that extend laterally and innervate the subepidermal or submuscular nerve nets. The region posterior to the brain has two kinds of nerves showing strong serotonin signals. There is a very strong staining of

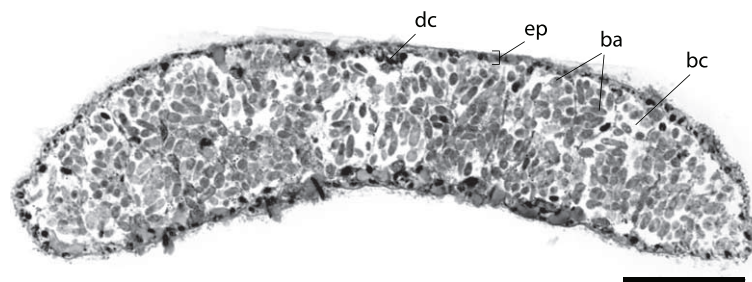


Figure 5. *Paracatenula galateia* sp. nov. Semi-thin cross-section through trophosome region showing the thin epidermis (ep), the dorsal cord (dc), the bacteriocytes (bc) filling most of the body and the symbiotic bacteria (ba) within the bacteriocytes. Scale bar 50 μ m.

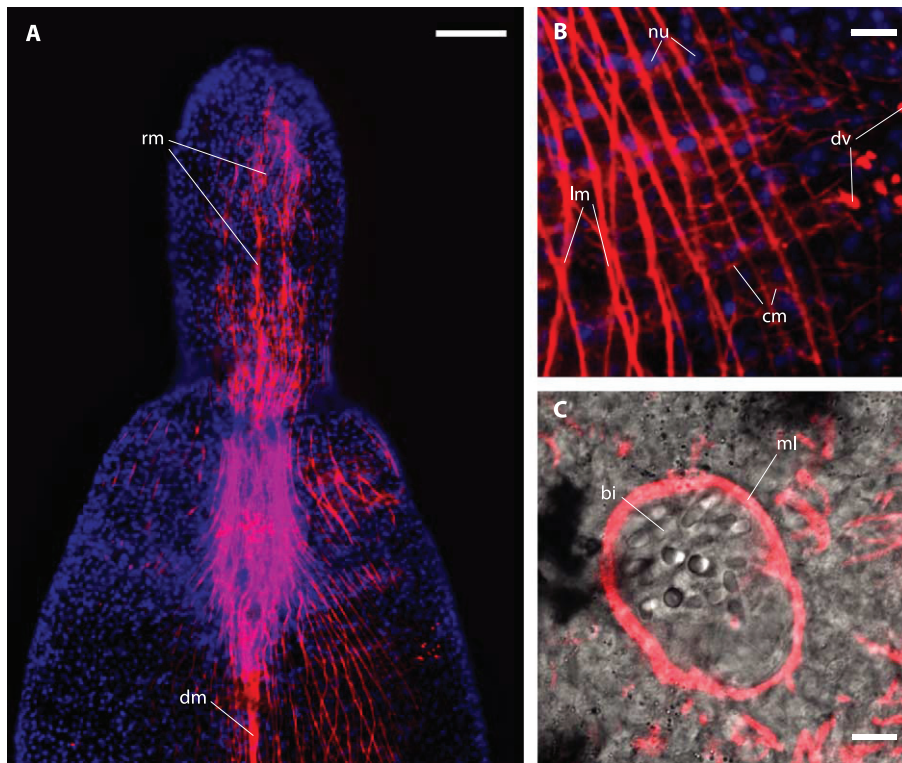


Figure 6. *Paracatenula galateia* sp. nov. Phalloidin staining of muscles. A. Anterior region showing rostrum muscles (rm) and dorsal cord muscles (dm) B. Detail showing longitudinal fibres (lm), thin circular fibres (cm), nuclei of the epidermis (nu) sunken into the muscle sheath and dorsoventral fibres (dv). C. Muscular layer (ml) surrounding the pouch that contains the bipartite inclusions (bi). Scale bars 50 μ m (A) and 5 μ m (B, C).

two main nerve cords that are direct extensions of the dorsal parts of the brain. These main nerves are associated with the ‘dorsal cord’ and extend through the entire posterior part of the worm. The other type of serotonergic nerve in the posterior part of the animal is the subepidermal or submuscular nerve net, which is ubiquitous and evenly distributed.

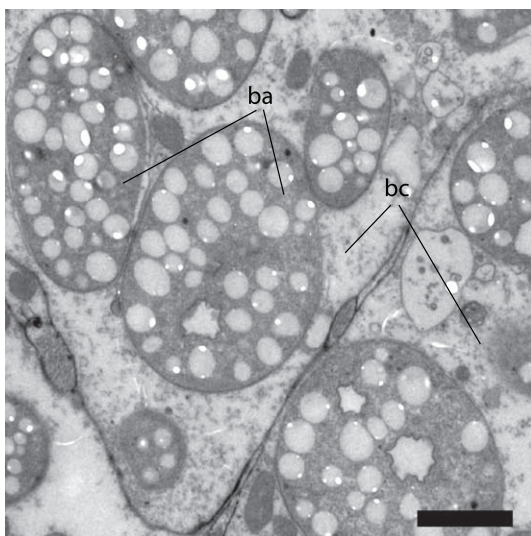


Figure 7. *Paracatenula galateia* sp. nov. symbiotic bacteria. TEM section of the trophosome region with several bacteria (ba) localized in a bacteriocyte (bc). Scale bar 2 μ m.

Cells containing characteristic bipartite inclusions (Figures 2B, 4, 6C, 9A,B), which could be interpreted as spermatozoa, were encountered in

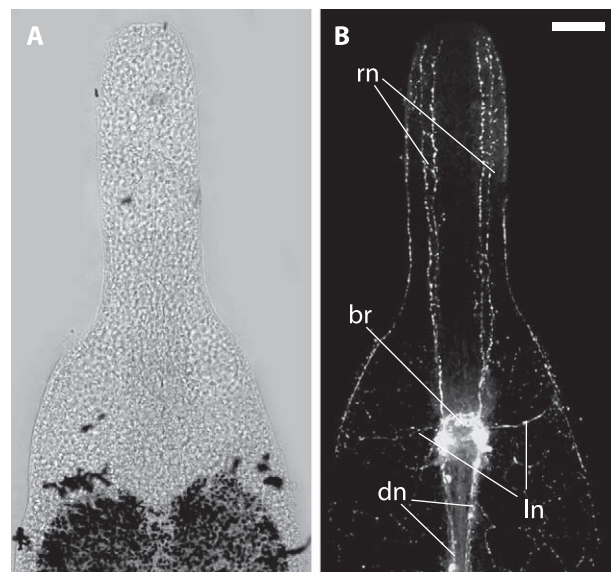


Figure 8. *Paracatenula galateia* sp. nov. Serotonin staining of the nervous system in the anterior region. A. Light micrograph of anterior end. B. Projection of several immunofluorescent micrographs of the same specimen showing the brain (br), rostrum nerves (rn), lateral nerves (ln) and dorsal cord nerves (dn). Scale bar 50 μ m.

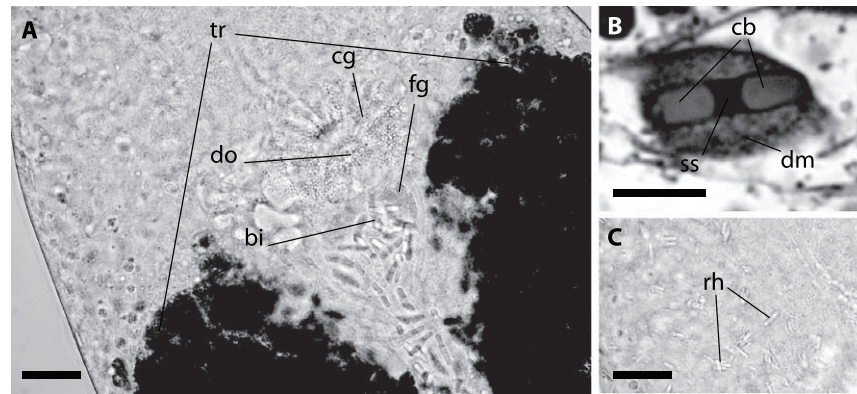


Figure 9. *Paracatenula galateia* sp. nov. bipartite inclusions and rhabdoids. A, Anterior end of trophosome (tr) region. Focus on dorsal side showing the bipartite inclusions (bi) along the dorsal chord and concentrated in the circular pouch with finely granulated glands (fg), the dorsal opening (do) and the surrounding glands with coarse granules (cg). B, Bipartite inclusion in a semi-thin section showing two slightly cone-shaped bodies (cb) connected by a short strand (ss) surrounded by a dense matrix (dm). C, Same region as A; focus on ventral side, showing bundles of rhabdoids (rh). Scale bars 25 μm (A, C) and 10 μm (B).

five of 19 large specimens. They are distributed throughout the trophosome region, especially along the dorsal cord (Figure 9A), but are concentrated behind the brain, between the anterior ends of the trophosome lobes, in a round pouch enclosed by a muscle layer (Figures 4, 6C, 9A), which we interpret as a *vesicula seminalis*. The rostral wall of the pouch is made up of fine-grained gland cells. Anterior and connected to this pouch there is a circular dorsal opening to the outside (genital

pore?), which is surrounded by gland cells containing coarse granules (Figure 9A).

The inclusion containing cells are oval, 20–24 μm long and 7–15 μm wide. The inclusions are made up of a pair of conical or ladyfinger-shaped bodies (Figure 2B, 4, 6C, 9A,B) that are arranged in either a straight line or at a 160° angle, without touching each other but joined together by a short bond; each pair measures 11.2–13.5 μm (mean 12.2 μm) in length and 2.6–3.6 μm (mean 3.0 μm) in width. The

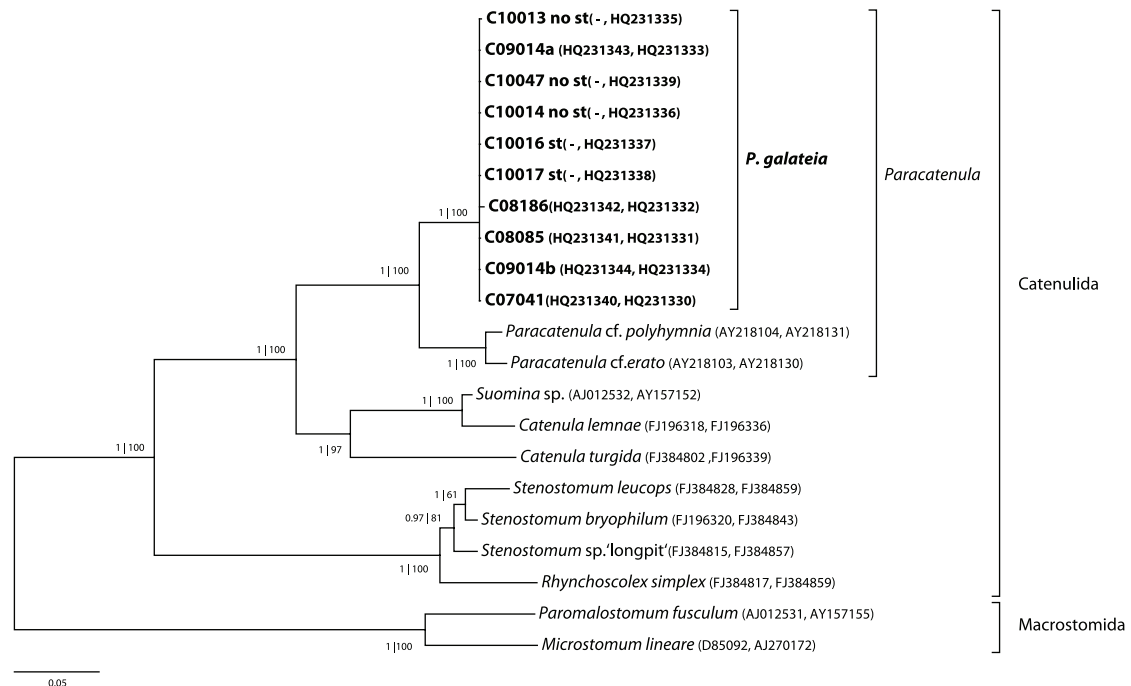


Figure 10. 18S and 28S rRNA-gene based phylogenetic reconstruction showing the position of the sequenced individuals of *P. galateia* sp. nov. in the Catenulida. The tree is based on the most likely PHYML tree (GTR + I + G model of substitution). Support in MrBayes and PHYML analysis is indicated (pp | aRLT) for each node. Microstomidae were used as outgroup. GenBank accession numbers are given in parentheses (first 18S and then 28S rRNA gene). Scale bar represents 5% estimated sequence divergence. st = statocyst.

Table I. Biometric comparison of the *Paracatenula* species.

	<i>P. galateia</i>	<i>P. urania</i>	<i>P. erato</i>	<i>P. polyhymnia</i>	<i>P. kalliope</i>
Maximal length	6 mm	3–7 mm	1.9 mm	0.83 mm	2.2 mm
Maximal width	271 µm	30 µm	100 µm	100 µm	170 µm
Cross section	Ribbon	Round?	Ribbon?	?	Ribbon
Rostrum	398 µm	220 µm	130 µm	200 µm	400 µm
Tail	No	No	?	100 µm	200 µm
Inclusion shape	Bipartite	Spindle	Spindle	Spicule	ribbon
Inclusion length	11–14 µm	10 µm	45 µm	34–36 µm	65 µm
Inclusion width	3 µm	1.5 µm	5 µm	1.5 µm	6 µm

conical or ladyfinger-shaped bodies are 3–6.1 µm long; the connecting bond is a 1.6–3.3 µm long electron-dense strand.

Bundles of 2–6 rhabdoids, rounded rods 10–12 µm long and 1–2 µm wide, may be found throughout the animal (Figure 9C).

Molecular phylogenetic analysis

Sequences of the 18S and 28S rRNA gene were obtained from 10 individuals of *Paracatenula galateia* sp. nov. They are highly similar, with 99.9% and 99.7% pairwise identity. Phylogenetic analysis based on a concatenated alignment of 18S and 28S rRNA genes from *Paracatenula galateia* and selected Catenulida as well as Macrostomida (Figure 10) shows that (1) our reconstruction of the Catenulida internal phylogeny supports the phylogeny presented by Larsson et al. (2008); (2) all sequences from the genus *Paracatenula* form one clade within the Catenulida; (3) sequences from *P. galateia* form a highly supported and well-separated cluster within the genus meriting the designation of a new species; and (4) there is no separation of sequences from individuals with statocyst to individuals without statocyst, showing that all specimens studied belong to the same species.

Discussion

The lack of mouth and pharynx together with the molecular data define the new species as belonging to the genus *Paracatenula*. *P. galateia* sp. nov. is the most massive species described so far. The width of the similarly long *P. urania* Sterrer and Rieger, 1974 is only a tenth of that of the new species. A comparison of biometric data is given in Table I. Furthermore, *P. galateia* sp. nov. is clearly distinguished from the four species described by Sterrer & Rieger (1974) by the structure of its ‘sperm nucleus’, which is spindle-shaped in *P. urania* and *P. erato*,

spicule-shaped in *P. polyhymnia* Sterrer & Rieger, 1974, and possibly ribbon-shaped in the lesser-known *P. kalliope* Sterrer & Rieger, 1974. The fact that in *P. galateia* sp. nov. the two ‘ladyfingers’ often diverge at a 160° angle might suggest an affinity with *P. polyhymnia* where the two arms of the spicules as a rule enclose a 160° angle (Sterrer & Rieger 1974, fig. 13g). However, the nature of the peculiar cells containing the variously shaped inclusions is still unclear. In *P. galateia* sp. nov. the location of the cells, and their concentration in a muscular pouch with a dorsal opening, strongly suggests them to be sperm. Attempts to stain the presumed nucleus with DAPI, however, failed. Most puzzling are the spicule shaped inclusions in *P. polyhymnia* and several other not yet described species (own unpublished observations) that seem to have a mineral nature.

Acknowledgements

This work was supported by the Austrian Science Fund (FWF) project 20394-B03 (JO, HG, NL and UD). We thank Renate Hodinka for suggesting the species name. Part of this work was carried out by using the resources of the Computational Biology Service Unit from Cornell University which is partially funded by The Microsoft Corporation. This is contribution 899 from the Carrie Bow Cay Laboratory, Caribbean Coral Reef Ecosystem Program, NMNH, Washington, DC.

References

- Anisimova M, Gascuel O. 2006. Approximate likelihood-ratio test for branches: A fast, Accurate, and powerful alternative. *Systematic Biology* 55:539–52.
- Borkott H. 1970. Geschlechtliche Organisation, Fortpflanzungsverhalten und Ursachen der sexuellen Vermehrung von *Stenostomum sthenum*; nov. spec. (Turbellaria, Catenulida). *Zoomorphology* 67:183–262.

- Dereeper A, Guignon V, Blanc G, Audic S, Buffet S, Chevenet F, et al. 2008. Phylogeny.fr: Robust phylogenetic analysis for the non-specialist. *Nucleic Acids Research* 36:W465–69.
- Doe D, Rieger RM. 1977. A new species of the genus *Retronectes* (Turbellaria, Catenulida) from the coast of North Carolina, U.S.A. *Mikrofauna des Meeresbodens* 66:1–10.
- Drummond A, Ashton B, Buxton S, Cheung M, Cooper A, Heled J, et al. 2010. Geneious v5.1, available from <http://www.geneious.com/>. Computer program.
- Faubel A. 1976. Eine neue Art der Gattung *Retronectes* (Turbellaria, Catenulida) aus dem Küstengrundwasser der Nordseeinsel Sylt. *Zoologica Scripta* 5:217–20.
- Guindon S, Dufayard J-F, Lefort V, Anisimova M, Hordijk W, Gascuel O. 2010. New algorithms and methods to estimate maximum-likelihood phylogenies: Assessing the performance of PhyML 3.0. *Systematic Biology* 59:307–21.
- Guindon S, Gascuel O. 2003. A simple, fast, and accurate algorithm to estimate large phylogenies by maximum likelihood. *Systematic Biology* 52:696–704.
- Katoh K, Kuma K-i, Toh H, Miyata T. 2005. MAFFT version 5: Improvement in accuracy of multiple sequence alignment. *Nucleic Acids Research* 33:511–18.
- Larsson K, Jondelius U. 2008. Phylogeny of Catenulida and support for Platyhelminthes. *Organisms Diversity & Evolution* 8:378–87.
- Loy A, Duller S, Baranyi C, Mussmann M, Ott J, Sharon I, et al. 2009. Reverse dissimilatory sulfite reductase as phylogenetic marker for a subgroup of sulfur-oxidizing prokaryotes. *Environmental Microbiology* 11:289–99.
- Noreña-Janssen C, Faubel A. 1996. *Myoretronectes paranaensis* n. gen. et sp., a new freshwater genus of the family Retronectidae (Turbellaria, Catenulida) from the Paraná, Argentina. *Hydrobiologia* 330:111–18.
- Nylander JAA. 2008. MrModeltest v2.3, Program distributed by the author, Evolutionary Biology Centre, Uppsala University. Computer program.
- Ott JA, Rieger G, Rieger R, Enderes F. 1982. New mouthless interstitial worms from the sulfide system: Symbiosis with Prokaryotes. *Publicazioni Stazione Zoologica Napoli I: Marine Ecology* 3:313–33.
- Pasteris JD, Freeman JJ, Goffredi SK, Buck KR. 2001. Raman spectroscopic and laser scanning confocal microscopic analysis of sulfur in living sulfur-precipitating marine bacteria. *Chemical Geology* 180:3–18.
- Pradillon F, Schmidt A, Peplies J, Dubilier N. 2007. Species identification of marine invertebrate early stages by whole-larvae in situ hybridisation of 18S ribosomal RNA. *Marine Ecology Progress Series* 333:103–16.
- Riedl R. 1959. Turbellarien aus submarinen Höhlen. I. Archioophora. *Publicazioni Stazione Zoologica Napoli Supplement* 30:178–208.
- Rieger PM. 1978. Multiple ciliary structures in developing spermatozoa of marine Catenulida (Turbellaria). *Zoomorphology* 89:229–36.
- Ronquist F, Huelsenbeck JP. 2003. MrBayes 3: Bayesian phylogenetic inference under mixed models. *Bioinformatics* 19:1572–74.
- Rützler K, Macintyre I. 1982. The Atlantic barrier reef ecosystem at Carrie Bow Cay, Belize, I. Structure and communities. Washington, DC: Smithsonian Institution Press. 539 pages.
- Schuchert P, Rieger RM. 1990. Ultrastructural examination of spermatogenesis in *Retronectes atypica* (Catenulida, Platyhelminthes). *Journal of Submicroscopical Cytology & Pathology* 22:379–87.
- Sterrer W. 1966. New polyolithophorus marine Turbellaria. *Nature* 210:436.
- Sterrer W, Rieger RM. 1974. Retronectidae – A new cosmopolitan marine family of Catenulida (Turbellaria). In: Riser N, Morse M, editors. *Biology of the Turbellaria*. New York, NY: McGraw-Hill, p 63–92.
- Tyler S, Schilling S, Hooge M, Bush L. 2006–2010. Turbellarian taxonomic database Version 1.6, available at <http://turbellaria.umaine.edu>.
- von Reumont B, Meusemann K, Szucsich N, Dell’Ampio E, Gowri-Shankar V, Bartel D, et al. 2009. Can comprehensive background knowledge be incorporated into substitution models to improve phylogenetic analyses? A case study on major arthropod relationships. *BMC Evolutionary Biology* 9:119.

Editorial responsibility: Tomas Cedhagen

V. *Paracatenula*, an ancient symbiosis between thiotrophic *Alphaproteobacteria* and catenulid flatworms

Authors: Harald Ronald Gruber-Vodicka, Ulrich Dirks, Nikolaus Leisch, Christian Baranyi, Kilian Stoecker, Silvia Bulgheresi, Niels Robert Heindl, Matthias Horn, Christian Lott, Alexander Loy, Michael Wagner and Jörg Ott

Publication status: published 2011 in *Proceedings of the National Academy of Sciences of the United States of America* Volume 108, Number 29, pages 12078-12083

Personal contributions of Harald Gruber-Vodicka

- a. designed the study together with JAO
- b. collected material on six field trips to Carrie Bow Caye (Belize), Dahab, Egypt, Lizard Island (Australia) and Elba (Italy)
- c. sequenced symbiont 16S, cbbL, apra and dsr genes and host 18S and 28S rRNA genes
- d. designed FISH probes
- e. performed all phylogenetic analyses, all statistical analyses and the element analyses based on energy dispersive x-ray analysis
- f. wrote the manuscript

Paracatenula, an ancient symbiosis between thiotrophic Alphaproteobacteria and catenulid flatworms

Harald Ronald Gruber-Vodicka^{a,1}, Ulrich Dirks^a, Nikolaus Leisch^a, Christian Baranyi^{b,2}, Kilian Stoecker^{b,3}, Silvia Bulgheresi^c, Niels Robert Heindl^{a,c}, Matthias Horn^b, Christian Lott^{d,e}, Alexander Loy^b, Michael Wagner^b, and Jörg Ott^a

Departments of ^aMarine Biology, ^bMicrobial Ecology, and ^cGenetics in Ecology, University of Vienna, A-1090 Vienna, Austria; ^dSymbiosis Group, Max Planck Institute for Marine Microbiology, D-28359 Bremen, Germany; and ^eElba Field Station, Hydra Institute for Marine Sciences, I-57034 Campo nell'Elba, Italy

Edited by Nancy A. Moran, Yale University, West Haven, CT, and approved May 31, 2011 (received for review April 8, 2011)

Harnessing chemosynthetic symbionts is a recurring evolutionary strategy. Eukaryotes from six phyla as well as one archaeon have acquired chemoautotrophic sulfur-oxidizing bacteria. In contrast to this broad host diversity, known bacterial partners apparently belong to two classes of bacteria—the *Gamma*- and *Epsilon*proteobacteria. Here, we characterize the intracellular endosymbionts of the mouthless catenulid flatworm genus *Paracatenula* as chemoautotrophic sulfur-oxidizing *Alphaproteobacteria*. The symbionts of *Paracatenula galateia* are provisionally classified as “*Candidatus Riegeria galateiae*” based on 16S ribosomal RNA sequencing confirmed by fluorescence in situ hybridization together with functional gene and sulfur metabolite evidence. 16S rRNA gene phylogenetic analysis shows that all 16 *Paracatenula* species examined harbor host species-specific intracellular *Candidatus Riegeria* bacteria that form a monophyletic group within the order *Rhodospirillales*. Comparing host and symbiont phylogenies reveals strict cocoladogenesis and points to vertical transmission of the symbionts. Between 33% and 50% of the body volume of the various worm species is composed of bacterial symbionts, by far the highest proportion among all known endosymbiotic associations between bacteria and metazoans. This symbiosis, which likely originated more than 500 Mya during the early evolution of flatworms, is the oldest known animal-chemoautotrophic bacteria association. The distant phylogenetic position of the symbionts compared with other mutualistic or parasitic *Alphaproteobacteria* promises to illuminate the common genetic predispositions that have allowed several members of this class to successfully colonize eukaryote cells.

intracellular symbiosis | marine catenulid | meiofauna | subtidal sand

Marine catenulid flatworms of the genus *Paracatenula* have no mouth or gut (1). Instead, they harbor intracellular microbial endosymbionts in bacteriocytes (2) that form a tissue known as the trophosome (Fig. 1A) in functional analogy to the trophosome of the mouthless Siboglinidae (Annelida) (3). The trophosome almost completely fills the posterior part of the body behind the brain (2, 3). The worms inhabit the interstitial space of warm temperate to tropical subtidal sands together with other animals such as nematodes, gutless oligochaetes, and lucinid or solemyid bivalves that all harbor chemoautotrophic sulfur-oxidizing bacteria (SOB). By migrating through the redox potential gradient in the uppermost 5- to 15-cm sediment layer, millimeter-sized worms can supply chemoautotrophic symbiotic bacteria alternately with spatially separated electron donors and acceptors such as sulfide and oxygen, as has been described for Nematoda and Oligochaeta (4, 5).

Chemosynthetic carbon fixation by using reduced sulfur compounds (i.e., thiotrophy) is widespread in free-living members of the microbial domains *Bacteria* and *Archaea*. This metabolic capability has been found in members of the *Actinobacteria*, *Aquificae*, *Bacilli*, *Chloroflexi*, *Chlorobi*, and *Spirochaeta*, and all classes of the *Proteobacteria* and the archaeal order *Sulfolobales*. One archaeon, “*Candidatus Giganthauma karukerense*” (6), as well as

a wide range of protists and animals, including Ciliata (e.g., *Zoothamnium*), Nematoda (*Stilbonematinae* and *Astomonema*), Arthropoda (*Rimicaris* and *Kiwa*), Annelida (e.g., *Riftia* or *Olivinus*), along with bivalve and gastropod Mollusca (e.g., *Solemya* or *Neomphalina*; reviewed in ref. 7), have established themselves as hosts in symbioses with SOB. They all derive some or all of their energy demands from the primary production of the symbionts (7). Interestingly, despite this great taxonomic variety of hosts—from habitats as divergent as deep-sea hydrothermal hot vents, cold seeps, whale or wood falls, and peat and shallow-water sediments—the SOB symbiont diversity seemed to be limited to *Proteobacteria* of the *Gamma* and *Epsilon* classes (7). Here, we present evidence that the symbionts of *Paracatenula* form an ancient clade of sulfur-oxidizing *Alphaproteobacteria* that are strictly coevolved with their hosts and that equal host biomass in the consortium.

Results and Discussion

The body plan of *Paracatenula* suggests that the symbionts make up a substantial proportion of the worms. To specify symbiont-to-host tissue ratios, cross-sections in the trophosome region of three species of *Paracatenula* were analyzed by transmission EM (TEM). The symbionts make up 36.7% of the cross section area in *Paracatenula galateia* (3) (Carrie Bow Cay, Belize), 41.2% in *P. cf. galateia* (Dahab, Egypt), and 51.9% in *P. cf. polyhymnia* (Dahab, Egypt; Fig. S1). The symbiont-housing trophosome region accounts for 90% to 98% of the total worm length: multiplying these two factors, we roughly estimate symbiont-to-host tissue ratios of 33% in *P. galateia*, 40% in *P. cf. galateia*, and 50% in *P. cf. polyhymnia*. These are the highest proportions of all known endosymbioses between bacteria and metazoans, far higher

Author contributions: H.R.G.-V., S.B., N.R.H., M.H., A.L., M.W., and J.O. designed research; H.R.G.-V., U.D., N.L., C.B., K.S., C.L., and J.O. performed research; M.W. contributed new reagents/analytic tools; H.R.G.-V., U.D., N.L., C.B., K.S., and J.O. analyzed data; and H.R.G.-V. wrote the paper.

The authors declare no conflict of interest.

This article is a PNAS Direct Submission.

Freely available online through the PNAS open access option.

Data deposition: The sequences reported in this paper have been deposited in the GenBank database [accession nos. HQ689139 (*aprA*); HQ840958 (*cbmM*); HQ689138 (*dsrAB*); HQ689029–HQ689053, HQ689087–HQ689095, HQ689123, HQ689124, HQ689128, HQ689129, and HQ845108–HQ845110 (16S rRNA); HQ689054–HQ689068, HQ689096–HQ689108, HQ689125, and HQ689130–HQ689133 (18S rRNA); and HQ689069–HQ689086, HQ689109–HQ689122, HQ689126, HQ689127, and HQ689134–HQ689137 (28S rRNA)].

¹To whom correspondence should be addressed. E-mail: harald.gruber@univie.ac.at.

²Present address: Department of Marine Biology, University of Vienna, A-1090 Vienna, Austria.

³Present address: Project Group Bioresources, Fraunhofer Institute for Molecular Biology and Applied Ecology, D-35394 Giessen, Germany.

This article contains supporting information online at www.pnas.org/lookup/suppl/doi:10.1073/pnas.1105347108/-/DCSupplemental.

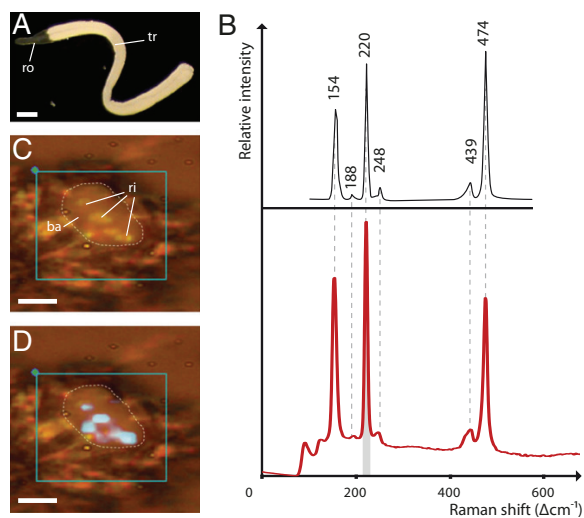


Fig. 1. Sulfur storage in *Candidatus Riegeria galateiae*. (A) Living specimen of *P. galateia*, with *Cand. Riegeria galateiae* endosymbionts in trophosome (tr) appearing white in incident light in contrast to the bacteria-free rostrum (ro). (Scale bar: 250 μm .) (B) Raman spectrum of individual cellular inclusion (red) with reference spectrum (black) of elemental sulfur in S_8 ring configuration. (C) Air-dried *Cand. Riegeria galateiae* cell (ba) with light refractile inclusions (ri). (Scale bar: 5 μm .) (D) Mapping of the Raman sulfur spectrum peak indicated in B in gray onto C, with the mapped area indicated with turquoise rectangle. (Scale bar: 5 μm .)

than, e.g., in the deep-sea tubeworm *Riftia pachyptila*, in which bacteria make up only 24.1% of the trophosome, which in turn occupies less than one third of the body volume (8). The exceptional proportion of bacterial biomass in this intracellular symbiosis questions the common view that animals exploit the metabolic skills of their microbial partners because the *Paracatenula* worms in return appear to serve as a protective vehicle for their symbionts.

The bacteria of all *Paracatenula* species contain highly light refractive spherical inclusions (0.5–2 μm in diameter), which render the bacteria white in incident light (Fig. 1A). This white coloring, typical for SOB that store elemental sulfur (9), was an initial clue that the symbionts could be sulfur oxidizing (2). We selected the symbionts of *P. galateia* for a detailed analysis because the worms are abundant, comparatively large, and morphologically distinct (3). Sulfur oxidizing capabilities were assessed by examining sulfur storage and functional genes used in thiotrophy. All inclusions of extracted symbiont cells from *P. galateia* analyzed by Raman microspectroscopy consist of elemental sulfur in S_8 ring configuration (Fig. 1B–D). Energy dispersive X-ray microanalysis shows that in the trophosome this bacterial sulfur storage can make up 5% to 19% of the tissue mass (Fig. S2). In many SOB that store elemental sulfur, the sirohaem dissimilatory sulfite reductase (i.e., DsrAB) enzyme system functioning in reverse is an important part of the sulfur oxidation machinery (10). Our phylogenetic analysis of a collection of dissimilatory sulfite reductase (i.e., DsrB) sequences from SOB, including the sequence of the *P. galateia* symbionts determined in the present study, demonstrates that the sequences of *Paracatenula* symbionts form a well supported monophyletic clade with sequences from other thiotrophic *Alphaproteobacteria* [approximate likelihood-ratio test (aLRT), 0.90; posterior probability (pp), 1.00; Fig. S3]. This corroborates the results from a previous study placing the DsrAB sequences from bacteria associated with two species of *Paracatenula* together with sequences of the alphaproteobacterial genus *Magnetospirillum*, albeit with weak node support (10). Additionally, the

gene coding for AprA, the α -subunit of dissimilatory adenosine-5'-phosphosulfate (APS) reductase, another key enzyme in sulfur energy metabolism, was partially sequenced for the *P. galateia* symbionts. APS reductase is used by SOB to oxidize sulfite to APS and by sulfate-reducing microorganisms to reduce APS to sulfite (11). The symbionts' AprA sequence clusters with the AprA lineage II of SOB with good statistical support (aLRT, 0.89; pp, 1.00; Fig. S4). The Calvin–Benson–Basham pathway with ribulose-1,5-bisphosphate carboxylase/oxygenase (RubisCO) as the central enzyme is a key mechanism of carbon fixation in autotrophic organisms (12). The partial sequence coding for RubisCO form II (CbbM) sequenced for the *P. galateia* symbionts is related to sequences from the alphaproteobacterial genus *Magnetospirillum* and other chemoautotrophs (Fig. S5).

Taken together, three lines of evidence point to a chemoautotrophic sulfur-oxidizing lifestyle of the symbionts: (i) the habitat that *P. galateia* shares with many other hosts of thiotrophic bacteria, (ii) intracellular storage of elemental sulfur by the symbionts, and (iii) the presence of *cbbM* as well as *dsrAB* and *aprBA*, both related to sequences from SOB, in the symbionts' genome.

16S rRNA gene based approaches were used to assess the diversity within and between the symbiont populations of individual worms of *Paracatenula galateia*. The PCR products obtained separately from 10 specimens using general bacterial 16S rRNA gene primers comprise the same phylotype based on (i) clone libraries, (ii) direct sequencing, and (iii) denaturing gradient gel electrophoresis (DGGE) analysis [pairwise identity of 99.7–100; a species-level phylotype threshold of $\geq 99\%$ 16S rRNA gene sequence identity was used (13)]. According to the ribosomal database project classifier (14) and our comprehensive phylogenetic analysis (as detailed later), this bacterial phylotype is a member of the alphaproteobacterial order *Rhodospirillales* (Fig. 2). FISH with a phylogenetically nested probe set specifically targeting most *Bacteria*, most *Alphaproteobacteria*, and the symbiont confirms that *P. galateia* contains only one alphaproteobacterial species-level phylotype (Fig. 3).

To infer host specificity of the symbionts from different *Paracatenula* hosts and to elucidate the symbionts' evolutionary relationships, we sequenced symbiont 16S rRNA genes from additional 31 worms belonging to 15 species, all morphologically distinct from *P. galateia*: five species from the Caribbean Sea (Carrie Bow Cay,

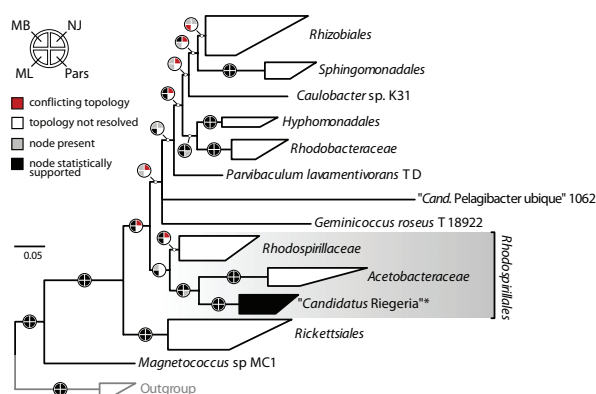


Fig. 2. Phylogeny of the family level *Candidatus Riegeria* clade in the *Alphaproteobacteria*. Based on comparative 16S rRNA gene analysis, the *Cand. Riegeria* clade is the sister group of the family *Acetobacteraceae* within the order *Rhodospirillales*. The tree shown was estimated by using MrBayes (MB), and node support is additionally indicated for three alternative methods (NJ, neighbor joining; Pars, parsimony; ML, maximum likelihood). **Cand. Riegeria* clade; the detailed phylogeny of this clade is shown in Fig. S6. (Scale bar: 5% estimated sequence divergence.)

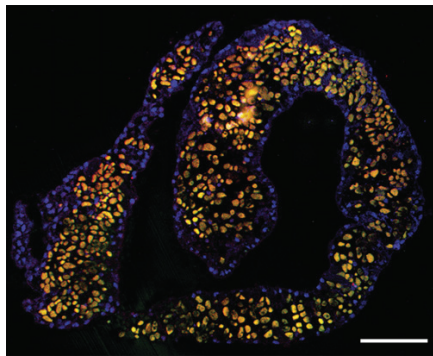


Fig. 3. *Candidatus Riegeria galateiae* in the host trophosome. Laser scanning confocal micrograph of FISH on LR-White cross-section; Overlay of three images with a bacteria-specific probe (green), symbiont-specific probe (red), and eukaryote-specific probe (blue). Because of the overlay of colors, the symbionts appear in yellow. (Scale bar: 50 μ m.)

Belize), one from the Mediterranean Sea (Elba, Italy), five from the Red Sea (Dahab, Egypt), and four from the Pacific Ocean (Lizard Island, Australia). Our 16S rRNA gene-based tree of the *Alphaproteobacteria* (Fig. 2) is largely congruent with the topologies presented in recent phylogenomic studies of this class (15, 16). The placement of the symbiont sequences shows that (i) the symbionts form a distinct and well supported sister clade to the *Acetobacteraceae* within the order *Rhodospirillales* (Fig. 2), (ii) the symbionts are present in all worms (Fig. S6), and (iii) each host species harbors only one phylotype, which is specific for the respective host (Fig. S6). Based on these phylogenetic data and our detailed metabolic analysis, we propose the provisional classification (17) “*Candidatus Riegeria galateiae*” for the symbionts of *P. galateia*. Short description is as follows: coccoid alphaproteobacterium of the order *Rhodospirillales*, 5 to 8 μ m in diameter with intracellular storage of elemental sulfur, present in bacteriocytes of the catenulid flatworm *Paracatenula galateia*. The basis of assignment is as follows: 16S rRNA gene, *cbbM*, *dsrAB*, and *aprA* sequences (HQ689043, HQ840958, HQ689138, and HQ689139, respectively) and hybridization with the phylotype-specific oligonucleotide probe PAR1151 (5'-CTT GTC ACC GGC AGT TCC CTC-3').

Riegeria refers to the late zoologist Reinhard Rieger, who described the host genus, together with W. Sterrer (1); and *galateiae* to its specific flatworm host *P. galateia*.

Our phylogenetic analysis also revealed that only a single 16S rRNA sequence in public databases (GQ402753) belongs to the clade of *Paracatenula* symbionts (Fig. S6). This clone was retrieved from a permanently waterlogged tropical peat swamp forest sample in Thailand (18), but only scarce details are available for the sample.

The maximum 16S rRNA gene sequence divergence within the symbiont clade is 12.7%, and members of the clade show a minimum sequence divergence of 11.5% to the next described relative *Elioraea tepidiphila* TU-7 (EF519867). This high degree of phylogenetic distinctness is in the range reported for other proteobacterial families (19) and would thus merit, from a 16S rRNA-based point of view, the proposal of a family within the *Rhodospirillales* to classify the *Paracatenula* symbionts.

With the exception of the genus *Paracatenula*, all groups of Catenulida have a cosmopolitan distribution ranging from tropical to cold temperate; several species of the marine catenulid genus *Retronectes*, which have no chemosynthetic symbionts, have been found as far north as Kristineberg on the Swedish west coast (1, 20). As all cultured *Rhodospirillales* related to the symbionts are mesophilic or slightly thermophilic (21), it is tempting to speculate that the limitation of *Paracatenula* to warm temperate or tropical waters reflects the temperature requirements of its symbionts.

To molecularly characterize the different hosts, we sequenced their 18S and 28S rRNA genes. Our phylogenetic analysis corroborates the placement of *Paracatenula* within the Catenulida as the monophyletic sister clade to the limnic *Catenula/Suomina* species complex (20) (Fig. S7). A strict consensus tree based on several phylogenetic methods using all hosts with both 18S and 28S rRNA genes sequenced (15 species) is highly congruent to the 16S rRNA gene tree obtained for their symbionts (Fig. 4). Bayesian inference-based reconstructions for this dataset are fully resolved on the host species level and completely congruent between host and symbiont (Fig. S6). The cocladogenesis of both groups indicates that a common ancestor of the host worms had acquired an alphaproteobacterial progenitor of the *Cand. Riegeria* clade and that this association has been stably maintained up to the present day by vertical transmission of the symbionts from one host generation to the next (22). In chemoautotrophic associations, vertical symbiont transmission has been reported

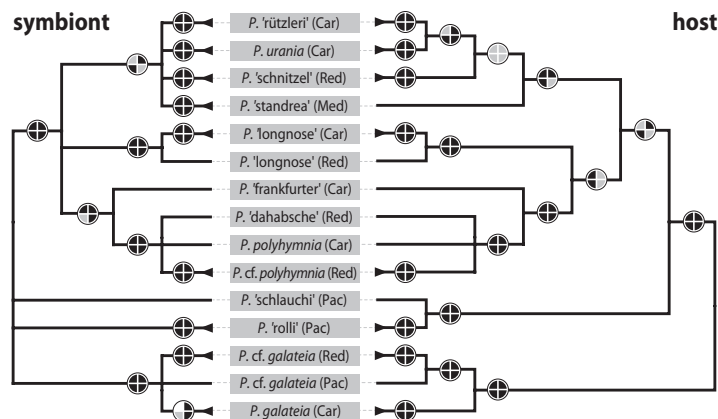


Fig. 4. Cocladogenesis between *Paracatenula* and *Candidatus Riegeria*. Tanglegram of strict consensus cladograms of four reconstruction methods for both symbiont 16S rRNA and host concatenated 18S and 28S rRNA. Node support is indicated as in Fig. 3. Provisional working names for undescribed species are given in parentheses. Sample origins: Car, Caribbean Sea; Med, Mediterranean Sea; Red, Red Sea; Pac, Pacific Ocean. No conflicting nodes are statistically supported in the results of the four phylogenetic reconstruction algorithms, indicating close coevolution between the partners.

only for the deep-sea clam family Vesicomidae (23). Recent studies, however, have shown that host–symbiont phylogenies are decoupled for some vesicomid clams, suggesting a mixed mode of symbiont transmission with vertical transmission occasionally interrupted with lateral symbiont acquisition (24, 25). Vertically transmitted symbionts tend to have an accelerated nucleotide substitution rate compared with free-living bacteria (26, 27). Sequence divergence of 16S rRNA for inheritable symbionts averages approximately 4% for every 100 million years (Ma), ranging from 2.5% to 11%, whereas free-living bacteria have rates ranging from 2% to 4% for 100 Ma (26, 28, 29). Based on this range of rates, the symbiosis in the ancestor of *Paracatenula* was established between 100 and 635 Mya. The maximum estimated divergence time for flatworms is 620 Ma and must be used as the maximum age of this symbiosis (30). As the *Cand. Riegeria* symbionts have no detectable nucleotide substitution rate heterogeneity in their 16S rRNA gene sequences compared with free-living *Acetobacteraceae* (Tajima rate test, $P > 0.05$ for all *Cand. Riegeria* against the *Acetobacteraceae* used in the phylogenetic analysis), we suppose a divergence rate of 2.5% in the phylogenetic analysis, we suppose a divergence rate of 2.5% in the phylogenetic analysis, we suppose a divergence rate of 2.5% in the phylogenetic analysis. This delimits the estimated age to 500 to 620 Ma. In comparison, the ancient solemyid and lucinid bivalve lineages in which all living taxa harbor chemoautotrophic symbionts have a paleontological record dating back to the late Ordovician/early Silurian 445 to 435 Mya (31). Even with the uncertainties involved when using evolutionary rates established for other groups of symbionts (29), the *Cand. Riegeria*–*Paracatenula* association can be considered the oldest known mutualistic bacteria–metazoan symbiosis, likely dating back to the early evolution of bilaterian diversity in the late Ediacaran/early Cambrian.

Coevolving inherited endosymbionts tend to have guanine and cytosine (GC) depleted genomes (27, 32). The alphaproteobacterial families closely related to the *Cand. Riegeria* clade, the *Acetobacteraceae* and *Rhodospirillaceae*, have a very high genomic guanine and cytosine content (gGC; 60–71% and 62–69%, respectively). Although there are no gGC data for *Cand. Riegeria galatiae* yet, the *dsrAB*, *aprA*, and *cbmM* genes combined have a GC content of 51.4%. This significantly lower GC content compared with closely related free-living groups has two possible non mutually exclusive explanations: (i) the intracellular symbiosis has relieved the symbionts from the selection pressure that leads to the high gGC in *Rhodospirillales* and the symbiont gGC therefore decreased to approximately 50%; or (ii) population bottlenecks leading to high genetic drift (33) have been driving the nucleotide bias in *Cand. Riegeria galatiae*, but at a much slower pace compared with that documented in the less than 50 Ma old symbiosis in vesicomid clams (symbiont genome sizes of 1.02–1.16 Mb, gGC of 31.6–34%; closely related free-living *Thiomicrospira crunogena* genome size, 2.43 Mb, gGC of 43.1%) (23, 34, 35). The close coevolution of *Paracatenula* and *Cand. Riegeria*, in which each host maintains a monoculture of its specific symbiont, will allow comparative genomic studies to test these hypotheses and other theoretical predictions of genome evolution developed for intracellular symbionts (36). Moreover, this ancient clade of endosymbionts, with their distant phylogenetic position and their different function compared with other symbiotic *Alphaproteobacteria*, could help illuminate the common genetic predispositions that have allowed several members of this class to become successfully incorporated into eukaryotic cells—be it as intracellular parasites such as members of the order *Rickettsiales* or mutualists such as members of the order *Rhizobiales* or of the *Cand. Riegeria* clade.

Methods

TEM. TEM specimens were fixed in glutaraldehyde, postfixated with osmium tetroxide, and, after dehydration, embedded in Low Viscosity Resin (Agar Scientific). Complete ultrathin cross-sections mounted on formvar-coated slot

grids were poststained with uranyl acetate and lead citrate. To estimate tissue ratios, digital images of the sections were merged and host and bacterial tissue were digitally traced into vector-based black and white representations. Area calculations were performed with ImageJ software based on these trace images using the “analyze particles” function.

SEM and Energy-Dispersive X-Ray Microanalysis. Specimens were immediately fixed as for TEM analysis. The samples were partly dehydrated in an acetone series up to 75% to preserve a maximum amount of sulfur (37). The samples were embedded in Spurr epoxy resin. Semithin cross sections (2.5 μm) of embedded samples were cut, mounted on carbon-padded stubs, and carbon-coated. The analysis was carried out on a Philips XL20 SEM with an EDAX P-505 sensor using EDAX eDXi V2.11 software. Sulfur was mapped against carbon and at least two other elements prominent in the given spectrum (e.g., phosphorous and osmium) to rule out structural and edge effects.

Raman Microspectroscopy. Extracted symbiont cells of PFA-fixed specimens were mounted on a calcium fluoride slide and analyzed with a LabRAM HR800 confocal Raman microspectroscopy (HORIBA Jobin-Yvon). A 532-nm Nd:YAG laser provided the excitation for Raman scattering. Cells were selected haphazardly using a 50 \times objective, and the signal was acquired over a period of 5 s using a D0.6 intensity filter. The pinhole of the Peltier-cooled CCD detector was adjusted to 250 μm (optical slice, 4.6 μm). Spectra were measured between 0 and 2,000 cm^{-1} . They were baseline-corrected and normalized with LabSpec software 5.25.15 (HORIBA Jobin-Yvon). Reference spectra for elemental sulfur in S_8 ring configuration (Merck) were obtained by using the same settings and methods.

DNA Extraction, PCR Amplification, and Sequencing. DNA was extracted from individual worms by using the Blood and Tissue DNA extraction kit (Qiagen), and 2 μL of each extraction were used as PCR templates. Symbiont 16S rRNA-gene fragments (approximately 1,500 nt) were amplified with bacterial primers 616V (5'-AGAGTTTGATYMTGGCTC-3') (38) and 1492R (5'-GGYACCT-GTTACGACTT-3') (39). PCR products were purified by using the MinElute PCR purification kit (Qiagen) and either directly sequenced with the PCR primers or cloned by using pCR2.1-TOPO and the TOPO TA Cloning Kit (Invitrogen Life Technologies). Host 18S and 28S rRNA-gene fragments (approximately 1,750 and 1,350 nt long, respectively) were amplified for each worm with general eukaryote primers 1f (5'-CTGGTTGATYTGCCAGT-3') and 2023r (5'-GGTTC-ACCTACGGAACC-3') for 18S (40) and the primers D1a (5'-CCSCGTAAYTT-AAGCATAT-3') and D5b2 (5'-CGCCAGTTCTGCTACC-3') for 28S (41). PCR products were purified as described earlier and directly sequenced with the PCR primers. From *P. galatiae* samples, *aprBA* was amplified with primers AprB-1-FW (5'-TGCGTGATAYATHGYCC-3') (11) and AprA-9-RV (5'-CKGWAG-TAGTARCCSGGSYA-3') (42), *dsrAB* was amplified with primers rDSR1fA (5'-AARGNTAYTGGAARG-3') and rDSR4Rb (5'-GGRWARCAIGCNCRCRA-3') (10), and *cbmM* was amplified with shortened primers after Blazejak et al. (43): CbbMF_bl_s (5'-ATCATCAARCCSAARCTSGGYC-3') and CbbM1R_bl_s (5'-SGC-RCRTGRCCRCGCMC-3'). We used touchdown PCR cycling programs for *cbmM*, *aprBA* and *dsrAB* as described for *aprBA* in Meyer and Kuever (42). The 395 nt-long *cbmM* fragment was directly sequenced by using the PCR primers, whereas the *aprBA* (2,178 nt) and *dsrAB* (1,911 nt) PCR products were gel purified using the MinElute gel extraction kit (Qiagen) and cloned as described earlier. For all cloned products, at least four clones were randomly picked and fully sequenced with the vector-specific primers M13F and M13R; for *aprBA* and *dsrAB*, we additionally used internal sequencing primers AprA-1-FW and AprB-5-RV (42) and DSR874F (10).

DGGE Analysis. DGGE analysis of 16S rRNA genes was performed as described by Meyer et al. (44). In every lane, only one band was observed, which was excised from the DGGE gel, and gel slices were stored in 50 mL MQ overnight at 4 $^{\circ}\text{C}$. One microliter of this elution was used as a template for PCR reamplification using the forward primer (341f) without the GC clamp. Reamplified DNA was purified and directly sequenced as described above.

rRNA Gene Based Phylogenetic Analyses. A 16S rRNA gene dataset for *Alphaproteobacteria* was constructed including 41 *Cand. Riegeria* sequences, three BLAST (45) hits from GenBank longer than 1,400 bp with sequence identities more than 89% to *Cand. Riegeria galatiae* (FJ152947, EU440696, and GQ402753), all *Alphaproteobacteria* with completely sequenced genomes used in a previous phylogenomic study (16), and sequences for landmark genera of cultivated *Rhodospirillales*. Table S1 provides details on the *Cand. Riegeria* 16S rRNA sequences used, including accession numbers. Table S2 provides accession numbers of sequences from reference *Alphaproteobacteria* and the deltaproteobacterial outgroup. The sequences were

aligned by using MAFFT Q-INS-i, which considers the secondary structure of RNA (46), and the alignments were trimmed at the 5' and 3' ends. We evaluated the optimal substitution model of sequence evolution with MrModeltest (47), and the general time-reversible (GTR) model with invariable sites (I) and a γ -correction for site-to-site rate variation (G) model was selected using the Akaike information criterion. No filters based on sequence conservation were used. We reconstructed the phylogenies using neighbor joining-, parsimony- (both MEGA 4 software) (48), maximum likelihood- (PHYML; phylogeny.fr Web service) (49, 50), and Bayesian inference-based (MrBayes) (51) algorithms. MrBayes was run for 5 million generations and trees were sampled every 1,000 generations after a burn-in of 40%. Node stability was evaluated using bootstrap (1,000 \times neighbor joining and parsimony), pps (Bayesian inference), and aLRT [maximum likelihood (52, 53)]. Bootstrap support of at least 70%, aLRT of at least 80%, and posterior probabilities of at least 0.80 were considered statistically significant. Strict consensus trees were constructed by collapsing all nodes conflicting in different phylogenetic methods up to the lowest node supported by all methods.

18S and 28S rRNA gene datasets were constructed from *Paracatenula* host sequences and from selected Catenulida sequences available in GenBank, with sequences of rhabditophoran flatworms (Macrostomida) as outgroup. Accession numbers of all sequences are shown in Fig. S7 and Table S1. The 18S and 28S rRNA gene datasets were separately aligned and trimmed as for the 16S gene analysis. Substitution models were evaluated for each gene, and the GTR+I+G model was selected for both. We concatenated the alignments and then reconstructed and evaluated the phylogenies as described earlier for 16S rRNA genes.

Phylogenetic Analyses of DsrB, AprA, and CbbM. Analyses of all genes were based on amino acid translations by using MAFFT alignments of full-length reference sequences obtained from available genomes and partial, PCR-amplified fragments. The optimal Wehlan and Goldman substitution model

(WAG) for the DsrB alignment (500 aa positions; WAG+G), the AprA alignment (376 aa positions; WAG+G+I), and the CbbM alignment (478 aa positions; WAG+G+I) was evaluated with MrModeltest. Phylogenies were reconstructed for all genes using PHYML as well as MrBayes (3 million generations, 1 million burn-in). Node support in all gene trees is indicated for the ML analysis by using PHYML (aLRT) and Bayesian inference (pp). aLRT of at least 80% and posterior probabilities of at least 0.80 were considered statistically significant.

FISH. We designed oligonucleotide FISH probes by using the arb probe design tool included in the arb software package (54) (Table S3) and evaluated their specificity in silico by using the probe match tool probeCheck (55). Fluorescently labeled probes were purchased from Thermo, and FISH was performed according to Manz et al. (56) as adapted for LR-white resin (British BioCell International) sections described in Nussbaumer et al. (57). As a negative control, a nonsense probe (NON-338) was used. To determine stringent hybridization conditions for the PAR1151 probe, a formamide series was conducted by using *Cand. Riegeria galateiae* cell extractions. All FISH experiments were examined by using a Leica TCS-NT confocal laser-scanning microscope.

ACKNOWLEDGMENTS. We thank the Core facility for Cell Imaging and Ultrastructural Research at the University of Vienna and M. Stachowitsch. This work was supported by Austrian Science Fund Projects P17710 (to S.B. and N.R.H.), P20185 (to A.L.), P20394 (to H.R.G.-V., U.D., and J.O.), P20775 (to K.S.), and Y277-B03 (to M.H.) and is contribution 902 from the Carrie Bow Cay Laboratory, Caribbean Coral Reef Ecosystem Program, National Museum of Natural History, Washington, DC. Part of this work was carried out with the use of the resources of the Computational Biology Service Unit of Cornell University, which is partially funded by Microsoft Corporation.

1. Sterrer W, Rieger RM (1974) Retronectidae - a new cosmopolitan marine family of Catenulida (Turbellaria). *Biology of the Turbellaria*, eds Riser N, Morse M (McGraw-Hill, New York), pp 63-92.
2. Ott JA, Rieger G, Rieger R, Enderes F (1982) New mouthless interstitial worms from the sulfide system: Symbiosis with Prokaryotes. *Pubblazioni Stazione Zoologica Napoli I. Mar Ecol (Berl)* 3:313-333.
3. Dirks U, Gruber-Vodicka HR, Leisch N, Sterrer WE, Ott JA (2011) A new species of symbiotic flatworms, *Paracatenula galateia* n. sp. (Platyhelminthes: Catenulida: Retronectidae) from Belize (Central America). *Mar Biol Res*, 10.1080/17451000.2011.574880.
4. Ott JA, et al. (1991) Tackling the sulfide gradient: A novel strategy involving marine nematodes and chemoautotrophic ectosymbionts. *Pubblazioni Stazione Zoologica Napoli I. Mar Ecol (Berl)* 12:261-279.
5. Giere O, Conway N, Gastrock G, Schmidt C (1991) "Regulation" of gutless annelid ecology by endosymbiotic bacteria. *Mar Ecol Prog Ser* 68:287-299.
6. Muller F, Brissac T, Le Bris N, Felbeck H, Gros O (2010) First description of giant *Archaea* (*Thaumarchaeota*) associated with putative bacterial ectosymbionts in a sulfidic marine habitat. *Environ Microbiol* 12:2371-2383.
7. Dubilier N, Bergin C, Lott C (2008) Symbiotic diversity in marine animals: The art of harnessing chemosynthesis. *Nat Rev Microbiol* 6:725-740.
8. Bright M, Sorigo A (2003) Ultrastructural reinvestigation of the trophosome in adults of *Riftia pachyptila* (Annelida, Siboglinidae). *Invertebr Biol* 122:347-368.
9. Pasteris JD, Freeman JJ, Goffredi SK, Buck KR (2001) Raman spectroscopic and laser scanning confocal microscopic analysis of sulfur in living sulfur-precipitating marine bacteria. *Chem Geol* 180:3-18.
10. Loy A, et al. (2009) Reverse dissimilatory sulfite reductase as phylogenetic marker for a subgroup of sulfur-oxidizing prokaryotes. *Environ Microbiol* 11:289-299.
11. Meyer B, Kuever J (2007) Molecular analysis of the diversity of sulfate-reducing and sulfur-oxidizing prokaryotes in the environment, using *aprA* as functional marker gene. *Appl Environ Microbiol* 73:7664-7679.
12. Badger MR, Bek EJ (2008) Multiple Rubisco forms in proteobacteria: Their functional significance in relation to CO₂ acquisition by the CBB cycle. *J Exp Bot* 59:1525-1541.
13. Stackebrandt E, Ebers J (2006) Taxonomic parameters revisited: Tarnished gold standards. *Microbiol Today* 33:152-155.
14. Wang Q, Garrity GM, Tiedje JM, Cole JR (2007) Naive Bayesian classifier for rapid assignment of rRNA sequences into the new bacterial taxonomy. *Appl Environ Microbiol* 73:5261-5267.
15. Williams KP, Sobral BW, Dickerman AW (2007) A robust species tree for the *Alphaproteobacteria*. *J Bacteriol* 189:4578-4586.
16. Wu D, et al. (2009) A phylogeny-driven genomic encyclopaedia of Bacteria and Archaea. *Nature* 462:1056-1060.
17. Murray RGE, Stackebrandt E (1995) Taxonomic note: implementation of the provisional status Candidatus for incompletely described prokaryotes. *Int J Syst Bacteriol* 45:186-187.
18. Kanokratana P, et al. (2011) Insights into the phylogeny and metabolic potential of a primary tropical peat swamp forest microbial community by metagenomic analysis. *Microb Ecol* 61:518-528.
19. Loy A, et al. (2005) 16S rRNA gene-based oligonucleotide microarray for environmental monitoring of the betaproteobacterial order "Rhodocyclales". *Appl Environ Microbiol* 71:1373-1386.
20. Larsson K, Jondelius U (2008) Phylogeny of Catenulida and support for Platyhelminthes. *Org Divers Evol* 8:378-387.
21. Albuquerque L, Rainey FA, Nobre MF, da Costa MS (2008) *Elioraea tepidiphila* gen. nov., sp. nov., a slightly thermophilic member of the Alphaproteobacteria. *Int J Syst Evol Microbiol* 58:773-778.
22. Bright M, Bulgheresi S (2010) A complex journey: transmission of microbial symbionts. *Nat Rev Microbiol* 8:218-230.
23. Hurtado LA, Mateos M, Lutz RA, Vrijenhoek RC (2003) Coupling of bacterial endosymbiont and host mitochondrial genomes in the hydrothermal vent clam *Calyptogena magnifica*. *Appl Environ Microbiol* 69:2058-2064.
24. Stewart FJ, Young CR, Cavanaugh CM (2008) Lateral symbiont acquisition in a maternally transmitted chemosynthetic clam endosymbiosis. *Mol Biol Evol* 25:673-687.
25. Stewart FJ, Young CR, Cavanaugh CM (2009) Evidence for homologous recombination in intracellular chemosynthetic clam symbionts. *Mol Biol Evol* 26:1391-1404.
26. Moran NA, McCutcheon JP, Nakabachi A (2008) Genomics and evolution of heritable bacterial symbionts. *Annu Rev Genet* 42:165-190.
27. Moran NA, McLaughlin HJ, Sorek R (2009) The dynamics and time scale of ongoing genomic erosion in symbiotic bacteria. *Science* 323:379-382.
28. Ochman H, Elwyn S, Moran NA (1999) Calibrating bacterial evolution. *Proc Natl Acad Sci USA* 96:12638-12643.
29. Kuo CH, Ochman H (2009) Inferring clocks when lacking rocks: The variable rates of molecular evolution in bacteria. *Biol Direct* 4:35.
30. Douzery EJP, Snell EA, Baptiste E, Delsuc F, Philippe H (2004) The timing of eukaryotic evolution: does a relaxed molecular clock reconcile proteins and fossils? *Proc Natl Acad Sci USA* 101:15386-15391.
31. Distel DL (1998) Evolution of chemoautotrophic endosymbioses in bivalves. *Bioscience* 48:277-286.
32. Moran NA (1996) Accelerated evolution and Muller's ratchet in endosymbiotic bacteria. *Proc Natl Acad Sci USA* 93:2873-2878.
33. Dale C, Wang B, Moran N, Ochman H (2003) Loss of DNA recombinational repair enzymes in the initial stages of genome degeneration. *Mol Biol Evol* 20:1188-1194.
34. Kuwahara H, et al. (2008) Reductive genome evolution in chemoautotrophic intracellular symbionts of deep-sea *Calyptogena* clams. *Extremophiles* 12:365-374.
35. Scott KM, et al. (2006) The genome of deep-sea vent chemolithoautotroph *Thiomicrospira crunogena* XCL-2. *PLoS Biol* 4:e383.
36. Sachs JL, Essenberg CJ, Turcotte MM (2011) New paradigms for the evolution of beneficial infections. *Trends Ecol Evol* 26:202-209.
37. Rieger J, Giere O, Dubilier N (2000) Localization of RubisCO and sulfur in endosymbiotic bacteria of the gutless marine oligochaete *Inanidrilus leukodermatus* (Annelida). *Marine Biology (Berlin)* 137:239-244.
38. Juretschko S, et al. (1998) Combined molecular and conventional analyses of nitrifying bacterial diversity in activated sludge: *Nitrosococcus mobilis* and *Nitrospira*-like bacteria as dominant populations. *Appl Environ Microbiol* 64:3042-3051.
39. Kane MD, Poulsen LK, Stahl DA (1993) Monitoring the enrichment and isolation of sulfate-reducing bacteria by using oligonucleotide hybridization probes designed

from environmentally derived 16S rRNA sequences. *Appl Environ Microbiol* 59: 682–686.

40. Pradillon F, Schmidt A, Peplies J, Dubilier N (2007) Species identification of marine invertebrate early stages by whole-larvae in situ hybridisation of 18S ribosomal RNA. *Mar Ecol Prog Ser* 333:103–116.
41. von Reumont BM, et al. (2009) Can comprehensive background knowledge be incorporated into substitution models to improve phylogenetic analyses? A case study on major arthropod relationships. *BMC Evol Biol* 9:119.
42. Meyer B, Kuever J (2007) Molecular analysis of the distribution and phylogeny of dissimilatory adenosine-5'-phosphosulfate reductase-encoding genes (*aprBA*) among sulfur-oxidizing prokaryotes. *Microbiology* 153:3478–3498.
43. Blazejak A, Kuever J, Erséus C, Amann R, Dubilier N (2006) Phylogeny of 16S rRNA, ribulose 1,5-bisphosphate carboxylase/oxygenase, and adenosine 5'-phosphosulfate reductase genes from gamma- and alphaproteobacterial symbionts in gutless marine worms (oligochaeta) from Bermuda and the Bahamas. *Appl Environ Microbiol* 72: 5527–5536.
44. Meyer H, et al. (2006) Soil carbon and nitrogen dynamics along a latitudinal transect in Western Siberia, Russia. *Biogeochemistry* 81:239–252.
45. Altschul SF, Gish W, Miller W, Myers EW, Lipman DJ (1990) Basic local alignment search tool. *J Mol Biol* 215:403–410.
46. Katoh K, Kuma K-i, Toh H, Miyata T (2005) MAFFT version 5: Improvement in accuracy of multiple sequence alignment. *Nucleic Acids Res* 33:511–518.
47. Nylander JAA (2008) *MrModeltest v2.3 Program Distributed by the Author* (Uppsala Univ, Uppsala, Sweden).
48. Tamura K, Dudley J, Nei M, Kumar S (2007) MEGA4: Molecular Evolutionary Genetics Analysis (MEGA) software version 4.0. *Mol Biol Evol* 24:1596–1599.
49. Guindon S, Gascuel O (2003) A simple, fast, and accurate algorithm to estimate large phylogenies by maximum likelihood. *Syst Biol* 52:696–704.
50. Dereeper A, et al. (2008) Phylogeny.fr: Robust phylogenetic analysis for the non-specialist. *Nucleic Acids Res* 36(suppl 2):W465–W469.
51. Ronquist F, Huelsenbeck JP (2003) MrBayes 3: Bayesian phylogenetic inference under mixed models. *Bioinformatics* 19:1572–1574.
52. Anisimova M, Gascuel O (2006) Approximate likelihood-ratio test for branches: A fast, accurate, and powerful alternative. *Syst Biol* 55:539–552.
53. Guindon S, et al. (2010) New algorithms and methods to estimate maximum-likelihood phylogenies: Assessing the performance of PhyML 3.0. *Syst Biol* 59:307–321.
54. Ludwig W, et al. (2004) ARB: A software environment for sequence data. *Nucleic Acids Res* 32:1363–1371.
55. Loy A, et al. (2008) probeCheck—a central resource for evaluating oligonucleotide probe coverage and specificity. *Environ Microbiol* 10:2894–2898.
56. Manz W, Amann R, Ludwig W, Wagner M, Schleifer K-H (1992) Phylogenetic oligodeoxynucleotide probes for the major subclasses of proteobacteria: Problems and solutions. *Syst Appl Microbiol* 15:593–600.
57. Nussbaumer AD, Fisher CR, Bright M (2006) Horizontal endosymbiont transmission in hydrothermal vent tubeworms. *Nature* 441:345–348.

Supporting Information

Gruber-Vodicka et al. 10.1073/pnas.1105347108

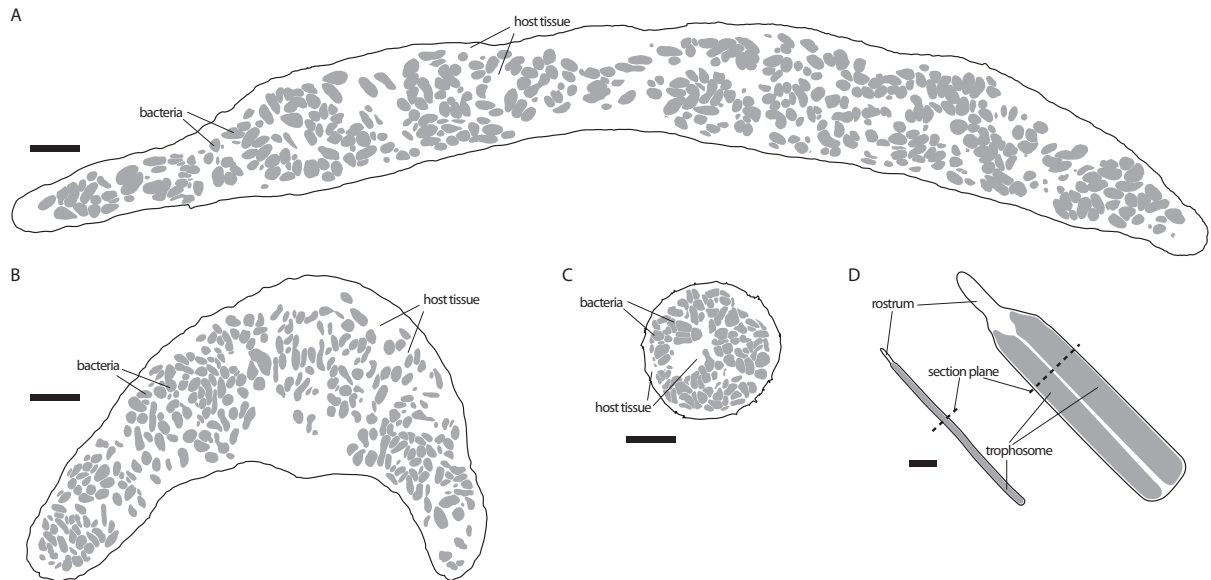


Fig. S1. Symbiont-to-host tissue ratio of three different *Paracatenula* species. (A–C) Vector trace images of TEM cross sections. Bacteria are indicated in gray; host epidermal outline indicated in black line. (Scale bars: 20 μm .) (A) Cross-section of *P. cf. galateia* from Dahab, Egypt: symbionts make up 41.2% of cross-section area. (B) Cross-section of *P. galateia* from Carrie Bow Cay, Belize: symbionts make up 36.7% of cross-section area. (C) Cross-section of *P. cf. polyhymnia*: symbionts make up 51.9% of cross-section area. (D) Schematic habitus of *P. cf. polyhymnia* (Left) and *P. galateia* (Right). Trophosome tissue with bacteria is indicated in gray, host outline indicated in black line, and dashed lines indicate positions of cross sections in A–C. (Scale bar: 200 μm .)

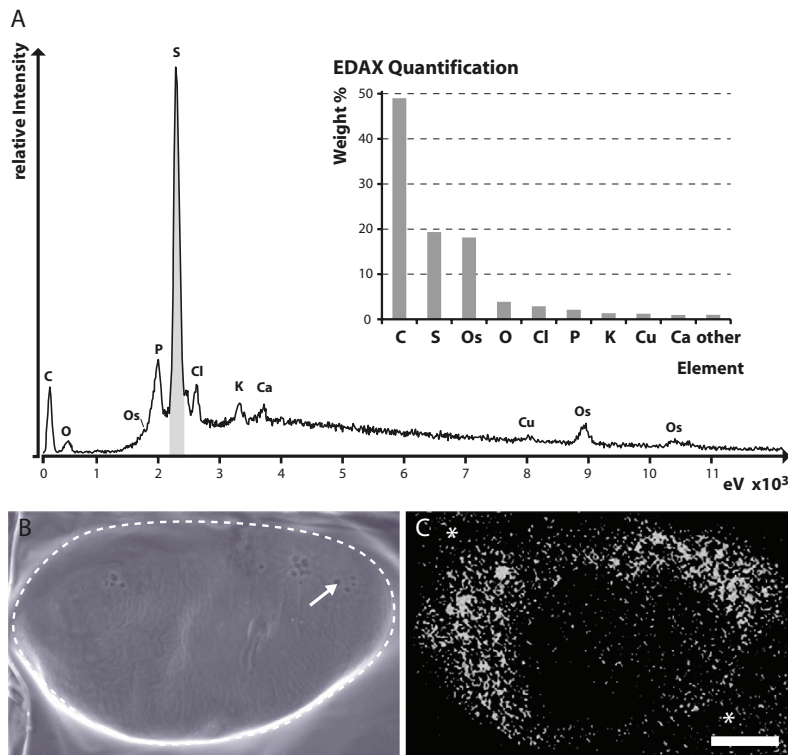


Fig. S2. Sulfur measurements of the trophosome material of *P. galateia*. (A) Energy dispersive X-ray spectrum of trophosome region. Measurement location marked with arrow in *B*; peaks of the nine most frequent elements are indicated above the peaks, and their weight (atomic mass) proportions are also shown (*Inset*). (B) Scanning EM image of partially dehydrated semithin cross-section of *P. galateia* embedded in Spurr resin; arrow indicates locality of spectrum in *A*. (C) Mapping of sulfur using the peak indicated with gray in spectrum (*A*) on the trophosome cross-section in *B*. *Regions of high sulfur content in resin outside of the worm caused by partial loss of sulfur in the embedding process. *B* and *C* are shown at the same scale. (Scale bar: 50 μm .)

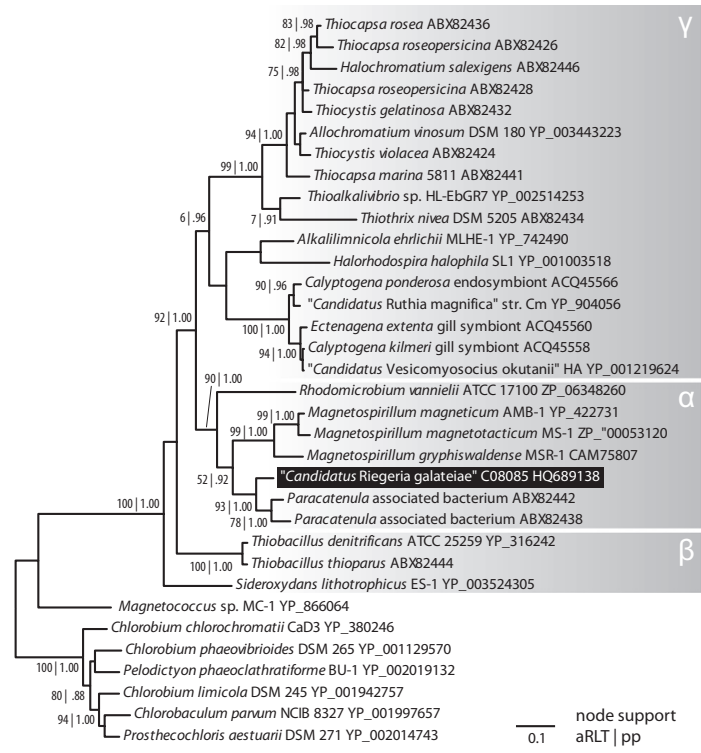


Fig. S3. Phylogenetic reconstruction of DsrB sequences from symbiotic and free-living SOB. *Alpha*-, *Beta*-, and *Gammaproteobacteria* are indicated with gray boxes, and the sequence from *Candidatus Riegeria galateiae* obtained in this study is marked in black. The analysis is based on a MAFFT amino acid alignment with 500 positions. The tree shown was estimated under the WAG+G model using PHYML and the tree was rooted with *Chlorobi*. Node support is indicated for ML analysis using PHYML (aRLT) as well as Bayesian inference (pp) with MrBayes (three Mio generations and one Mio burn-in). Accession numbers are given after the name and strain indicator. (Scale bar: 10% estimated sequence divergence.)

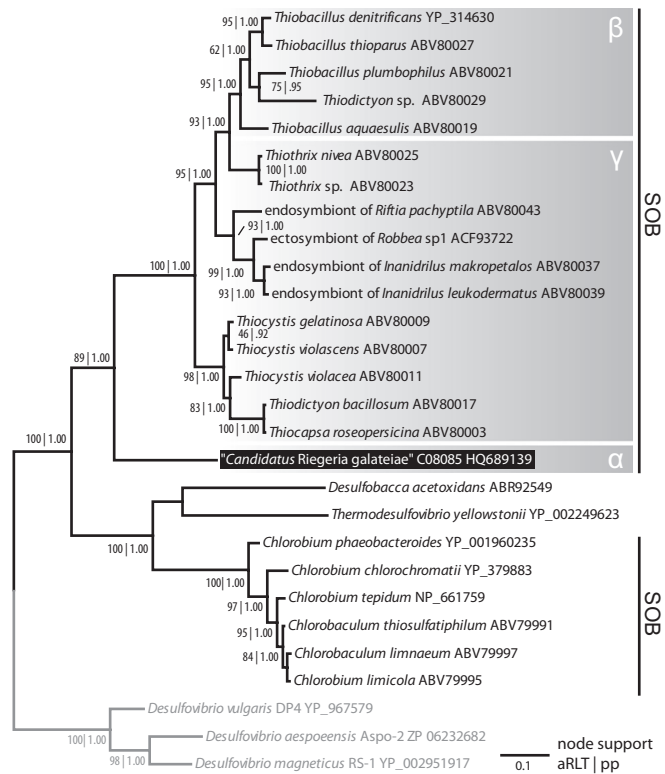


Fig. S4. Phylogenetic reconstruction of AprA lineage II sequences from SOB and sulfate-reducing bacteria. The different classes of Protecd sequences (AprA lineage I) were used as outgroup. The analysis is based on a MAFFT amino acid alignment with 376 positions, and the tree shown was estimated under the WAG+Gamma model using MrBayes with three Mio generations and one Mio burn-in; node support is indicated for ML \pm aRLT and Bayesian inference (MrBayes; pp). Accession numbers are given after the name and strain indicator. (Scale bar: 10% estimated seque

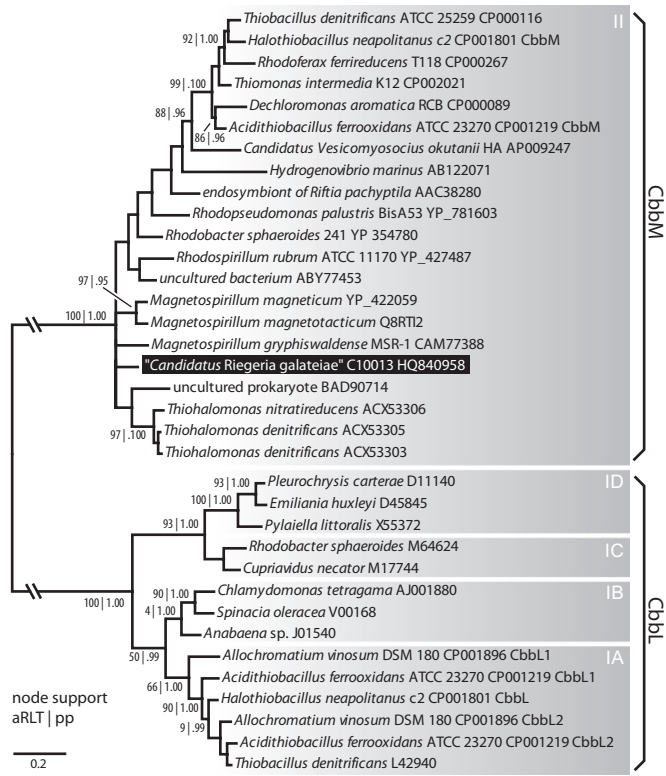


Fig. S5. Phylogenetic reconstruction of RubisCO (CbbM and CbbL) sequences. The different forms of RubisCO are indicated with gray box lineages with black brackets, and the sequence from *Candidatus Riegeria galateiae* obtained in this study is marked in black. The analysis is based on amino acid alignment with 478 positions. The tree shown was estimated under the WAG+G+I model using MrBayes with one Mio generation in, rooted with the CbbL clade, and node support is indicated for ML analysis (PHYML; aRLT) and Bayesian inference (MrBayes; pp). (Scale bar: 20% estimated sequence divergence.)

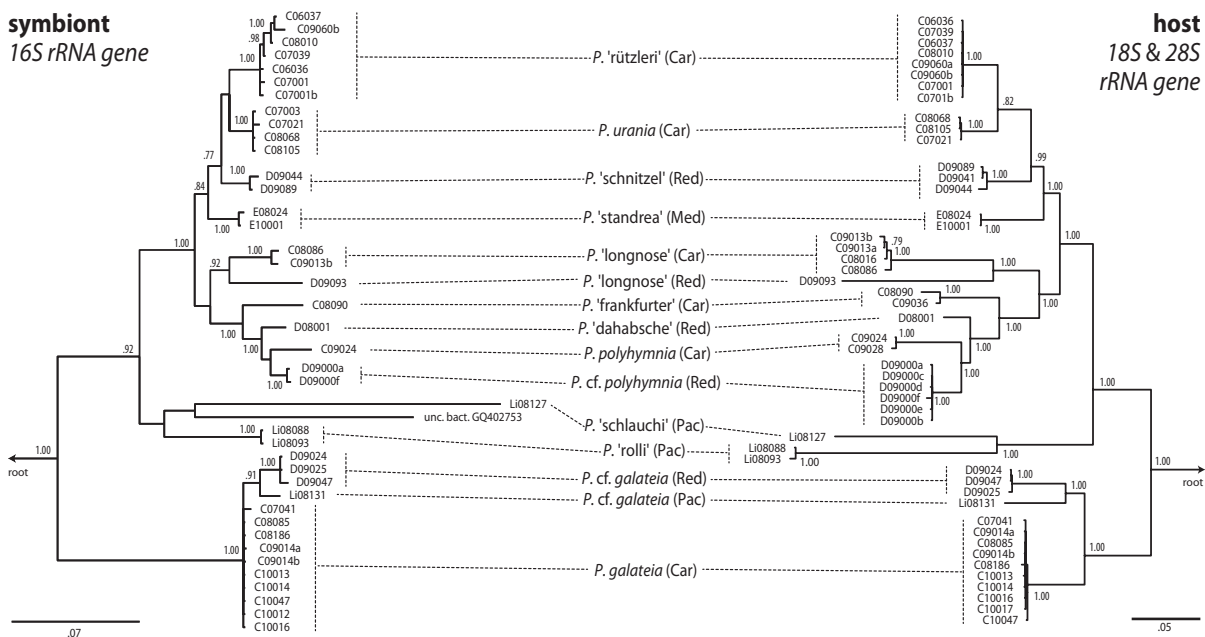


Fig. S6. Co-cladogenesis between *Paracatenula* and *Candidatus Riegeria*. Tangle-gram of the trees of symbiont 16S rRNA (1,542 positions) and host concatenated 18S and 28S rRNA genes (3,492 positions) sequenced from worm sampled in the Caribbean Sea (Car), Mediterranean Sea (Med), Red Sea (Red), and Pacific Ocean (Pac). Both trees are based on MAFFT nucleotide alignments incorporating predicted secondary structure information and were estimated under the GTR+G+I model using MrBayes with five Mio generations and two Mio burn-in; node support in both trees is indicated (pp). The root part of the host phylogeny including other catenulids and the outgroup is shown in Fig. S7. The trees were calculated by using all available *Paracatenula* sequences (Table S2). Specimens where either host or symbiont data were lacking completely were pruned from the tree for clarity. Accession numbers for sequences from *Paracatenula* hosts and symbionts are given in Table S1. The accession numbers for the sequences used in the root part of the host tree are given in Fig. S7; for the symbiont tree, refer to Tables S1 and S2. [Scale bars: 7% (symbiont) and 5% (host) estimated sequence divergence.]

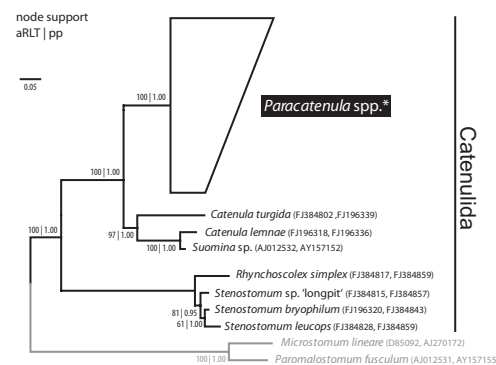


Fig. S7. Catenulid phylogeny based on concatenated 18S and 28S rRNA gene analysis. Root part of the tree presented in Fig. S6, indicating the position of the genus *Paracatenula* within Catenulida. Asterisks indicates the *Paracatenula* clade of this tree that is shown in Fig. S6 (host tree). The tree shown is based on a MAFFT nucleotide alignment incorporating predicted secondary structure information with 3,492 positions and was estimated under the GTR+G+I model using MrBayes with five Mio generations and two Mio burn-in; node support is indicated for maximum likelihood (PHYML; aRLT) as well as Bayesian inference (MrBayes; pp). The tree was rooted by using sequences of two rhabditophoran flatworms (Macrostomida) as outgroup (indicated in gray). Accession numbers are given after the organism name (18S and 28S rRNA gene, respectively) except for the *Paracatenula* spp. sequences, which are listed in Table S1. (Scale bar: 5% estimated sequence divergence.)

Table S1. Accession numbers of *Paracatenula* and “*Cand. Riegeria*” rRNA sequences used

Host name	Geographic origin	Sampling location	Specimen	“ <i>Cand. Riegeria</i> ” 16S	18S	28S
<i>Paracatenula</i> “rützleri”	Caribbean Sea	Belize, CBC	C06036	HQ68053*	HQ689068*	HQ689086*
<i>Paracatenula</i> “rützleri”	Caribbean Sea	Belize, CBC	C06037	HQ68052*	HQ689067*	HQ689085*
<i>Paracatenula</i> “rützleri”	Caribbean Sea	Belize, CBC	C07001	HQ68051*	—	HQ689084*
<i>Paracatenula</i> “rützleri”	Caribbean Sea	Belize, CBC	C07001b	HQ68050*	—	HQ689083*
<i>Paracatenula urania</i>	Caribbean Sea	Belize, CBC	C07003	HQ68049*	—	—
<i>Paracatenula urania</i>	Caribbean Sea	Belize, CBC	C07021	HQ68048*	HQ689066*	HQ689082*
<i>Paracatenula</i> “rützleri”	Caribbean Sea	Belize, CBC	C07039	HQ68047*	HQ689065*	HQ689081*
<i>Paracatenula galateia</i>	Caribbean Sea	Belize, CBC	C07041	HQ68046*	HQ231340	HQ231330
<i>Paracatenula</i> “rützleri”	Caribbean Sea	Belize, CBC	C08010	HQ68045*	HQ689064*	HQ689080*
<i>Paracatenula</i> “longnose”	Caribbean Sea	Belize, CBC	C08016	—	HQ689063*	HQ689079*
<i>Paracatenula urania</i>	Caribbean Sea	Belize, CBC	C08068	HQ68044*	HQ689062*	HQ689078*
<i>Paracatenula galateia</i>	Caribbean Sea	Belize, CBC	C08085	HQ68043*	HQ231341	HQ231331
<i>Paracatenula</i> “longnose”	Caribbean Sea	Belize, CBC	C08086	HQ68042*	HQ689061*	—
<i>Paracatenula</i> “frankfurter”	Caribbean Sea	Belize, CBC	C08090	HQ68041*	HQ689060*	HQ689077*
<i>Paracatenula urania</i>	Caribbean Sea	Belize, CBC	C08105	HQ68040*	—	HQ689076*
<i>Paracatenula galateia</i>	Caribbean Sea	Belize, CBC	C08186	HQ68039*	HQ231342	HQ231332
<i>Paracatenula</i> “longnose”	Caribbean Sea	Belize, CBC	C09013a	—	HQ689059*	HQ689075*
<i>Paracatenula</i> “longnose”	Caribbean Sea	Belize, CBC	C09013b	HQ68038*	HQ689058*	HQ689074*
<i>Paracatenula galateia</i>	Caribbean Sea	Belize, CBC	C09014a	HQ68037*	HQ231343	HQ231333
<i>Paracatenula galateia</i>	Caribbean Sea	Belize, CBC	C09014b	HQ68036*	HQ231344	HQ231334
<i>Paracatenula polyhymnia</i>	Caribbean Sea	Belize, CBC	C09024	HQ68035*	HQ689057*	HQ689073*
<i>Paracatenula polyhymnia</i>	Caribbean Sea	Belize, CBC	C09028	—	—	HQ689072*
<i>Paracatenula</i> “frankfurter”	Caribbean Sea	Belize, CBC	C09036	—	HQ689056*	—
<i>Paracatenula</i> “rützleri”	Caribbean Sea	Belize, CBC	C09060a	—	HQ689055*	HQ689071*
<i>Paracatenula</i> “rützleri”	Caribbean Sea	Belize, CBC	C09060b	HQ68034*	HQ689054*	HQ689070*
<i>Paracatenula galateia</i>	Caribbean Sea	Belize, CBC	C10012	HQ68033*	—	—
<i>Paracatenula galateia</i>	Caribbean Sea	Belize, CBC	C10013	HQ68032*	—	HQ231335
<i>Paracatenula galateia</i>	Caribbean Sea	Belize, CBC	C10014	HQ68031*	—	HQ231336
<i>Paracatenula galateia</i>	Caribbean Sea	Belize, CBC	C10016	HQ68030*	—	HQ231337
<i>Paracatenula galateia</i>	Caribbean Sea	Belize, CBC	C10017	—	—	HQ231338
<i>Paracatenula galateia</i>	Caribbean Sea	Belize, CBC	C10047	HQ68029*	—	HQ231339
<i>Paracatenula</i> “dahabsche”	Red Sea	Egypt, Dahab	D08001	HQ69095*	HQ689108*	HQ689122*
<i>Paracatenula cf polyhymnia</i>	Red Sea	Egypt, Dahab	D09000a	HQ69094*	HQ689107*	HQ689121*
<i>Paracatenula cf polyhymnia</i>	Red Sea	Egypt, Dahab	D09000b	—	—	HQ689120*
<i>Paracatenula cf polyhymnia</i>	Red Sea	Egypt, Dahab	D09000c	—	HQ689106*	HQ689119*
<i>Paracatenula cf polyhymnia</i>	Red Sea	Egypt, Dahab	D09000d	—	HQ689105*	HQ689118*
<i>Paracatenula cf polyhymnia</i>	Red Sea	Egypt, Dahab	D09000e	—	HQ689104*	HQ689117*
<i>Paracatenula cf polyhymnia</i>	Red Sea	Egypt, Dahab	D09000f	HQ69093*	HQ689103*	—
<i>Paracatenula</i> “spaghetti”	Red Sea	Egypt, Dahab	D09003	—	—	HQ689116*
<i>Paracatenula cf galateia</i>	Red Sea	Egypt, Dahab	D09024	HQ69092*	HQ689102*	HQ689115*
<i>Paracatenula cf galateia</i>	Red Sea	Egypt, Dahab	D09025	HQ69091*	—	HQ689114*
<i>Paracatenula</i> “schnitzel”	Red Sea	Egypt, Dahab	D09031	—	—	HQ689113*
<i>Paracatenula</i> “schnitzel”	Red Sea	Egypt, Dahab	D09041	—	HQ689101*	HQ689112*
<i>Paracatenula</i> “schnitzel”	Red Sea	Egypt, Dahab	D09044	HQ69090*	HQ689100*	—
<i>Paracatenula cf galateia</i>	Red Sea	Egypt, Dahab	D09047	HQ69089*	HQ689099*	HQ689111*
<i>Paracatenula</i> “schnitzel”	Red Sea	Egypt, Dahab	D09089	HQ69088*	HQ689098*	HQ689110*
<i>Paracatenula</i> “speedy”	Red Sea	Egypt, Dahab	D09091	—	HQ689097*	—
<i>Paracatenula</i> “longnose”	Red Sea	Egypt, Dahab	D09093	HQ69087*	HQ689096*	HQ689109*
<i>Paracatenula</i> “stanadrea”	Mediterranean Sea	Italy, Elba	E08024	HQ69124*	HQ689125*	HQ689127*
<i>Paracatenula</i> “stanadrea”	Mediterranean Sea	Italy, Elba	E10001	HQ69123*	—	HQ689126*
<i>Paracatenula</i> “rolli”	Pacific Ocean	Australia, LI	LI08088	HQ69129*	HQ689133*	HQ689137*
<i>Paracatenula</i> “rolli”	Pacific Ocean	Australia, LI	LI08093	HQ69128*	HQ689132*	HQ689136*
<i>Paracatenula cf urania</i>	Pacific Ocean	Australia, LI	LI08098	HQ845108*	—	—
<i>Paracatenula</i> “schlauch”	Pacific Ocean	Australia, LI	LI08127	HQ845109*	HQ689131*	HQ689135*
<i>Paracatenula cf galateia</i>	Pacific Ocean	Australia, LI	LI08131	HQ845110*	HQ689130*	HQ689134*

—, no PCR product obtained. CBC, Carrie Bow Cay; LI, Lizard Island.
*Sequence generated in the present study.

Table S2. Accession numbers of alphaproteobacterial and deltaproteobacterial 16S rRNA sequences used

Bacteria	Sequence
Alphaproteobacteria	
<i>Rhizobiales</i>	
<i>Bartonella bacilliformis</i> KC583	NC_008783
<i>Bartonella quintana</i> Toulouse	NC_005955
<i>Beijerinckia indica</i> subsp. <i>indica</i> 9039	NC_010581
<i>Bradyrhizobium</i> sp. ORS278	NC_009445
<i>Brucella melitensis</i> 16M	NC_003317, NC_003318
<i>Mesorhizobium loti</i> MAFF303099	NC_002678
<i>Mesorhizobium</i> sp. BNC1	NC_008254
<i>Methylobacterium radiotolerans</i> JCM 2831	NC_010505
<i>Methylobacterium</i> sp. 4-46	NC_010511
<i>Nitrobacter winogradskyi</i> Nb-255	NC_007406
<i>Rhizobium leguminosarum</i> bv. <i>viciae</i> 3841	NC_008380
<i>Rhodopseudomonas palustris</i> BisB18	NC_007925
<i>Xanthobacter autotrophicus</i> Py2	NC_009720
<i>Sphingomonadales</i>	
<i>Erythrobacter litoralis</i> HTCC2594	NC_007722
<i>Novosphingobium aromaticivorans</i> DSM 12444	NC_007794
<i>Sphingomonas wittichii</i> RW1	NC_009511
<i>Sphingopyxis alaskensis</i> RB2256	NC_008048
<i>Zymomonas mobilis</i> subsp. <i>mobilis</i> ZM4	NC_006526
<i>Hyphomonadales</i>	
<i>Hyphomonas neptunium</i> ATCC 15444	NC_008358
<i>Maricaulis maris</i> MCS10	NC_008347
<i>Rhodobacteraceae</i>	
<i>Paracoccus denitrificans</i> PD1222	NC_008686, NC_008687
<i>Dinoroseobacter shibae</i> DFL 12	NC_009952
<i>Jannaschia</i> sp. CCS1	NC_007802
<i>Roseobacter denitrificans</i> OCh 114	NC_008209
<i>Silicibacter pomeroyi</i> DSS-3	NC_003911
<i>Rhodobacter sphaeroides</i> 2.4.1	NC_007494, NC_007493
<i>Rhodospirillaceae</i>	
<i>Azospirillum lipoferum</i>	Z29619
<i>Insolitispirillum peregrinum</i> LMG 4340	EF612767
<i>Magnetospirillum magneticum</i> AMB-1	NC_007626
<i>Novispirillum itersonii</i> IAM 14945	AB074520
<i>Rhodocista pekingensis</i> 3-p	AF523824
<i>Rhodospirillum rubrum</i> ATCC 11170	NC_007643
<i>Roseospira marina</i> CE2105	AJ298879
<i>Acetobacteraceae</i>	
<i>Acidiphilium cryptum</i> JF-5	NC_009484
<i>Elioraea tepidiphila</i> TU-7	EF519867
<i>Gluconacetobacter diazotrophicus</i> PAI 5	NC_010125
<i>Gluconobacter oxydans</i> 621H	NC_006677
<i>Granulibacter bethesdensis</i> CGDNIH1	NC_008343
<i>Rickettsiales</i>	
<i>Anaplasma marginale</i> str. St. Maries	NC_004842
<i>Anaplasma phagocytophilum</i> HZ	NC_007797
<i>Ehrlichia canis</i> str. Jake	NC_007354
<i>Ehrlichia ruminantium</i> str. Welgevonden	NC_005295
<i>Neorickettsia sennetsu</i> Miyayama	NC_007798
<i>Orientia tsutsugamushi</i> Boryong	NC_009488
<i>Rickettsia bellii</i> RML369-C	NC_007940
<i>Rickettsia typhi</i> Wilmington	NC_006142
<i>Wolbachia</i> endosymbiont TRS of <i>Brugia malayi</i>	NC_006833
<i>Wolbachia pipientis</i> symbiont of <i>Dipetalonema gracile</i>	AJ548802
<i>Incertae sedis</i>	
" <i>Candidatus</i> Pelagibacter ubique" HTCC1062	NC_007205
<i>Caulobacter</i> sp. K31	NC_010338
<i>Geminicoccus roseus</i> 18922	AM403172
<i>Magnetococcus</i> sp. MC-1	NC_008576
<i>Parvibaculum lavamentivorans</i> DS-1	NC_009719

Table S2. Cont.

Bacteria	Sequence
<i>Deltaproteobacteria</i> (outgroup)	
<i>Geobacter sulfurreducens</i> PCA	U13928
<i>Geobacter uraniireducens</i> Rf4	EF527427
<i>Pelobacter propionicus</i> DSM 2379	NC_008609

For 16S rRNA genes extracted from genomes, the genome accession numbers are given.

Table S3. Probes used for FISH

Probe	Standard probe name [†]	Specificity	Sequence 5' modification	Target RNA	Position [‡]	Formamide, %/hybridization time, h/probe concentration, ng/μL	Reference
EUB338	S-*BactV-0338-a-A-18	Most bacteria	5'-GCT GCC TCC CGT AGG AGT-3' FLUOS	16S	338–355	40%/3/4.6	1
ALF968	L-C-gProt-1027-a-A-17	<i>Alphaproteobacteria</i> , except for <i>Rickettsiales</i> no mismatch to " <i>Cand. Riegeria galateiae</i> "	5'-GCC TTC CCA CAT CGT TT-3' Cy5	16S	968–985	40%/3/2.7	2
Par1151	S-*CRg-1151-a-A-21	" <i>Cand. Riegeria galateiae</i> " [§]	5'-CTT GTC ACC GGC AGT TCC CTC-3' Cy3	16S	1,151–1,171	40%/3/2.7	Present study
NON338	Not named	Antisense	5'-ACT CCT ACG GGA GGC AGC-3' Cy3	16S	338–355	40%/3/2.7	3

[†]According to Alm et al. (4).

[‡]16S rRNA position, *E. coli* numbering (5).

[§]The probe as 4/2231/9474 bacterial non target hits in the RDP database with 0/1/2 mismatches (6).

1. Amann RI, Krumholz L, Stahl DA (1990) Fluorescent-oligonucleotide probing of whole cells for determinative, phylogenetic, and environmental studies in microbiology. *J Bacteriol* 172: 762–770.
2. Neef A (1997) Anwendung der in situ-Einzelzell-Identifizierung von Bakterien zur Populationsanalyse in komplexen mikrobiellen Biozönosen [Application of in-situ single cell identification of bacteria in population analysis of complex microbial communities]. PhD thesis (Technische Universität München, Munich).
3. Wallner G, Amann R, Beisker W (1993) Optimizing fluorescent in situ hybridization with rRNA-targeted oligonucleotide probes for flow cytometric identification of microorganisms. *Cytometry* 14:136–143.
4. Alm EW, Oerther DB, Larsen N, Stahl DA, Raskin L (1996) The oligonucleotide probe database. *Appl Environ Microbiol* 62:3557–3559.
5. Brosius J, Palmer ML, Kennedy PJ, Noller HF (1978) Complete nucleotide sequence of a 16S ribosomal RNA gene from *Escherichia coli*. *Proc Natl Acad Sci USA* 75:4801–4805.
6. Cole JR, et al. (2009) The Ribosomal Database Project: Improved alignments and new tools for rRNA analysis. *Nucleic Acids Res* 37(suppl 1):D141–D145.

VII. Conclusions and Outlook

As the presented papers in Chapters II-VI discuss the used methods and the obtained results in their individual context, this part of the thesis does not recapitulate these chapters but rather gives a broader synthesis with discussions and outlooks to several selected topics.

Transmission in the MONTS cluster

In Chapter II we characterized the Marine Oligochaete and Nematode Thiotrophic Symbiont (MONTS) cluster (Heindl et al. 2011), a monophyletic clade of *Gammaproteobacteria* related to *Chromatiaceae* that has a unique diversity of lifestyles from free-living to ecto- and endosymbiotic. Three different host-symbiont systems are present in the MONTS: the ectosymbionts on stilbonematin nematodes (e.g. *Laxus oneistus* or *Stilbonema majum*) (Ott et al. 2004; Bulgheresi et al. 2011), the extracellular Gamma1-endosymbionts in gutless oligochaetes (e.g. *Olavius* spp.) (Dubilier et al. 2006), and the intracellular endosymbionts in mouthless nematodes of the genus *Astomonema* (Ott et al. 1982; Musat et al. 2007) see Figure 4. As the common ancestor to these diverse animal hosts was certainly non-symbiotic, the symbionts of this clade have been acquired by their hosts independently several times. The 16S rRNA gene based phylogenies show significant differences between the symbionts of different hosts (Figure 4) (Musat et al. 2007; Bayer et al. 2009; Heindl et al. 2011). Sequence divergence of 16S rRNA for inheritable symbionts ranges from 2.5% to 11%, while free-living bacteria have rates ranging from 2% to 4% for 100 million years (Moran et al. 2008; Kuo and Ochman 2009). Based on this range of rates and a sequence divergence of 3%-5% within the MONTS cluster, the first symbioses in this clade have been established between 25 and 250 million years ago. With this rough age estimate and species level differences on the 16S rRNA gene level it can be expected that the associations with different hosts have left distinct signatures in the genomes of the symbionts, making this group an ideal model to study the genomic differences in free-living vs. ecto- vs. endosymbiotic lifestyles.

The transmission of MONTS symbionts in the different host systems is relatively unexplored. There are indications that at least some of the gutless oligochaete symbionts are transmitted vertically from mother to offspring (Giere and Langheld 1987). With the existence of host – symbiont specific variations of the host-lectin Mermaid as we described in Chapter III, environmental transmission of the *Laxus oneistus* or *Stilbonema majum* symbionts seems feasible. Another possible scenario could be that Mermaid isoforms play

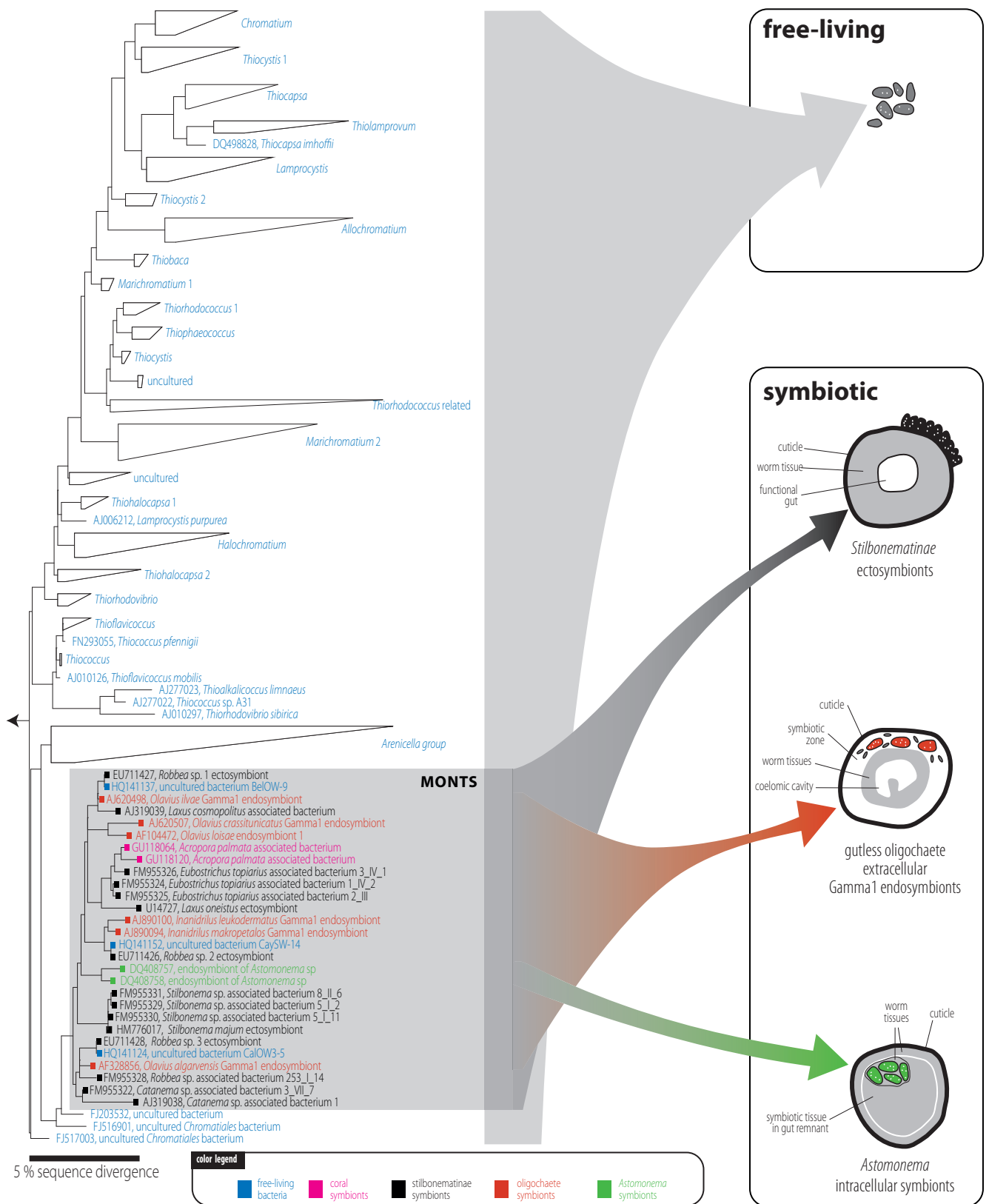


Figure 4: Left part – 16S rRNA gene based phylogeny of *Chromatiaceae* closely related to the MONTS cluster as provided by the arb-silva rRNA database (www.arb-silva.de). Right part – lifestyles of the different *Chromatiaceae* shown in the tree to the left. The symbionts are color coded as in the tree and their type of host association is illustrated.

a role in the maintenance of a specific ectosymbiont coat, but transmission could be largely or completely vertical. Recent advances in the comprehension of the genome evolution in symbiotic bacteria provide a novel framework that allows inferences on the mode of transmission based on genomic features of the symbionts (Newton and Bordenstein 2011; Sachs et al. 2011) and could be combined with e.g. behavioral and developmental studies.

Cand. Riegeria genome evolution

In Chapters IV and V we characterized the *Paracatenula* – *Cand. Riegeria* symbiosis, a new thiotrophic symbiosis model that has several outstanding features. Besides the remote phylogenetic position of both the host and the symbiont compared to other thiotrophic symbioses, the reproductive biology of *Paracatenula* and its implications to symbiont transmission and symbiont genomics are fascinating. Genome evolution in bacteria can be mechanistically interpreted as a flux of DNA: the genomic content is largely governed by the opposing forces of acquisition and erosion (Mira et al. 2001). Bacteria have a deletional bias leading to constant loss of DNA through pseudogenization by mutation followed by subsequent deletion. Other factors that lead to erosion are the loss of larger fragments through mobile DNA. New DNA can be accumulated through lateral gene transfer or duplication. Several symbiont lineages such as the mitochondria, have been ‘captured’, as they are strictly vertically transmitted within their hosts lineages (Bright and Bulgheresi 2010). This major evolutionary transition, where the captured microbial partner loses the ability to replicate independently of its host, limits the population size and reduces the chance of lateral gene transfer. This leads to high rates of genetic drift, reflected by high substitution rates, the fixation of slightly deleterious traits, codon usage biases, lowered G+C content and genome reduction (Mira et al. 2001; Moran et al. 2008; Toft and Andersson 2010). The G+C content of 51 % in the functional genes sequenced from *Cand. Riegeria galateiae* is, however, significantly higher than in the two other available thiotrophic symbiont genomes (31.6 and 34%) from two vesicomid clam symbionts, which is puzzling, considering that the *Paracatenula-Riegeria* symbiosis is substantially older than the vesicomid clams symbiosis (Gruber-Vodicka et al. 2011). One possible explanation for the slow pace of change of nucleotide substitutions and genomic G+C content could be the reduction of genetic drift through the transmission of ten-thousands of symbionts at any one reproductive event by paratomy (U.Dirks, pers. communication). This could be tested in a comparative genomics approach relating the

Cand. Riegeria symbionts to its closest cultivated free-living relatives (e.g. *Elioraea tepidiphila* based on 16S rRNA analysis) and other related free-living alphaproteobacterial genera such as *Magnetospirillum* or *Rhodospirillum*, focussing on the evolution of symbiosis related aspects such as gene order, mobile DNA content, lateral gene transfer, deletion patterns and compositional bias.

SOBs in shallow water sediments

Besides symbiosis specific insights in the MONTS cluster and the *Paracatenula* symbiosis the papers that resulted from this thesis, together with several other recent publications, suggest a need to evaluate the role symbiotic bacteria play globally in sulfur oxidation in reduced shallow water sediments, the largest biota on earth largely dominated by chemosynthetic production. These coastal marine sediments harbor a broad diversity of uncultivated SOB (Lenk et al. 2011). While some might be free-living, it is highly feasible that at least in some habitats most of the key players are actually associated to eukaryotic meiofauna hosts that help them access both electron acceptors and electron donors that are spatially separated. Already in his groundbreaking work in the late 1950s Wolfgang Wieser described meiofauna communities dominated by taxa that are now known to harbor chemoautotrophic symbionts (Wieser 1960). Several meiofauna based studies have since found different nematode hosts of the MONTS cluster to be highly abundant or dominating in shallow water sediments (Ott and Novak 1989; Leonardis et al. 2008; Semprucci et al. 2010) and even in depths down to 1000m (Ingels et al. 2011). The fixation techniques used in these and many other meiofauna studies hardly allow for an assessment of the non-cuticulate meiofauna members that harbor SOBs such as *Paracatenula* flatworms or even more fragile karyorelictid ciliates like *Kentrophoros*, both taxa that reached very high abundances and dominated the meiofaunal communities in several samples analyzed during this PhD thesis (personal observation). In recent years the taxonomic coverage of publicly available eukaryotic marker genes such as the 18S rRNA has increased substantially and most known meiofauna hosts to SOBs are now represented in the databases. This will allow future studies to integrate host based SOBs in a microbial ecology perspective by analyzing the presence of hosts using 18S rRNA gene libraries in parallel to the prokaryote specific 16S rRNA gene based methods.

The genomic capacities of most of these uncultured SOBs have been inaccessible before the advent of single-cell techniques such as cell sorting and whole genome amplification based single-cell genomics

(Swan et al. 2011), but even with cell sorting it is hard to pinpoint the one organism one would like to study even if it is dominating the chosen bacterial community. Here one great advantage of symbiosis research that was 'exploited' throughout this thesis easily bridges this problem - the fact that the hosts do the selection and culturing job for the researchers and provide the bacteria in ample amounts.

Literature cited

- Bayer C, Heindl NR, Rinke C, Lückner S, Ott JA, Bulgheresi S (2009) Molecular characterization of the symbionts associated with marine nematodes of the genus *Robbea*. Environmental Microbiology Reports 1: 136-144
- Bright M, Bulgheresi S (2010) A complex journey: transmission of microbial symbionts. Nature Reviews Microbiology 8: 218-230
- Bulgheresi S, Gruber-Vodicka HR, Heindl NR, Dirks U, Kostadinova M, Breiteneder H, Ott JA (2011) Sequence variability of the pattern recognition receptor Mermaid mediates specificity of marine nematode symbioses. ISME J 5: 986-998
- Dubilier N, Blazejak A, Rühland C (2006) Symbioses between Bacteria and Gutless Marine Oligochaetes. In: Overmann J (ed) Molecular Basis of Symbiosis. Springer Berlin, Heidelberg, pp 251-275
- Giere O, Langheld C (1987) Structural organisation, transfer and biological fate of endosymbiotic bacteria in gutless oligochaetes. Marine Biology 93: 641-650
- Gruber-Vodicka HR, Dirks U, Leisch N, Baranyi C, Stoecker K, Bulgheresi S, Heindl NR, Horn M, Lott C, Loy A, Wagner M, Ott J (2011) *Paracatenula*, an ancient symbiosis between thiotrophic Alphaproteobacteria and catenulid flatworms. Proceedings of the National Academy of Sciences 108: 12078-12083

- Heindl NR, Gruber-Vodicka HR, Bayer C, Lüscher S, Ott JA, Bulgheresi S (2011) First detection of thiotrophic symbiont phylotypes in the pelagic marine environment. *FEMS Microbiology Ecology* 77: 223-227
- Ingels J, Tchessunov AV, Vanreusel A (2011) Meiofauna in the Gollum Channels and the Whittard Canyon, Celtic Margin—How Local Environmental Conditions Shape Nematode Structure and Function. *PLoS One* 6: e20094
- Kuo CH, Ochman H (2009) Inferring clocks when lacking rocks: the variable rates of molecular evolution in bacteria. *Biology Direct* 4: 35
- Lenk S, Arnds J, Zerjatke K, Musat N, Amann R, Mußmann M (2011) Novel groups of *Gammaproteobacteria* catalyse sulfur oxidation and carbon fixation in a coastal, intertidal sediment. *Environmental Microbiology* 13: 758-774
- Leonardis C, Sandulli R, Vanaverbeke J, Vincx M, de Zio S (2008) Meiofauna and nematode diversity in some Mediterranean subtidal areas of the Adriatic and Ionian Sea. *Scientia Marina* 70: 5-13
- Mira A, Ochman H, Moran NA (2001) Deletional bias and the evolution of bacterial genomes. *Trends in genetics* : TIG 17: 589-596
- Moran NA, McCutcheon JP, Nakabachi A (2008) Genomics and evolution of heritable bacterial symbionts. *Annual Review of Genetics* 42: 165-190
- Musat N, Giere O, Gieseke A, Thiermann F, Amann R, Dubilier N (2007) Molecular and morphological characterization of the association between bacterial endosymbionts and the marine nematode *Astomonema* sp. from the Bahamas. *Environmental Microbiology* 9: 1345-1353
- Newton I, Bordenstein S (2011) Correlations Between Bacterial Ecology and Mobile DNA. *Current Microbiology* 62: 198-208
- Ott JA, Bright M, Bulgheresi S (2004) Symbioses between Marine Nematodes and Sulfur-oxidizing Chemoautotrophic Bacteria. *Symbiosis* 36: 103-126

- Ott JA, Novak R (1989) Living at an interface: Meiofauna at the oxygen/sulfide boundary of marine sediments. In: Ryland JS, Tyler PA (eds) 23rd European Marine Biology Symposium. Olsen & Olsen, pp 415–422
- Ott JA, Rieger G, Rieger R, Enderes F (1982) New mouthless interstitial worms from the sulfide system: Symbiosis with Prokaryotes. *Pubblicazioni Stazione Zoologica Napoli I: Marine Ecology* 3: 313-333
- Sachs JL, Essenberg CJ, Turcotte MM (2011) New paradigms for the evolution of beneficial infections. *Trends in Ecology & Evolution* 26: 202-209
- Semprucci F, Colantoni P, Baldelli G, Rocchi M, Balsamo M (2010) The distribution of meiofauna on back-reef sandy platforms in the Maldives (Indian Ocean). *Marine Ecology* 31: 592-607
- Swan BK, Martinez-Garcia M, Preston CM, Szyrba A, Woyke T, Lamy D, Reinthaler T, Poulton NJ, Masland EDP, Gomez ML, Sieracki ME, DeLong EF, Herndl GJ, Stepanauskas R (2011) Potential for Chemolithoautotrophy Among Ubiquitous Bacteria Lineages in the Dark Ocean. *Science* 333: 1296-1300
- Toft C, Andersson SGE (2010) Evolutionary microbial genomics: insights into bacterial host adaptation. *Nat Rev Genet* 11: 465-475
- Wieser W (1960) Benthic studies in Buzzards Bay. II. The meiofauna. *Limnology and Oceanography* 5: 121–137

Summary

Harnessing chemosynthetic symbionts is a recurring evolutionary strategy in marine invertebrates, with the most prominent host groups being the giant polychaetes at deep-sea hydrothermal vents. Eukaryotes from six phyla are known to harbor chemoautotrophic sulfur-oxidizing (thiotrophic) bacteria.

Three meiofaunal worm groups that are hosts to thiotrophic symbionts occur in shallow water subtidal sands: gutless oligochaetes and Stilbonematinae and *Astomonema* nematodes. Their thiotrophic gammaproteobacterial symbionts form a phylogenetic cluster (the Marine Oligochaete and Nematode Thiotrophic Symbionts – MONTS) within the *Chromatiaceae*. At least for the ectosymbionts that live on the nematode cuticle, environmental transmission is likely, but until now no free-living relatives have been found. The first publication of this thesis reports the detection of members of the MONTS clade closely related to several symbiont phylotypes in offshore surface seawater of both the Caribbean and Mediterranean Sea.

The successful selection of such likely environmentally transmitted partners is crucial for hosts. As typical for several of the stilbonematine host species, *Laxus oneistus* is covered by a single bacterial phylotype. The symbionts are embedded in a layer of mucus containing the host secreted lectin Mermaid, which mediates symbiont attachment. In the second publication of this thesis, we show that *Stilbonema majum*—another symbiotic stilbonematine nematode co-occurring with *L. oneistus*—is covered by bacteria that are also MONTS members but phylogenetically distinct from those covering *L. oneistus*. *Mermaid* analyses based on the transcriptomes of both host species revealed several isoforms that differ in only one to three of the 105 aa positions in the active carbohydrate recognition domain. The isoforms show higher affinities to the symbionts of the host species they were found in. This indicates that particular isoforms of the same molecule play a role in the attachment and selection of specific symbionts, very similar to what has been documented for pathogen recognition in the innate immune system of several animals.

Co-occurring with both gutless oligochaetes and the nematode hosts are mouth- and gutless catenulid flatworms of the genus *Paracatenula*. The third publication of this thesis for the first time describes the largest and most abundant *Paracatenula* species from subtidal sands in the Belize Barrier reef: *P. galateia* nov. spec.. All bacterial partners in thiotrophic symbioses apparently belong to two classes of bacteria – the *Gamma*- and *Epsilon*proteobacteria. In the fourth publication of this thesis, the intracellular endosymbionts of *Paracatenula* flatworms are shown to be a novel family-level clade of chemoautotrophic sulfur-oxidizing

Alphaproteobacteria. We describe the symbionts of *P. galateia* as ‘*Candidatus* Riegeria galateiae’ and show their elemental sulfur storage as well as their genetic capabilities to oxidize reduced sulfur and to fix inorganic carbon. All studied *Paracatenula* species collected from the Caribbean, the Mediterranean, the Red Sea and the Pacific harbor species-specific *Candidatus* Riegeria symbionts. The symbionts can occupy up to 50% of the body volume in some host species. Our phylogenetic reconstructions imply that the *Cand.* Riegeria - *Paracatenula* species association is 500 million years old. The host and symbiont phylogenies are congruent and the branching pattern is independent of the hosts’ geographic origin, indicating vertical transmission of the symbionts from each host generation to the next.

The results of the first two publications document that the MONTS clade has a unique diversity of bacterial lifestyles, free-living and symbiotic. The ectosymbionts associated with Stilbonematinae are shown to be amendable for experimental fieldwork as they can be efficiently separated from their hosts. The symbionts are highly specific, with host-lectins acting as one of the selective agents ensuring this host specificity. Despite the advances presented it remains intriguing what factors lead to this exceptional case of multiple convergent transitions of free-living bacteria to mutualistic symbionts in the different MONTS hosts. With Stilbonematinae and *Astomonema* specimens dominating several meiofaunal assemblages ranging from shallow waters to 1000m depth, and with *Paracatenula* worms completely overlooked in meiofaunal studies due to their fragile bauplan, the results of this thesis clearly warrant a reevaluation of the role thiotrophic symbionts play in the sulfur cycling in reduced sediments. This thesis provides an extended framework for future research into the evolution of chemoautotrophic symbiosis, a process that has occurred many times and has created some of the most alien animals encountered to date, animals that live on inorganic sources of carbon and energy.

Zusammenfassung

Die ‚Domestikation‘ von chemosynthetischen Bakterien ist eine wiederholt umgesetzte Strategie in der Evolution. Eukaryoten aus sechs Stämmen und sogar ein Archaeon beherbergen chemoautotrophe schwefeloxidierende (thiotrophe) Symbionten, wobei die bekanntesten Vertreter die Riesenröhrenwürmer an hydrothermalen Quellen in der Tiefsee darstellen.

Drei wurmförmige Wirtsgruppen in der Meiofauna subtidaler Flachwassersande haben thiotrophe Symbionten - darmlose Oligochaeten sowie Nematoden der Subfamilie der Stilbonematinae und der

Gattung *Astomonema* - die eine eigene Clade von Chromatiaceae innerhalb der Gammaproteobakterien, die MONTS, formen. Zumindest für die als Ektosymbionten auf der Cuticula lebenden Symbionten der Stilbonematinae ist eine Übertragung aus der Umwelt wahrscheinlich, allerdings wurden noch nie freilebende Verwandte gefunden. Die erste Publikation dieser Doktorarbeit berichtet vom Fund von Mitglieder der MONTS-Clade aus küstenfernen Oberflächenwassern sowohl aus der Karibik als auch aus dem Mittelmeer, die teilweise nahe Verwandte zu Symbionten darstellen.

Die erfolgreiche Selektion solcher sehr wahrscheinlich aus der Umwelt aufgenommenen Partner ist ein essentieller Vorgang für die Wirte. Wie es für mehrere Stilbonematinae Wirte üblich ist, hat *Laxus oneistus* einen von nur einer einzigen Art aufgebauten bakteriellen Überzug. Die Symbionten sind in eine Schleimschicht eingebettet. Diese enthält das vom Wirt abgegebene Lektin Mermaid, das an der Anheftung der Symbionten maßgeblich beteiligt ist. In der zweiten Publikation der vorliegenden Arbeit zeigen wir, dass *Stilbonema majum* – ein weiterer Vertreter der Stilbonematinae, der mit *L. oneistus* gemeinsam vorkommt – ebenfalls von einem monospezifischen Symbiontenüberzug besiedelt ist. Diese Symbionten sind eine nahe verwandte, jedoch deutlich eigenständige Linie innerhalb der MONTS. Analysen von Mermaid-Transkripten beider Wirtsarten brachten mehrere Isoformen ans Licht, bei denen von den 105 Aminosäuren im aktiven Zuckerbindungszentrum des Moleküles nur eine bis drei unterschiedlich sind. Die verschiedenen Isoformen zeigen höhere Bindungsaktivitäten bei den Symbionten des Wirtes, in dessen Transkriptom sie gefunden wurden. Dies bedeutet, dass spezielle Isoformen desselben Moleküles eine Rolle in der Anheftung und der Selektion spezifischer Symbionten einnehmen. Ein ähnlicher Mechanismus wurde für die Erkennung von Krankheitserregern im angeborenen Immunsystem bei mehreren Tiergruppen beschrieben.

Gemeinsam mit den beschriebenen darmlosen Oligochaeten und Nematoden findet man oft mund- und darmlose catenulide Plattwürmer der Gattung *Paracatenula*. Die dritte Publikation dieser Doktorarbeit beschreibt die größte und häufigste *Paracatenula* Art aus subtidalen Sanden im Barriere Riff von Belize: *P. galateia* spec. nov..

Die bakteriellen Partner in allen thiotrophen Symbiosen schienen bisher nur aus zwei Klassen von Bakterien zu stammen – den Gamma- und Epsilonproteobakterien. In der vierten Publikation dieser Doktorarbeit zeigen wir, dass die intrazellulären Symbionten der *Paracatenula* Plattwürmer eine neue Familie von chemoautotrophen schwefel-oxidierenden Alphaproteobakterien darstellen. Wir beschreiben die Symbionten von *P. galateia* als ‚*Candidatus* Riegeria galateiae‘ und zeigen, dass sie elementaren Schwefel einlagern und

die genetische Ausstattung besitzen, reduzierte Schwefelverbindungen zu oxidieren und anorganischen Kohlenstoff zu fixieren. Alle untersuchten *Paracatenula* Spezies, die im Mittelmeer, dem Roten Meer, der Karibik und dem Pazifik stammten, beherbergen jeweils wirtsartsspezifische *Candidatus* Riegeria Symbionten. Die Symbionten machen dabei bis zu 50% des Gewebes einiger Wirtsspezies aus. Unsere phylogenetischen Rekonstruktionen weisen darauf hin, dass die Symbiose zwischen *Paracatenula* und *Cand.* Riegeria 500 Millionen Jahre alt ist. Die kongruenten Stammbäume der Wirte und Symbionten und die Unabhängigkeit der Verwandtschaftsverhältnisse von der geographischen Herkunft der Wirte weisen auf eine vertikale Weitergabe Symbionten von einer Wirtsgeneration zu nächsten hin.

Die Ergebnisse der ersten zwei Publikationen dokumentieren, dass die MONTS Clade eine einzigartige Diversität an bakteriellen Lebensformen, mit freilebenden als auch symbiotischen Formen besitzt. Die Ektosymbionten der stilbonematinen Nematoden haben sich dabei als flexibles Modell für Experimente bewährt, da sie effizient von ihren Wirten getrennt werden können. Die Symbionten sind hoch spezifisch und Lektine des Wirtes tragen wesentlich zu dieser Spezifität bei. Trotz aller Fortschritte im Verständnis dieser Symbiosen bleiben die Mechanismen, die zu den mehrfach konvergent entstandenen Symbiosen der MONTS in ihren verschiedenen Wirtgruppen geführt haben, ungeklärt. Da einerseits die beiden Nematodengruppen mit MONTS Symbionten die Meiofauna in mehreren Studien, die in von Flachwassersedimenten bis in 1000m Tiefe reichten, dominierten und andererseits *Paracatenula* wie viele Plattwürmer durch ihren empfindlichen Bauplan in Meiofauna Studien übersehen werden, legen die Ergebnisse dieser Doktorarbeit eine Neubewertung der Rolle von thiotrophen Symbionten im Schwefelkreislauf reduzierter Sedimente nahe. Insgesamt schafft diese Doktorarbeit erweiterte Rahmenbedingungen für zukünftige Forschungsarbeiten zur Evolution der chemoautotrophen Symbiosen, ein Prozess der oftmals abgelaufen ist und der einige der fremdartigsten Tiere hervorgebracht hat, die man bisher gefunden hat – Tiere die sich von anorganischen Kohlenstoff- und Energiequellen ernähren können.

Acknowledgements

First of all I want to thank **Jörg Ott**, the supervisor of this thesis. He gave me the opportunity to join his working group many years ago and from the first time he presented a little vial with crumbs of *Paracatenula* to me for my diploma thesis to the submission of this thesis he gave me the confidence and the support to do the quality of science the little worms deserved.

I am especially indebted to **Silvia Bulgheresi**. Silvia gave me data to work on that led to my first and first author publication and she was always more than helpful with anything I needed (and she is the best party host anyone could imagine).

Another great warm thank you goes to **Uli Dirks**. Without Uli the mastering of all the basic molecular techniques would have come much harder and all the field trips would have been way less fun. Your company in the office, your thoughtful and honest comments on many things made this thesis so much more pleasant to accomplish.

I really want to thank our former master student **Niko Leisch**. He has turned into a true friend over the fieldtrips, the Sprühwurst and all the rest we handled together.

I also want to thank the changing members of the shallow water symbiosis group, namely **Niels** and **Christoph** for their support, from my first steps in a molecular lab to all our joint publications we have been an awesome team.

I am very grateful for the support **Gerhard Herndl** has provided to this thesis and to my career. He is one of the most outstanding scientists at our University, yet he always had the time to read and comment on my work in time, however unrelated to his work it ever was. Without his support my tracks would likely look very different.

I also thank all other member of this Department, so many of you have become friends over the past year or two – this goes out to **Pedro**, to **Daniele**, to **Eva** and **Kristin** and to all of you that shared their jokes during lunchtimes and their wit in the lab.

A special thank you goes out to **Christian Baranyi** who already at his times at the DOME always gave me good (mostly perfect!) advice and who continued to do so since he moved to the Marine Biology Department. There are three members of the DOME that also had a great deal of influence on this thesis, **Matthias Horn** and **Alex Loy** who helped me from the beginning of this project and **Michi Wagner** who gave a good final

touch to our joint publication, thanks for putting you time and effort into a guy you hardly knew.

I also want to thank **Wolfgang Sterrer** for the big times we had before the buckets and behind the microscopes, hunting for worms as well as for the meaning of life - his instructions helped all of us to get the *Paracatenula* stories right.

I also want to express my appreciation for the great job the people from the National Museum of Natural History, Washington D.C. did in running the Carrie Bow Cay Laboratory when I was visiting - Thank you **Klaus**, thank you **Mike**.

I owe this study of Marine Biology to my parents **Susanne** and **Ronald Gruber**, who got me to the sea almost every year of my life until I had professional interests and funding. Swimming, snorkeling, boating and the appreciation for the wonders of Nature are crucial tools for a Viennese Marine Biologists studying shallow water worms and you taught it all to me.

Finally I want to thank my family, my wife **Jana** for enduring my weeks-long fieldtrips and my girls **Mia**, **Merle** and **Sirii** for always appreciating the little things I brought home. You gave me the strength to get this done and you kept me focused when things got rough.

Mag. Harald Gruber-Vodicka

Born April 17, 1978, married, 3 children

2006 – Ph.D. Biology/Zoology at the Dep. of Marine Biology, University of Austria;

Supervisor: Prof. Dr. Jörg Ott

Ph.D. committee: Prof. Dr. Matthias Horn, Dr. Alexander Loy and Prof. Dr. Gerhard Steiner

1996 – 2005 M.Sc. Biology/Zoology at the University of Vienna, Austria

Publications

Bulgheresi S*, **Gruber-Vodicka HR***, Heindl NR, Dirks U, Kostadinova M, Breiteneder H, Ott JA (2011)

Sequence variability of the pattern recognition receptor Mermaid mediates specificity of marine nematode symbioses. *ISME J* 5: 986-998 (*authors contributed equally)

Heindl NR, **Gruber-Vodicka HR**, Bayer C, Lückner S, Ott JA, Bulgheresi S (2011) First detection of thiotrophic symbiont phylotypes in the pelagic marine environment. *FEMS Microbiology Ecology* 77: 223-227

Gruber-Vodicka HR, Dirks U, Leisch N, Baranyi C, Stoecker K, Bulgheresi S, Heindl NR, Horn M, Lott C, Loy A, Wagner M, Ott J (2011) *Paracatenula*, an ancient symbiosis between thiotrophic *Alphaproteobacteria* and catenulid flatworms. *Proceedings of the National Academy of Sciences*: 108: 12078-12083

Dirks U*, **Gruber-Vodicka HR***, Leisch N, Sterrer WE, Ott JA (2011) A new species of symbiotic flatworms, *Paracatenula galateia* n. sp. (Platyhelminthes: Catenulida: Retronectidae) from Belize (Central America). *Marine Biology Research*: 7:769-777 (*authors contributed equally)

Leisch N, Dirks U, **Gruber-Vodicka HR**, Schmid M, Sterrer W, Ott JA (2011) Microanatomy of the trophosome region of *Paracatenula* cf. *polyhymnia*, a catenulid flatworm with intracellular symbionts. *Zoomorphology* online first DOI 10.1007/s00435-011-0135-y

Dirks U, **Gruber-Vodicka HR**, Leisch N, Bulgheresi S, Egger B, Ladurner P, Ott JA (submitted) Continued De Novo Formation and Asexual Transmission of Bacteriocytes in the Symbiotic Flatworm *Paracatenula galateia*. Submitted to PLOS one

Dirks U, **Gruber-Vodicka HR**, Egger B, Ott JA (submitted) Proliferation pattern during rostrum regeneration in the symbiotic flatworm *Paracatenula galateia* – a pulse-chase-pulse analysis. Submitted to Cell and Tissue

Selected training courses attended

- 2007** Fluorescence-in-situ-Hybridization (FISH) course, Dep. f. Microbial Ecology, University of Vienna
- 2007** “Phylogenie der Prokaryoten” – Phylogenetic analysis with the ARB-package, Dep. f. Microbial Ecology, University of Vienna
- 2006** Micro-sensor Analysis in the Environmental Sciences, Rønbjerg, Denmark
- 2002** advanced techniques in SEM and TEM – heavy metal tolerance and detoxification in selected crustaceans
- 2000** SEM and TEM in biological applications

Research field trips

6 field trips to Australia, Belize, Egypt and Italy

Selected Talks

- 2011** ‘Ocean swimming’ and ‘No sex on the beach’ – transmission stories in shallow water thiotrophic symbiosis - invited talk, all expenses covered - Max Plank Institute for Marine Microbiology, Invitational seminar series. May 2011
- 2010** “Mermaids and holobionts in shallow water sands” in Würzburg, Germany at the workshop symbiotic interactions at the University of Würzburg - October 2010
- 2010** “An ancient symbiosis of thiotrophic *Alphaproteobacteria* and marine catenulid flatworms” ISME 13, Seattle, U.S.A.
- 2009** “Shallow water interstitial worms and their thiotrophic bacterial partners” in Munich, Germany at the workshop symbiotic interactions at the Helmholtz Zentrum München - German Research Center for Environmental Health - November 2009
- 2009** “*Alphaproteobacteria* as Coevolved Thiotrophic Symbionts in Marine Catenulid Flatworms with a Worldwide Distribution” 6th ISS Congress, Madison, Wisconsin, U.S.A

Poster presentations

2008 A novel marine flatworm/thiotrophic bacteria symbiosis model system. ISME 12, Cairns, Australia

2005 Localization of sulfur in the symbionts of a retronectid plathelminth by EDX and EFTEM. 40th EMBS, Vienna University, Vienna, Austria

Scholarships & Awards

2010 The talk “Alphaproteobacteria as coevolved thiotrophic symbionts in marine catenulid flatworms” presented at the Science day at the Vienna Ecology Centre, Vienna, Austria was selected as “Best PhD student presentation”. This award included travelling money for a conference visit.

2006 University of Vienna travelling scholarship “Kurzfristige Wissenschaftliche Arbeiten im Ausland”, to Rønbjerg, Denmark